SPECTROSCOPIC TECHNIQUES TO STUDY THE OPTICAL PROPERTIES AND INTERACTION OF SOME DRUGS WITH BIOACTIVE COMPOUNDS OF COFFEE BEANS

Ataklti Abraha

DEPARTMENT OF PHYSICS,

THE GRADUATE PROGRAM OF ADDIS ABABA UNIVERSITY

A THESIS SUBMITTED IN PARTIAL FULFILMENT OF THE REQUIREMENT FOR THE DEGREE OF DOCTOR OF PHILOSOPHY IN PHYSICS (LASER SPECTROSCOPY)

Addis Ababa University

Addis Ababa, Ethiopia

June 22, 2018

Declaration

DEPARTMENT OF PHYSICS, ADDIS ABABA UNIVERSITY

The undersigned hereby certify that they have read and recommend to the Graduate program of AAU for acceptance a thesis entitled "***Spectroscopic Techniques to Study the Optical Properties and Interaction of some Drugs with Bioactive Compound of Coffee Beans***" by **Ataklti Abraha** in partial fulfilment of the requirements for the degree of **Doctor of Philosophy in physics (Laser Spectroscopy)**.

Dated:June 22, 2018

External Examiner:_____ _____

Prof. Kalambuka Hudson Angeyo,

Department of Physics, University of Nairobi, Kenya

Internal Examiner:_____ _____

Dr. Alemu Kebede,

Applied Physics Program, ASTU, Ethiopia

Main Supervisor:_____ _____

Prof. Ashok V. Gholap,

Department of Physics, AAU, Ethiopia

Co-Supervisor:_____ _____

Dr. Abebe Belay,

Applied Physics Program, ASTU, Ethiopia

Examining Chair Person:_____ _____

Dr. Teshome Senbeta,

Department of Physics, AAU, Ethiopia

ADDIS ABABA UNIVERSITY

Date:**June 22, 2018**

Author: **Ataklti Abraha**

Title: **Spectroscopic techniques to study the optical properties and interaction of some drugs with bioactive compound of coffee Beans**

Department: **Physics** Degree: **PhD** Date: **June 22, 2018**

Permission is herewith granted to Addis Ababa University (AAU) to circulate and to have copied for non-commercial purposes, at its discretion, the above title upon the request of individuals or institutions.

_____

Signature of Author

Declaration of originality

This dissertation contains no material which has been accepted for a degree or diploma by the University or any other institution, except by way of background information and duly acknowledged in the dissertation. Moreover, to the best of my knowledge and belief no material previously published or written by another person except where due acknowledgement is made in the text of the dissertation, nor does the dissertation contain any material that infringes copyright.

Date:June 22, 2018

The author:_____ _____

Ataklti Abraha

PhD Student, AAU, Addis Ababa, Ethiopia

Coauthorship

Chapter 5 contains material that was published in A. Abraha, AV. Gholap and A. Belay. In all cases, the design and implementation of the research, data analysis, interpretation of the results and manuscript preparation was the responsibility of the candidate. AV. Gholap (Department of Physics, Addis Ababa University (AAU)) and A. Belay (Applied Physics program, Adama Science and Technology University) played great role in assisting with valuable insight, direction and guidance and supervision in all aspects of the PhD and with help producing publishable quality manuscripts.

Date:June 22, 2018

Main Supervisor:_____ _____

Prof. Ashok V. Gholap

Physics Department

Addis Ababa University, Addis Ababa, Ethiopia

Co-Supervisor:_____ _____

Dr. Abebe Belay

Applied Physics Program,

Adama Science and Technology University,

Adama, Ethiopia

Acknowledgements

Above all, I would like to thank the Almighty God, who offered me everything. *"Trust in the Lord with all your heart. Don't put your confidence in your own understanding. In all your way acknowledge Him, and He will direct your path."* Proverbs 3:5-6.

My long journey has come to end with a pleasant success. One can easily estimate the existed difficulties during this long period of time, because this work has been done in laboratory where there is no basic laboratory apparatus available. In fact, I may face more difficulty if the contributions of some individual people did not exists. Therefore, I would like to take the opportunity to thank all of them.

I would like to express my sincere gratitude to my supervisors, Professor A.V. Gholap and Dr. Abebe Belay for their valuable insight, direction, encouragement, limitless help, close guidance and effective supervision through out these years. It is with great appreciation to thank my supervisors not only for sharing their experience and enlightening discussion all the way through from the beginning but also for their tireless effort, commitment and great contribution in Laser spectroscopy in AAU in particular and throughout the country at large.

Special thanks go to graduate program of AAU for accepting my application as PhD student and in particularly academic and administrative staff of Department of Physics. Especially, thanks go to the following individuals, Dr. Teshome Senbeta (department head), Dr. Mulugeta Bekele, Dr. Belayneh Mesfin, and Mr. Tesfaye Mamo (Physics Lab Assistance) for their consistent help, motivations, discussions, support and for every opportunity for successful completion of my work. Besides, I would like to thank Mrs. Tsilat Adinew, secretary Department of Physics for her efforts in facilitating my dealings with the department and providing resources and research facilities.

Moreover, I would like to thank the Polymer Physics, Inorganic and Analytical Chemistry lab-

oratory group staff of AAU. Especially thanks go to Sintayehu Yigzaw, Dr. Mesfun Redi and Mr. Hagos Yisak for allowing me to use their facilities and constructive discussions. I acknowledge Samara University for offering me the opportunity for study leave and their consistent financial support over the last three years for the PhD fellowship, in general for investing so much resource to train me as a part of academic staff development.

I also thank to my family, my wife and my best friend (Tesfaye yemane), who have been a constant source of support and encouragement during the challenges of my research time. And, this work is dedicated for them since it was through their encouragement over the years to get me to where I am now.

Lastly but not least, I would like to pay tribute to my parents, office mates, class mates and friends for their continuing support and tolerance. To my brothers and sister who have been a source of strength and motivation from the beginning, and to all people who supported me with this dissertation.

Ataklti Abraha

Addis Ababa, Ethiopia

June 22, 2018

Dedication

Dedicated to my FAMILY, WIFE and best friend TESFAY YEMANE

Father And Mother I Love You

Abstract

Drug-drug/food interactions are major source of patient's inconvenience and non-adherence through disruption in a patient's daily schedule. Hence, lack of knowledge of potentially significant drug-drug/food interactions lead to poor clinical outcomes. Thus, investigation of different incompatibilities of drugs using spectroscopic techniques is most important inquiry of solving these problems. For this reason, the optical transition probabilities and interactions of some drugs (nicotinamide (NIC), neomycin sulfate (NOMS), norfloxacin (NOR) and ciprofloxacin (CIP)) with biologically active compounds of coffee beans (chlorogenic acid (CGA) and caffeine (CAF)) have been investigated using Ultraviolet visible (UV-Vis) absorption and fluorescence spectroscopic techniques. From the UV-Vis spectroscopic technique, the self-, hetero-association, thermodynamic properties, and optical transition probabilities of the drugs were investigated in aqueous solution. The parameters were analysed using Dimer model and Bensi-Hildebrand equations respectively for the self-and hetero-associations. The obtained equilibrium dimerization constant (K_C) values are 2.379×10^4, 1.06×10^5, 5.424×10^3, 4.377×10^3, 4.3135×10^3 and $6.67 \times 10^3 M^{-1}$ for NIC, NOMS, NOR, CIP, interaction of nicotinamide with chlorogenic acid (NIC-CGA), and interaction of norfloxacin with caffeine (NOR-CAF) respectively. In order to understand the interaction mechanisms of the self and hetero-associations, thermodynamic properties were determined using Vant's Hoff's equation. The molar enthalpy changes were found to be 4.826 ± 0.415, 3.76 ± 0.66, $-(5.35 \pm 0.459)$, $-(1.98 \pm 0.25)$,$-(16.927 \pm 0.836)$ and $-(1.277 \pm 0.103) kJ.mol^{-1}$ for NIC, NOMS, NOR, CIP, NIC-CGA and NOR-CAF respectively. Thus, hydrophobic interactions are dominant for the interaction of NIC and NOMS molecules, and electrostatic forces play the major role in the interactions of NOR, CIP, NIC-CGA and NOR-CAF molecules. The op-

tical transition probabilities of the drugs were determined using integrating absorption technique from the absorption spectra of the drugs. The values of the oscillator strengths are 0.07, 0.1,0.37 and 0.46 for NIC, NOMS, NOR and CIP respectively. Besides, the binding of CAF with NIC using fluorescence quenching technique was analysed at temperatures of 295 and 303 K and it was confirmed with the absorption spectra of the binding molecules. From this fluorescence quenching spectral analysis the quenching constant ($1.775 \times 10^4 L/mol$), quenching rate constant ($5.052 \times 10^{13} L/mol/s$) and number of binding sites 0.88 were determined at 295 K. The thermodynamic properties of interaction of nicotinamide with caffeine (NIC-CAF) indicates that electrostatic forces play the major rule in the binding of the molecules. The effect of solvent polarity on the absorption and fluorescence spectra of NIC were investigated. The ground state and excited state dipole moments of NIC are estimated from solvatochromic shifts of absorption and fluorescence spectra as a function of the dielectric constant and refractive index functions. Thus, the ground and excited dipole moments were found to be $0.02D$ and $0.268D$ respectively using Bilot-Kawski method. The excited state dipole moment is found to be higher than those of ground state for all of the used methods, and the higher values are attributed to more polar excited state of NIC. Therefore, the results of the study are very important for understanding the binding reaction in biological system, nature and strength of the transition, absorption spectral interpretation, and in providing stringent test of atomic and molecular structure calculations for theoretical work of the compounds. Thus, understanding the interaction properties of the drugs may help in the field of pharma technology and food companies in improving the efficiency and the capabilities of absorption of the drugs in biological system and in induce rapid recovery of patient's.

Ataklti Abraha

AAU,June 22, 2018

Table of Contents

List of Figures

List of Tables

Abbreviations and Acronyms

NOMS neomycin sulfate

UV-Vis Ultraviolet visible

NIC nicotinamide

CGA chlorogenic acid

NOR norfloxacin

CAF caffeine

NIC-CGA interaction of nicotinamide with chlorogenic acid

CIP ciprofloxacin

NOR-CAF interaction of norfloxacin with caffeine

NIC-CAF interaction of nicotinamide with caffeine

NAD nicotinamide adenine dinucleotide

NADP nicotinamide adenine dinucleotide phosphate

ATP adenosine triphosphate

DNA deoxyribonucleic acid

CNS central nervous system

LC-MS/MS liquid chromatography with mass spectrometry

NMR nuclear magnetic resonance spectroscopy

RPTLC reversed-phase thin-layer chromatography

IR infrared

HOMO highest occupied molecular orbital

LUMO lowest unoccupied molecular orbital

HOMO-LUMO highest occupied molecular orbital-lowest unoccupied molecular orbital

Chapter 1

Introduction

"Throughout this century, unraveling the physics of atoms and molecules has provided a rich source of new ideas and techniques. Today, we no longer ask what really goes on in an atom; we ask what is likely to be observed—and with what likelihood—when we subject atoms to any specified influences such as light or heat, magnetic fields or electric currents."

Gordon W. F. Drake and Otto Robert Frisch

The major difficulty of scientists is studying what happens at the atomic and molecular level without physically visualizing atoms and molecules. Fortunately, in order to solve this problem, they adapted to use light to learn every detail information about the structure, composition and interactions of the atoms and molecules. Accordingly, the relation of light with matter has always fascinated mankind. At the end of the nineteenth century, when the discrete nature of the spectral lines was explained, a deeper understanding of the interaction between light and matter was improved. In fact, most of our knowledge about the structure and properties of atoms and molecules is based on spectroscopic investigations [1]. Until today, these investigations rely on the mutual support of theory and experiment.

Spectroscopy is a technique that investigates the structure and the interaction of atoms

and molecules with their surroundings. It contains interaction of electromagnetic radiation with matter in order to obtain the structural and compositional information of the molecules from their spectrum. Most of the spectroscopic methods are based upon the principles of either absorption, emission, fluorescence, ionization or scattering [2–4]. A variety of spectroscopic techniques are regularly applied to solid, liquid and gaseous samples, exploiting a manifold of physical and chemical phenomena [5, 6]. The most powerful experimental technique available to scientists to study the interaction of light with matter is molecular spectroscopic techniques.

The foundations of molecular spectroscopy were laid at the beginning of the nineteenth century. This field was exploded following the invention of the laser in the 1960's equipped with a monochromatic, intense and tunable light source[7, 8]. A further step was taken in the 1980's, when laser spectroscopy emerged from the universities as an analytical discipline in an investigations of atomic and molecular information with increasingly commercial applications in physics, chemistry, pharmacy, medicine, geology, biology and engineering. High resolution spectroscopy was rapidly developed associated with the study of spectra of atoms and molecules in general, and to assess the information associated with the structure, size, and the atomic and molecular number densities, etc [8]. The experimental spectroscopic data that provides the frequencies, or wavelength of the radiation and amount of radiation emitted or absorbed by the sample of molecules can be used to determine the quantitative and qualitative values of various molecular properties such as the detailed and exact measurements of the size, shape, flexibility and electronic arrangements of the molecules. This makes molecular spectroscopy the most powerful tool for a great variety of molecular-structure studies, and has an outstanding contributions for the present state of different research disciplines [1].

The absorption spectroscopy and fluorescence spectroscopy are widely used to characterize the structure and dynamics of varieties of molecules. Besides, the information obtained from the absorption and fluorescence spactra can be useful for various kinds of analyses such as for the qualitative and quantitative chemical analysis [1, 5, 9]. Moreover, these techniques are the most useful techniques that have various applications such as for studies the rate of chemical reaction, molecular interactions, and the solvent and the temperature effect on the molecules. In this research, it is intended to investigate the molecular interactions, solvent effect, temperature effect, quantum mechanical and optical properties of some drug compounds (nicotinamide, norfloxacin, ciprofloxacin and neomycin sulphate) using computational and experimental methods.

Previously many workers have reported on the impact of the interactions, safety and efficiency of the drug compounds [10, 11]. Theses compounds can be found in various pharmaceutics and food stuffs and they can be very useful in different activities of the body system [12–16]. Moreover, the interaction of the drug compounds with other drugs and food stuff components may affect the pharmacodynamics and pharmacokinetics of the drugs [17]. Thus, with the increase use of food supplements and the rapid development of new types of drugs, the interaction of the drug compounds with biologically active compounds of coffee beans is important and is great field of interest.

Today intensive researches have been conducted on the quantitative and qualitative investigations of these compounds by chemical and physical methods to use for various applications in biological system and in optical characterization [10, 11]. The molecular interaction of these compounds with biologically active compounds have also been reported by theoretical as well as spectroscopic techniques to design more advanced and controllable carriers of drugs and food components. In view of the beneficial properties

of the drug compounds, it is of interest to investigate the molecular interactions, solvent effect, temperature effect and optical properties of the compounds.

The most economical, time saving and simple method for investigating the above mentioned properties are based on absorption (UV-Vis) and fluorescence spectroscopy. The techniques are non-destructive and of interest due to the recent development of powerful optical and molecular instruments, which permits the detection of numerous substances at low concentration. Therefore, this project is with the following general and specific objectives.

General Objective

The general objective of the dissertation is to explore "spectroscopic techniques to study the optical properties and interaction of some drugs with bioactive compound of coffee beans".

Specific Objectives

The general objective of this thesis was achieved based on the specific objectives. Thus, the main specific objectives of the work are to;

1. Determine the concentration dependent self-association of the drugs using dimer model equation.
2. Calculate the hetero-association of the drugs with biologically active compounds of coffee beans using Bensi-Hildebrand approach.

3. Determine the thermodynamic properties of the self and hetero-association of the compounds using Van't Hoff's equation.
4. Determine the optical transition properties (transition dipole moment, oscillator strength, integrated absorption cross-section, molar extinction coefficients and Einstein coefficients) of the drug molecules.
5. Determine the binding of nicotinamide with caffeine using fluorescence quenching and UV-Vis Spectroscopy.
6. Analyse the solvent effect on absorption and fluorescence spectra of nicotinamide
7. Determine the ground and excited dipole moments from the effect solvent polarity.

Organization of the Thesis

The thesis is organized as follows.

Chapter 1: This chapter deals with the general overview of spectroscopy, applications of spectroscopy, types of spectroscopic techniques, the general and specific objectives of the study and the overall structure (organization) of the thesis.

Chapter 2: Literature review related to the drugs and bioactive compounds of coffee beans is presented. The chemical and physical properties of these compounds, the physiological and psychological effects on biological systems and their interaction with other compounds are discussed. Moreover, the different physical and chemical methods that are used to study these compounds and their interaction with other compounds are reviewed.

Chapter 3: The theories related to the absorption of UV-Vis light in matter, fluorescence spectroscopy and the effect of solvent polarity on absorption and fluorescence spec-

tra are discussed. The derivation of electromagnetic wave equation from Maxwell's equations and the quantum mechanical derivation that is often used for qualitative and quantitative understanding of how transitions are induced in molecular system when it interacts with electromagnetic radiation are presented. The Schrodinger's equation is introduced and simple problems to illustrate its relation to quantities that are important in molecular spectroscopy are solved. Moreover, the principles and characteristics and quenching mechanisms of fluorescence spectroscopy are discussed.

Chapter 4: Chapter four describes the materials and methods used in this work. This chapter has two sections, the first section of this chapter deals with the description of various chemicals, samples and instruments used to carry out this research and the second section of this chapter deals with the methods of measuring all the parameters.

Chapter 5: The results and discussion of the the study are presented. In this chapter, self- and hetero-association of the drug compounds with bioactive compounds of coffee beans, thermodynamic properties, optical transition probabilities, the binding and binding mechanisms, and the effect of solvent polarity on absorption and fluorescence spectra of the drug compounds are well studied and presented in detail.

Chapter 6: Finally, conclusions of all the investigations carried out in the present series of experiments are presented in this chapter.

Chapter 2

Literature Review

Many scientists have studied [18–20] in the impact of drug interactions on the safety and efficacy of drugs for many years, and a number of regulatory actions taken by relevant activities of the issue. Drug-drug interactions can be categorized into those originating from pharmacokinetic mechanisms that result in alterations of drug absorption, distribution, metabolism and elimination, and those originating from pharmacodynamic mechanisms that occurs when one drug affects the actions of another drug[10, 18–20].

Pharmacodynamic interactions are an alteration in the pharmacological response of a drug that may be caused by direct competition at certain sites of action or by indirectly involving altered physiological mechanisms. These interactions can be useful when an improved therapeutic response occurs or be detrimental in that toxicity may be heightened [10, 11, 19].

Some drug interactions can be predicted from the chemical structure of the agent, its pharmacological activity, its toxicological profile, and other characteristics. But, other interaction of drugs can only be investigated through intense and large-scale clinical, pharmaceutical or chemical studies [10, 11, 19].

Drug-food interactions can be a major source of patient inconvenience and nonadherence through disruptions in a patient's daily schedule. As a result, advices should be given to

the patients how and when they have to take drugs with meals. But, lack of knowledge of potentially significant drug-food interactions can lead to poor clinical outcomes[10, 20].

Since studying large numbers of interactions consistently for all drugs is not feasible, selective methods are required to identify drugs that are likely to interact. A spectroscopist or a chemist who is knowledgeable about drug interactions may be able to identify interactions involving chelation, physical binding, or other incompatibility[10, 21, 22].

In this chapter, the literature review related to the chemical and physical properties, the various physiological and psychological effects in biological system and the different methods developed to study the drug compounds are reviewed. The compounds presented in this thesis are NIC, NOMS, NOR, CIP, CGA and CAF.

2.1 Drugs

2.1.1 Nicotinamide

Since the 19th century, vitamins are discovered with a major scientific achievement on the development of dietary allowances, fortification of foods, vitamin supplementation, and wider recognition of nutritional deficiency disorders and so on[23]. Vitamins are a unique organic micronutrients: that are essential to human health and very important for an organism as a vital nutrient to sustain life since they play an important role in normal metabolism process, growth and vitality [12]. Thus, investigating on the roles of the vitamins and their integration with other compounds is a fruitful way to control human health and to develop the function of the compounds.

Nicotinamide, member of water soluble B-vitamin complex, is the amide form vitamin that derivate from niacin. It is white, solid and colourless crystalline substances[24, 25], which is very stable in dry form. Nicotinamide, 3-Pyridinecarboxamide, has a molecular waight of $122,13 g/mol$ with a chemical structure as shown in Fig (2.1).

The human body receives its necessary quantities of nicotinamide from different natu-

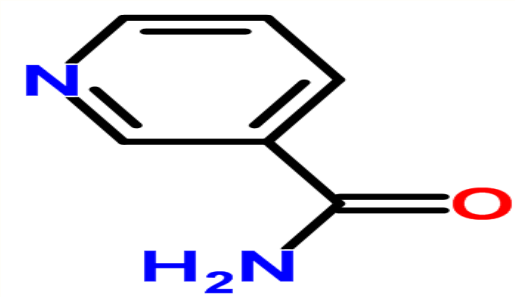

Figure 2.1: Molecular structure of nicotinomide

ral foodstuff [12], and can be obtained through synthesis in the body or as supplement of different food source such as sunflower seeds, chicken, pork, beef, fish, legumes, nuts, grain products, mushrooms, yeast extracts, coffee, e.t.c. [12, 26].

The nutritional significance of nicotinamide in its biochemical rule of electron-transfer reaction precedes to form the coenzymes nicotinamide adenine dinucleotide (NAD) and nicotinamide adenine dinucleotide phosphate (NADP) [25]. These co-enzymes are vital for reduction and oxidative reactions in which an individual is able to utilize the energy released by these reactions [25]. The increasing concentrations of nicotinamide increases NAD molecules availability in energy metabolism, and in return increases the amount of energy available in the cell.

As a precursor of NAD, nicotinamide is an essential cofactor in adenosine triphosphate (ATP) production that can replenishe cellular ATP levels in human keratinocytes after UV

exposure[27–31]. This energy-replenishing effect is the key mechanism by which nicotinamide enhances repair of ultraviolet radiation-induced deoxyribonucleic acid (DNA) damage in human keratinocytes and ex vivo skin [32, 33]. In addition, oral nicotinamide reduces nonmelanoma skin cancers in high-risk patients [34, 35].

Thus, it functions as a coenzyme and an antioxidant in numerous biological reduction and oxidation reaction systems in mammalian biological systems. It is required as a nutrient to prevent the niacin deficiency disorder pellagra, and also it is effective in arthritis and early-onset Type I diabetes[28, 29, 36]. It has also anti-inflammatory effects at pharmacological doses[37]. Moreover, Nicotinamide is used as a direct human food, therapeutic agent, skin and hair conditioning agent in cosmetics, and used as a food additive to enrich corn meal, farina, rice, and macaroni and noodle products.

2.1.2 Neomycin Sulfate

Aminoglycosides are an important group of wide spectrum antibiotics which are active against both gram-negative and gram- positive bacterial infections [38]. All aminoglycosides groups have similar structure that causes analogous chemical and pharmacological properties[38–40]. The compounds of this group are very stable, easily water soluble, wide antimicrobial spectrum and powerful sterilization capacity [41]. These drugs are used in both humans and veterinary medicines widely to treat infections caused by Gram-negative and Gram-positive bacteria [42, 43].

Neomycin sulfate is an antibiotic from the aminoglycoside group of drugs obtained from Streptomyces fradie and a complex of three separate compounds, neomycin A (neamine; inactive), neomycin C and neomycin B (framycetin).[44, 45]. It is a water soluble hy-

drophilic aminoglycoside antibiotic and calcium channel protein inhibitor that binds to prokaryotic ribosomes inhibiting translation, and is highly effective against Gram-positive and Gram-negative bacteria [13, 14]. It can be easily dissolved in water and stay in a stable solution. Neomycin sulfate has a molecular weight of 908.88 g/mol and its structure is represented in Fig (2.2). It can be found in many topical medications such as creams, ointments, and eyedrops.

In cell culture, neomycin sulfate is used as an antimicrobial agent to prevent contamination. It is also used as a selection agent for prokaryotic cells that have been transformed using the selectable marker gene. In vitro, neomycin sulfate is bactericidal and acts by inhibiting the synthesis of protein in susceptible bacterial cells. It is commonly used for the prevention of bacterial contamination of cell cultures and for treatment in various eye, skin and gastrointestinal infections[46–48]. It inhibits DNase I induced DNA degradation [14].

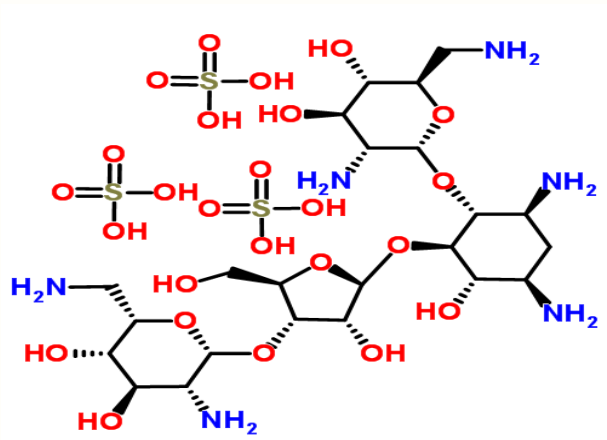

Figure 2.2: Molecular structure of neomycin sulfate

Since oral neomycin is absorbed systemically after oral administration, its use may result in nephrotoxicity, neurotoxicity and/or ototoxicity, even at recommended doses and in patients with normal renal function [49].

2.1.3 Norfloxacin and Ciprofloxacin

Quinolones are one of the largest classes of antimicrobial agents used worldwide with therapeutic indications having evolved from urinary tract infections to infections of almost all body compartments. Quinolone drugs are quinolone carboxylic acids, which are class of antibiotics or a group of synthetic antibacterial agents containing a $4-oxo-1,4-$dihydroquinoline skeleton that have found wide use in therapy[15, 16].

Accordingly, norfloxacin and ciprofloxacin are the second-generation of quinolones that introduced a fluorine atom at position 6 and a bulky piperidine at position 7, broadening the antimicrobial spectrum to Pseudomonas species[50].

Norfloxacin [l-ethyl-6-fluoro-l,4-dihydro-4-oxo-7- (1-piperazinyl)-3-quinolone carboxylic acid] is the first commercially available member of the modern fluoroquinolones with a fluorine atom and piperazine substituted at the C-6 position and C-7 position, respectively. The fluorine atom is responsible to increase potency against gram-negative organisms and the piperazine moiety is for antipseudomonal activity[51, 52]. It is a broad-spectrum antimicrobial used effectively to treat infections in humans and animals.

Norfloxacin is a light-yellow crystalline powder, odorless and has a bitter taste [53]. It has a molecular mass of $319.331 g/mol$ with structurally represented in Fig (2.3).
As norfloxacin is the first commercially available group of modern quinolone drugs, it possess various functions. It has broad-spectrum antibacterial activity against gram-positive and gram-negative [54, 55]. It is also used for the treatment of complicated urinary tract infections, gonorrhoea, Bladder, gynecological and infection of eyes [56]. The primary target of norfloxacin is to inhibit the DNA gyrase enzyme and topoisomerase II

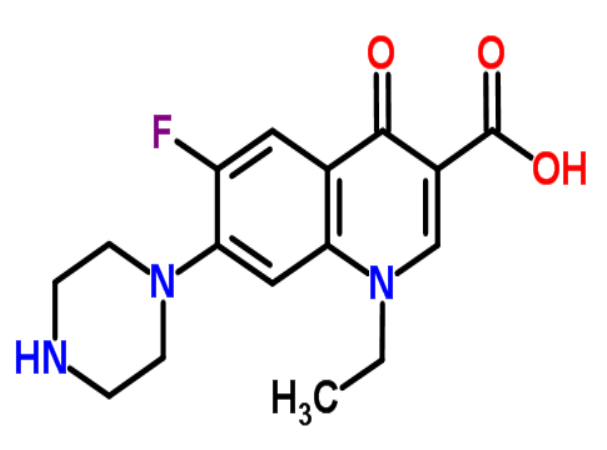

Figure 2.3: Molecular structure of norfloxacin

[15, 57, 58].

Similarly, ciprofloxacin (1-cyclopropyl-6-fluoro-1,4-dihydro-4- oxo-7-(1-piperazinyl)-3-quinolone carboxylic acid) belongs to the second generation of quinolone analogues of nalidix acid that show greater potency, lower toxicity and a broader antibacterial spectrum. The main difference between ciprofloxacin and other antibiotics is that it can be administered both parenterally and orally. It is well absorbed and widely distributed into various body tissues and fluids. It has a molecular mass of $331.347 g/mol$ and a chemical structure as shown in fig (2.4).

Ciprofloxacin is a group of fluoroquinolones that have a series of synthetic antimicro-

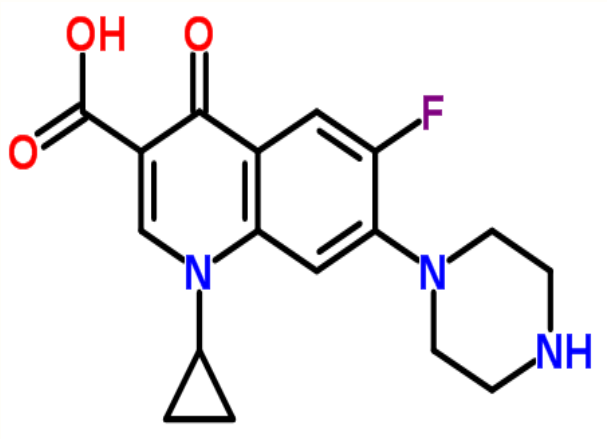

Figure 2.4: Molecular structure of ciprofloxacin

bials and active against both Gram-negative and Gram-positive microorganisms[16, 57]. It is the important bacterial enzyme DNA gyrase and topoisomerase IV, which are required for bacterial DNA replication, transcription, repair, strand supercoiling repair, and recombination[15, 57, 58].

Ciprofloxacin is extremely useful for the treatment of a variety of infections including urinary tract infections, skin and soft tissue infections, respiratory infections, gastrointestinal tract infection, bone and joint infections, intra abdominal infections, certain type of infectious diarrhea, typhoid fever, prostatitis, [16, 56, 59].

2.2 Biologically Active Compounds of Coffee Beans

Functional foods and bioactive components such as caffeine and chlorogenic acid of different fruits and vegetables are beneficial for human health [17, 60] and they are present in popular drinks and foods (that is, in coffee, tea, cola beverages and chocolates). They are the most widely consumed of all behaviorally active drugs in the world[61, 62].

2.2.1 Chlorogenic Acid

Chlorogenic acid (CGA) is the main phenolic natural products isolated from the leaves and fruits of dicotyledonous plants such as tea, coffee and wine[61, 63, 64]. The main known dietary source of CGA is coffee. It is a white crystal powder, which has a molecular weight of $354.31 g/mole$ and structurally it can be represented as shown in Fig (2.5).

Chlorogenic acid is the most abundant polyphenols in coffee which are responsible for substantial part of coffee antioxidants , antimutation, antibiotic, antihypercholesterolemia,

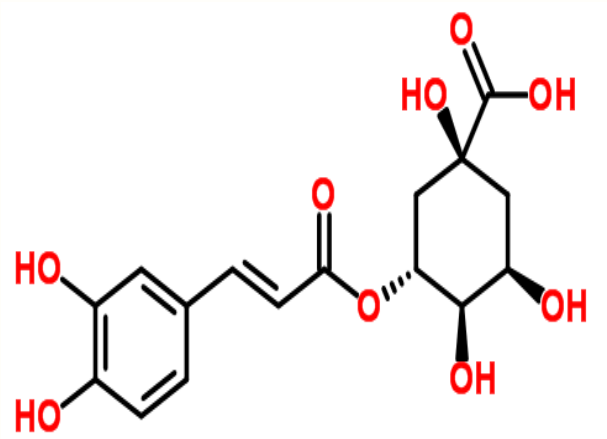

Figure 2.5: Molecular structure of chlorogenic acid

antihypertensive, metal chelation, in plant metabolism or glucose absorption [65–67], as a selective inhibitor for the production of glucose in liver [68] and used in disorders such as obesity, diabetes, and cancer [69, 70].

It is an important component of medicinal plants broadly used as anti-inflammatory agents[71, 72]. In vivo and in vitro studies show that CGA exhibits various biological properties, such as anti-bacterial and anti-carcinogenic activities [73, 74]. It is also a promising precursor compound for the development of medicine that can resist HIV / AIDS virus [75]. CGA can lower blood glucose level by 15-20 % and they are the most expected active component to antidiabetic effects according to clinical and pharmacology studies [76, 77].

2.2.2 Caffeine

Caffeine (1,3,7-trimethylxanthine) classified as the main alkaloid and the major pharmacological active group of methylxanthine. Naturally caffeine is found in leaves, seeds, or fruits of 63 plant species [78–80]. Because of it presence in popular drinks and foods (like coffee, tea, cola beverages and chocolates), it is one of the most widely consumed com-

pound in the form of caffeinated beverages over the entire world. The molecular weight of caffeine is 194.19$g/mole$ and it occurs as odorless, white crystalline with bitter taste. Structure of caffeine is shown in Fig (2.6).

Various researchers have reported that, Caffeine has various pharmacological, physio-

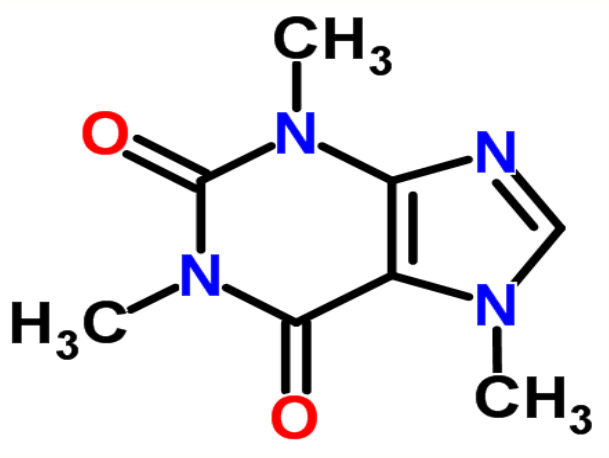

Figure 2.6: Molecular structure of caffeine

logical and psychological effects. These effects are depending on the concentration of caffeine consumption.

Psychologically, caffeine have a behavioural effects that produces more rapid, clearer flow of thought, suppresses mental exhaustion (fatigue), increases the capability of a greater sustained intellectual effort and more perfect association of ideas[62, 81]. Caffeine is used to regulate sleep quality that causes insomnia of sleep effect. Caffeine can improve the performance of a wide variety of mental tasks directly and indirectly by reducing decrements in performance under suboptimal conditions of alertness [82].

Physiologically, after caffeine is taken, relaxations of smooth muscles, like bronchial muscles, vascular and smooth muscles of the biliary and gastrointestinal tracts can occur[83, 84]. It can also stimulate the central nervous system that results in increase of gastric acid secretion and dieresis [83, 85, 86].

Pharmacologically, caffeine acts as an antagonistic effects on adenosine receptors [82, 87] or it can be used at lower dose adenosine receptors blockade. It also act as antifungal [88, 89], inhibition of phosphodiesterase [82, 90], a selective phytotoxicin [91], chemosterilant toward certain insects [92], and alterations in glucose metabolism [93]. Moreover, caffeine has a potential to decrease the antibacterial effect of tetracycline hydrochloride and chloramphenicol [94], and induce central nervous system (CNS) toxicity[95].

2.3 Drug-Drug and Drug-Food Interactions

With the increasing use of food supplements and the rapid development of new types of drugs, food/drug or drug/drug interactions are currently a great field of study. Interaction of such drug compounds with biological active compounds is one of the most common study areas, since the compounds can be found in various food sources and the interaction may affect the pharmacodynamics and pharmacokinetics of the compounds[17].

Drugs should undergo different chemical reactions before they reach their target sites to interact with biomolecules [96]. Accordingly, understanding their behaviour in a solution is very important in order to improve their pharmacological and biological activity. Thus, drugs may bind to different compounds either by a direct reaction, or weak interactions involving intermolecular bonds such as hydrogen bonding, hydrophobic interactions and so on [97].

Mixing of the compounds with different and complex molecular structure leads to various intermolecular interactions, resulting in non-ideal behaviour of mixtures[98]. Molecular interactions play a fundamental role in the behavior of the chemical and physical

properties of any physico-chemical system[98]. It involves the interaction of molecules through multiple intermolecular forces, such as dispersion (or London forces), orientation (dipole-dipole forces), induction (dipole-induced dipole or Debye forces), and electron donor-acceptor forces including hydrogen-bonding, leading to the partition of the solute between the gas and liquid phases[98]. Considering these facts, the interaction system of the selected drugs are discussed in this section.

Since nicotinamide is pharmacologically and physiologically active compound[99], it interacts with different types of compounds. Some of the interactions reported by different scholars are with metal precursors (Cr(III), Mn(II), Fe(III), Co(II), Ni(II), Cu(II) and Cd(II))[100], bipyridyl ruthenium(II)[101], moricizine [102], indomethacin [103], caffeine [104], chlorogenic acid [105], Ascorbic Acid [106], Ibuprofen [107], and so on .

The molecules of neomycin sulfate can also interact with other compounds such as monomolecular films of polyphosphoinositides and other lipids [108], Ribosomes and Ribosomal Ribonucleic Acid [109], phosphatidylinositol 4,5-bisphosphate [110], and so on. But, the self-association of of neomycin sulfate was not studied yet.

Moreover, caffeine can effectively form hetero association with many aromatic DNA intercalators that can change the biological activities of these drugs or make a computation with the drugs for the binding sites on DNA [111, 112]. Thus, as the norfloxacin molecules contain two fused aromatic rings just like caffeine, it can form interaction with caffeine [113]. This interaction may alter the pharmacokinetics or change the toxicity risk of the drugs [95, 113]. Also, the molecules of norfloxacin can make an interaction with antacids and minerals [114], rare earth [115], metal precursors (Fe(III), Co(II), and Zn(II)) [116], double-stranded DNA [117], Human Serum Albumin [118], trypsin [119], topoisomerase

IV [120], cyclosporine [121], Riboflavin [122], and so on.

In similar way, the molecular interaction of ciprofloxacin with different compounds was also studied by different scholars. Some of the interactions of ciprofloxacin are interactions with methotrexate [123], theophylline [124], cyclosporin A [125], DNA [126], warfarin [127], e.t.c.

The interest arises to study the optical, molecular interactions and thermodynamic properties of the compounds is because most probably these compounds could be found in many natural products, food/drug stuffs, and used in many patients for the purpose of treating different diseases. Thus, it is an important aspect to study the compounds in this matter in order to improve their efficiency in pharmaceutical and biological activities, understanding their binding in biological system, controling the effect of physicochemical properties, and to characterize their optoelectric properties. Moreover, the study is also important because knowledge of the optical, molecular interaction of the compounds are very important for understanding the binding reaction in biological systems, nature and strength of the molecular interaction in liquid solutions, to characterize the electron transition probabilities, interpreting the absorption spectra, and in providing stringent test of atomic and molecular structure calculation in theoretical works[128–132];.

2.4 Methods Developed to Study the Drug Compounds

Due to the fact of the drug/drug or drug food interactions mentioned above, many chemical and physical methods have been developed for the investigation of these compounds and their interactions with different compounds. Some of the methods/techniques used by different researchers to study the drug compounds for different purpose of applica-

tions are stated as follows.

Nicotinamide was studied by various researchers using Differential scanning calorimetry [107, 133], ultraviolet-visible [107, 134–136], fluorescence spectroscopy [135, 136], Fourier transform infrared [107, 134], nuclear magnetic resonance [107], powder X-ray diffraction [107], optical microscopy [107], millimeter-wave spectrometer [137], liquid chromatography with mass spectrometry (LC-MS/MS) [138], nuclear magnetic resonance spectroscopy (NMR) [134, 139], derivative spectrophotometry [140], electron diffraction[141], reversed-phase thin-layer chromatography (RPTLC) and microwave spectroscopy [137] for different applications such as for identify species of nicotinamide, interaction with different compounds, fluorescence decay kinetics and so on.

Similarly, in order to reduce the development of drug-resistant bacteria and maintain the effectiveness of Neomycin Sulfate, many studies have been carried out to investigate neomycin sulfate by LC-MS/MS [142, 143], Nitrogen-15 nuclear magnetic resonance spectroscopy [144], fluorescence [145, 146] and NMR spectroscopy [145], UV-Vis spectorscopy [146], high-performance liquid chromatographic [147], and so on.

Moreover, some of the methods developed previously to study the 4-quinolone drugs (norfloxacin and ciprofloxacin) are based on: LC-MS/MS [148, 149], UV-Vis [148–151], infrared (IR) [151], H NMR [151], chromatographic [149], fluorescence [149, 150], and so on. These methods was reported to use for different applications such as for the formation and properties of degradation, dose, charge transfer complexes (interaction) e.t.c.

As our knowledge concerning the methods to study the optical, molecular interaction and thermodynamic properties, binding and solvent polarity effect, the molecular spec-

troscopic techniques are the simplest, highly sensitive, rapid easily implemented techniques to study such kind of interactions. Among the molecular spectroscopic techniques UV-Vis and fluorescence spectroscopy are the most known and dominant methods to use in such type of study [128, 152–155].

Therefore, considering the importance of the compounds and the selectivity of the methods to study the optical and molecular interactions, molecular spectroscopic methods are the best way to achieve our goals. Moreover, to the best of our knowledge the self-association, hetero-association, thermodynamic parameters, optical transitional probability, the binding and the effect of solvent polarity of the drug compounds to elucidate structures, optical transition, solvent effect and binding mechanisms of the molecules are not yet investigated using UV-Vis and fluorescence spectroscopy. Thus, our objective is to investigate the optical properties and molecular interaction of some drugs with bioactive compounds of coffee beans using molecular spectroscopic methods (UV-Vis and fluorescence).

Chapter 3

Theory

The development of theoretical treatments of atomic and molecular systems have been closely correlated to the study of the experimental spectra of the systems since the nineteenth century. The theories can be introduced in order to obtain better understanding on the energy levels of the atom or molecule based on the spectral interpretation of the systems. More generally, they can be used to interpret the interaction of matter with electromagnetic radiation [156, 157].

The most interesting spectral method in order to analyse the interaction of electromagnetic radiation with matter is based on the molecular spectroscopic technique. It uses the theoretical frame work of the propagation of light through matter due to the electromagnetic radiation. To describe the interaction of electromagnetic radiation with molecules it is useful to adapt the semi-classical field theory which combines the classical picture of fields and the quantum picture of matter.

In this chapter, the general nature of the theoretical aspects of atomic and molecular systems are introduced to the extent needed for the treatments of experimental molecular systems of our interest. Here, the interaction of light with matter by classical and semi-classical theory are presented. Starting with Maxwell's equations, the wave equations in material media are described by classical electromagnetic theory to show the various theoretical molecular phenomena exhibited by medium (such as absorption and emission of

the light). This chapter will also deal with the theoretical derivation that can be used for understanding the optical transitions induced in molecular system. The time dependent Schrodinger equation relates to the theoretical treatment of the systems with that of the experimental spectra's. Moreover, the general nature of light in molecule systems in case of absorption and fluorescence processes such as the binding of molecules using fluorescence quenching and the solvent polarity effect on absorption and fluorescence are discussed.

3.1 Light Matter Interaction

3.1.1 Maxwell's Equation

Electromagnetic radiation is a kind of radiation including ultraviolet-visible light, radio waves, gamma rays, and X-rays, in which electric and magnetic fields vary simultaneously. Maxwell's equations in vacuum have been verified by many experiments[158, 159]. Besides, electromagnetic waves in vacuum, the interaction between media and electromagnetic waves is also an important subject. In the mid-nineteenth century, Maxwell showed that light of all kinds is radiated through conjoined electric and magnetic fields. Thus, all electromagnetic phenomena (static and dynamic) can be said to follow from Maxwell's equations[159, 160]. For a neutral isotropic charge-free homogeneous dielectric medium, Maxwell's equations can be simplified as:

$$\overrightarrow{\nabla}.\mathbf{E} = 0 \tag{3.1.1}$$

$$\overrightarrow{\nabla}.\mathbf{H} = 0 \tag{3.1.2}$$

$$\overrightarrow{\nabla} \times \mathbf{E} = -\frac{\partial \mathbf{B}}{\partial t} \tag{3.1.3}$$

$$\overrightarrow{\nabla} \times \mathbf{H} = \frac{\partial \mathbf{D}}{\partial t} \tag{3.1.4}$$

For most applications in molecular systems, we are interested only in non ferrous magnetic media, for which

$$\mathbf{B} = \mu_0 \mathbf{H} \tag{3.1.5}$$

The electric displacement D is defined as

$$\mathbf{D} = \epsilon_0 \mathbf{E} + \mathbf{P} \tag{3.1.6}$$

where ϵ_0 and μ_0 represent the dielectric permittivity and the magnetic permeability of the medium, and **E**, **H** and **P** represent the electric field, magnetic field and polarization respectively. The magnetic permeability of the medium for most dielectrics is almost equal to that of vacuum. The polarization **P** is the electric dipole moment per unit volume of the medium. **P** is the only term in the Maxwell's equations directly related to the medium.

If we take the curl of Eq. (3.1.3), we would obtain

$$\overrightarrow{\nabla} \times (\overrightarrow{\nabla} \times \mathbf{E}) = -\overrightarrow{\nabla} \times \frac{\partial \mathbf{B}}{\partial t} = -\frac{\partial}{\partial t}(\overrightarrow{\nabla} \times \mathbf{B}) \tag{3.1.7}$$

Now we use the general expression,

$$\overrightarrow{\nabla} \times (\overrightarrow{\nabla} \times \mathbf{E}) = \overrightarrow{\nabla}(\overrightarrow{\nabla}.\mathbf{E}) - \overrightarrow{\nabla}^2 \mathbf{E} \tag{3.1.8}$$

of a vector calculus, together with Eqn (3.1.5) and the maxwell's Eqn (3.1.4), to write

$$\overrightarrow{\nabla}(\overrightarrow{\nabla}.\mathbf{E}) - \overrightarrow{\nabla}^2 \mathbf{E} = -\mu_0 \frac{\partial^2 \mathbf{D}}{\partial t^2} \tag{3.1.9}$$

Finally we use the definition Eqn (3.1.6) of **D** and rearranging terms gives,

$$\overrightarrow{\nabla}^2 \mathbf{E} - \overrightarrow{\nabla}(\overrightarrow{\nabla}.\mathbf{E}) - \frac{1}{c^2}\frac{\partial^2 \mathbf{E}}{\partial t^2} = \frac{1}{\epsilon_0 c^2}\frac{\partial^2 \mathbf{P}}{\partial t^2} \tag{3.1.10}$$

Where $\epsilon_0 \mu_0 = \frac{1}{c^2}$ and $c = 2.998 \times 10^8 m/s$ is the speed of light in vacuum.

Eqn (3.1.10) is a partial differential equation that tells us how the electric field depends on the electric dipole moment density **P** of the medium. Here, we are particularly interested on the transverse fields or radiation fields when the charge density is zero that satisfy

$$\nabla.\mathbf{E} = 0 \tag{3.1.11}$$

Transverse wave therefore satisfies the inhomogeneous wave equation,

$$\nabla^2\mathbf{E} - \frac{1}{c^2}\frac{\partial^2\mathbf{E}}{\partial t^2} = \frac{1}{\epsilon_0 c^2}\frac{\partial^2\mathbf{P}}{\partial t^2} \tag{3.1.12}$$

The above Eqn (3.1.12) is the fundamental electromagnetic field equation that will be used for our purpose. **P** is the property of the material medium that the field **E** propagates in. The dipole moment density **P** produced in the medium leads to an explanation of many optical effects including dispersion and absorption. In order to make any use of it, it is necessary to specify the polarization. Now, Eqn (3.1.12) without the polarization term can be written as;

$$\nabla^2\mathbf{E} - \frac{1}{c^2}\frac{\partial^2\mathbf{E}}{\partial t^2} = 0 \tag{3.1.13}$$

And, one dimensional solution of Eqn (3.1.13) for a wave propagating in the z-direction in free space is given by

$$\mathbf{E}(R,t) = \widehat{\varepsilon}E_0 cos(\omega t - kz) \tag{3.1.14}$$

where the wave vector and phase velocity are

$$k_0^2 = \frac{\omega_0^2}{c^2} \tag{3.1.15}$$

and

$$v_p = \frac{\omega}{k_0} = c \tag{3.1.16}$$

3.1.2 Time Dependent Schroedinger Equation

One of the most useful applications of time dependent Schroedinger theory is to investigate the rate at which matter will absorb electromagnetic radiation. In this section we will find an expression for the rates of absorption and emission of radiation from the quantum mechanics and to relate these expressions with Einstein coefficients.

In molecular electronic structure, the transition of molecules is no longer stationary and we consider the time dependent Schroedinger equation that describes the system under the influence of a time dependent perturbation. Since the incident radiation on an atom is described by classical electromagnetic plane wave and the atom treated by quantum mechanically, the transition dipole moment of the molecules can be derived from the time dependent Schroedinger equation by semiclassical approach[1].

The time-dependent Schroedinger equation for a perturbed system can be described as

$$\widehat{H}\psi(x,t) = i\hbar\frac{\partial\psi}{\partial t} \tag{3.1.17}$$

where $\widehat{H}$ is the Hamiltonian due to interaction between the system and radiation, and ψ is the wave function for the perturbed system. And, if the system were initially in some stationary state, the time independent equation becomes [6, 161–163]

$$\widehat{H}^0\psi_n^0 = i\hbar\frac{\partial\psi_n^0}{\partial t} \tag{3.1.18}$$

where n is the transition state level and $\widehat{H}^0$ is the Hamiltonian of the system in the absence of radiation field. If the system is exposed to electromagnetic radiation for a limited time, the transition takes place to some other stationary state from its initial state. Thus, during this interval of time, the perturbation becomes

$$i\hbar\frac{\partial\psi}{\partial t} = (\widehat{H}^0 + \widehat{H})\psi \tag{3.1.19}$$

If the transition state level n is from the initial stationary state k to state m, then the system can be described by the time dependent linear combination of the two stationary states as

$$\psi(x,t) = c_k(t)\psi_k^0 e^{-iE_k^0 t/\hbar} + c_m(t)\psi_m^0 e^{-iE_m^0 t/\hbar} \tag{3.1.20}$$

which we require to normalize as

$$\int |\psi(x,t)|^2 d\tau = |c_k|^2 + |c_m|^2 = 1 \tag{3.1.21}$$

where c_k and c_m are the time dependent probability amplitudes of the two atomic states of k and m [1].

Now, if we substitute the time dependent wave function of Egn (3.1.20) in to the time dependent Schroedinger Eqn (3.1.17), multiplied in the left by $\psi^*_{n(n=k,m)} e^{-iE^0_{n(n=k,m)}t/\hbar}$ and integrated overall space, we obtain

$$c_k \int \psi_k^* \widehat{H} \psi_k d\tau + c_m e^{-i\omega_0 t} \int \psi_k^* \widehat{H} \psi_m d\tau = i\hbar \frac{dc_k}{dt} \tag{3.1.22}$$

where $\omega_0 = \frac{E_m^0 - E_k^0}{\hbar}$.

Now, let's denote the matrix element $\int \psi_k^* \widehat{H} \psi_k d\tau$ and $\int \psi_k^* \widehat{H} \psi_m d\tau$ as H_{kk} and H_{km}, with

$$H_{km} = \int \psi_k^* \widehat{H} \psi_m d\tau = -e\mathbf{E} \int \psi_k^* \widehat{r} \psi_m d\tau = -\mathbf{E} \bullet \overrightarrow{\mu}_{km} \tag{3.1.23}$$

where $\overrightarrow{\mu}_{km} = \overrightarrow{\mu}_{mk} = -e \int \psi_k^* \widehat{r} \psi_m d\tau$ is the transition dipole moment from state k to m. So we have

$$c_k H_{kk} + c_m e^{-i\omega_0 t} H_{km} = i\hbar \frac{dc_k}{dt} \tag{3.1.24}$$

and

$$c_k e^{i\omega_0 t} H_{mk} + c_m H_{mm} = i\hbar \frac{dc_m}{dt} \tag{3.1.25}$$

These two coupled equations define the quantum mechanical problem and the solution of the coefficients c_k and c_m defines the time evolution of the state wave function Eqn

(3.1.20). Moreover, the atomic transition dipole moment in Eqn (3.1.23) depends on the wave functions ψ_k and ψ_m of the two states and is determined by charge distribution in these states.[1, 163]. To further proceed with the atomic transition dipole moment, it is necessary to be more specific about the perturbation.

When a molecular system is exposed to electromagnetic radiation, the oscillating electric field of the radiation can disturb the energy of the molecule and the molecules escape from their initial stationary state[1, 162, 163]. Thus, for a single mode radiation source, the x-component of the classical electric field produced by this source at the position coupled by the molecule is

$$\mathbf{E}_x = \mathbf{E}_0(\frac{e^{i\omega t} + e^{-i\omega t}}{2}) \tag{3.1.26}$$

This electric field is responsible for the change in the Hamiltonian to produce a change in energy. Thus, using Eqns (3.1.23 and 3.1.26), the change in Hamiltonian is given by

$$\widehat{H} = -\mathbf{E}_x \bullet \overrightarrow{\mu}_x = (\mathbf{E}_0\frac{e^{i\omega t} + e^{-i\omega t}}{2})\overrightarrow{\mu}_x \tag{3.1.27}$$

Now, we have the probability of finding the population in the excited state at any time t is $|c_m(t)|^2$ [164], and the time rate of increase for the probability of finding the atom in its excited state is given by

$$\frac{|c_m(t)|^2}{t} \tag{3.1.28}$$

But, the excitation rate using the Einstein expression [164] is

$$B_{km}\rho_\omega d\omega \tag{3.1.29}$$

where B_{km} is the Einstein B-coefficient for absorption and ρ_ω is the spectral energy density. Thus, relating Eqns (3.1.28) and (3.1.29), we have

$$B_{km}\rho_\omega d\omega = \frac{|c_m(t)|^2}{t} \tag{3.1.30}$$

Now, in order to find the expression for B_{km} of Eqn (3.1.30), we have to find the solution of the coupled Eqns (3.1.24) and (3.1.25).

Consider a weak-field approximation that the field amplitude is sufficiently small for the time $t < T$ [1], and the population of E_m remains small compared to E_k. Besides, using the initial conditions for the coupled equations at $t = 0$ as $c_k(t = 0) = 1$ and $c_m(t = 0) = 0$, and substituting Eqn (3.1.26) in to Eqns (3.1.24 and 3.1.25), we have

$$\frac{dc_k}{dt} = 0 \tag{3.1.31}$$

$$\frac{dc_m}{dt} = \frac{i}{2\hbar}\mathbf{E}_0\langle\psi_m^0|\widehat{\mu}_x|\psi_k^0\rangle[e^{it(\omega+\omega_0)} + e^{it(\omega_0-\omega)}] \tag{3.1.32}$$

where

$$|\overrightarrow{\mu}_{km}| = \int \psi_m^0|\widehat{\mu}_x|\psi_k^0 dx$$

And, using the initial conditions and integration over the time interval 0 to t, the solution of $c_k(t)$ and $c_m(t)$ is given by

$$c_k(t) = 0 \tag{3.1.33}$$

$$c_m(t) = \frac{\mathbf{E}_0|\overrightarrow{\mu}_{km}|}{2\hbar}[\frac{e^{it(\omega+\omega_0)} - 1}{\omega + \omega_0} + \frac{e^{it(\omega_0-\omega)} - 1}{\omega_0 - \omega}] \tag{3.1.34}$$

If ω (driving wave frequency) approaches to ω_0 (transition resonance frequency), the exponential in the first term in bracket of the Eqn (3.1.34) will oscillate at about twice the atomic resonance frequency ω_0. And it go to zero over the time of the transition since it is very fast compared to the characteristic rate of weak field optical coupling [164]. Thus, the approximation will be

$$c_m(t) = \frac{E_0|\overrightarrow{\mu}_{km}|}{2\hbar}[\frac{e^{it(\omega_0-\omega)} - 1}{\omega_0 - \omega}] \tag{3.1.35}$$

Thus, the transition probability of absorption from k to m state becomes

$$(c_m^* c_m)(t) = \frac{E_0^2|\overrightarrow{\mu}_{km}|^2}{\hbar^2}[\frac{sin^2(\frac{(\omega_0-\omega)t}{2})}{(\omega_0 - \omega)^2}] \tag{3.1.36}$$

This equation is called the rotating wave approximation.

Now, the average field energy as an integral over the spectral energy density of the excitation source in the neighbourhood of the transition frequency with a spectral width of $\omega_0 \pm \triangle\omega$ can be expressed as

$$\frac{1}{2}\epsilon_0 E_0^2 = \int_{\omega_0-\triangle\omega}^{\omega_0+\triangle\omega} \rho_\omega d\omega \tag{3.1.37}$$

Substituting Eqn (3.1.37) into the rotating wave approximation Eqn (3.1.36), we have

$$|c_m(t)|^2 = \frac{2|\overrightarrow{\mu}_{km}|^2}{\epsilon_0\hbar^2} \int_{\omega_0-\triangle\omega}^{\omega_0+\triangle\omega} \rho_\omega \frac{sin^2(\frac{(\omega_0-\omega)t}{2})}{(\omega_0-\omega)^2} d\omega \tag{3.1.38}$$

$\rho_\omega = \rho_{\omega_0}$ by considering the spectral density for a conventional broadband excitation is constant over the line width of the atomic transition. But, this is not true for a narrowband excitation. Thus, assume a broadband continuous excitation with $t(\omega_0 - \omega) >> 1$, that gives

$$\int_{\omega_0-\triangle\omega}^{\omega_0+\triangle\omega} \frac{sin^2(\frac{(\omega_0-\omega)t}{2})}{(\omega_0-\omega)^2} d\omega = \frac{\pi t}{2} \tag{3.1.39}$$

Thus, the probability of finding the atom in the excited state is given by

$$|c_m(t)|^2 = \frac{\pi|\overrightarrow{\mu}_{km}|^2}{\epsilon_0\hbar^2}\rho_{\omega_0} t \tag{3.1.40}$$

Therefore, the quantum mechanical and classical expressions for the rate of excitation, using Eqn (3.1.30) gives the Einstein B coefficient in terms of the quantum mechanical transition moment as

$$B_{km}\rho(\omega_0) = \frac{|c_m(t)|^2}{t} = \frac{\pi|\overrightarrow{\mu}_{km}|^2}{\epsilon_0\hbar^2}\rho_{\omega_0} \tag{3.1.41}$$

This implies that

$$B_{km} = \frac{\pi|\overrightarrow{\mu}_{km}|^2}{\epsilon_0\hbar^2} \tag{3.1.42}$$

Finally, if the atoms move randomly with the confined space and using the quantum mechanical expression for the classical average of the dipole moment, the over all average

of the transition moment of the light field polarization with respect to the over all spacial directions is given by

$$|\mu_{km}|^2 = \frac{2}{3}|\overrightarrow{\mu}_{km}|^2 \tag{3.1.43}$$

And

$$B_{km} = \frac{2\pi|\overrightarrow{\mu}_{km}|^2}{3\epsilon_0\hbar^2} \tag{3.1.44}$$

This section implies how the time dependent Schroedinger equation relates with the Einstein coefficients in the presence of light matter interaction when the atom transit from the lower state to the upper state. Einstein coefficients and their relation with the experimental determinations of the absorption and emission of radiation will be discussed in the next section.

3.1.3 Transition Probability and Einstein Relations

Absorption and emission are the phenomena in which the electromagnetic radiation interacts with matter that originates from an electron transition between pairs of states[6, 161–163]. Transition is a quantum mechanical process expressed in molecular states by deriving the time-dependent Schrodinger equation which allows calculating the atomic scale phenomena as a function of time as well as space.

Beer-Lamberts Law

Absorption measurements involve placing a sample of atoms or molecules between a continuous light source and a spectrometer. The absorption coefficient, which can be derived from the material's dielectric function and conductivity, determines the absorption

of light as a function of path length. As the wave traverses the medium or sample, the transmitted intensity is exponentially attenuated:

$$I(z) = I_0 e^{-az} \tag{3.1.45}$$

where a is the absorption coefficient, z is the path length in the medium, and this equation is known as Beer-Lambert's law.

In optics, the Beer-Lambert's law relates the absorption of light to the properties of the materials through which the light travel. If the intensity I_0 and $I(t)$ are measured at two different positions $z = 0$ and $z = l$, then a can be obtained from the relation

$$al = ln\frac{I_0}{I(t)} \tag{3.1.46}$$

where l is the path length. And, this equation is strictly valid only if the detector is optically identical with the medium for which the absorption coefficient is to be measured [165].

The transmission $\frac{I(t)}{I_0}$ can be determined from the detector response with and without the sample interposed between source and detector.

Now, the absorption can be written as

$$a = \varepsilon C \tag{3.1.47}$$

where ε is the molar absorption coefficient of absorber and C is the concentration of the sample.

Thus, the absorbance for a liquid substance in terms of the ratio of the incident intensity I_0 and the transmitted intensity $I(t)$ is given by

$$A = Log(\frac{I_0}{I(t)}) = \varepsilon Cl \tag{3.1.48}$$

Extinction coefficient ε is the attenuation of an electromagnetic wave by an absorption as it traverses a particulate medium [166]. And, it can be related with the absornace of the system as in Eqn (3.1.48).

The Absorption Cross-Section

Absorption of light by a quantum system can be characterized by a frequency dependent absorption cross-section. Consider an excitation beam with intensity I propagating in the direction of z through a dilute sample of randomly oriented molecules. The absorption cross-section (σ), related to the absorption coefficient (a) at a single frequency for N number of molecules per unit volume can be expressed as[129]

$$a(\overline{v}) = N\sigma(\overline{v}) \tag{3.1.49}$$

However, in a UV-Vis spectrometer, the absorption of molecules in a liquid occurs over a certain range of frequencies rather than at a single frequency. Thus, integrated absorption coefficient which is the sum of absorption coefficients for all frequencies in the band can preferable in such cases [128, 167]. It is independent of line function which may be varying due to pressure, temperature, interaction of solute and solvent[129, 168], and the technique is also very important in the absence of a high-resolution spectrometer [128]. Thus, The integrated absorption coefficient (α_t) in the wavenumber from $\overline{v}$ to $(\overline{v} + d\overline{v})$ regions can be expressed by,

$$\alpha_t = \int \alpha(\overline{v}) d\overline{v} \tag{3.1.50}$$

Using Eqn (3.1.48) into (3.1.50) yields

$$\alpha_t = \frac{1}{l} \int Log(\frac{I_0}{I(t)}) d\overline{v} \tag{3.1.51}$$

Also, the integrated absorption cross-section (σ_t) is given by[129];

$$\sigma_t = \frac{1}{N} \int \alpha(\overline{v}) d\overline{v} = \frac{1}{Nl} \int Log(\frac{I_0}{I(t)}) d\overline{v} \tag{3.1.52}$$

Where, $\alpha(\overline{v})$ is absorption coefficient and N is number density of the molecules.

Oscillatory Strength

Oscillator strength which represents the average number of electrons per atom that can be excited by the incident radiation is important parameter for providing the relative strength of electron transition [169]. Oscillator strength can be found from measurements of absolute emission, absorption, dispersion, or through combined measurement techniques. The accuracy of oscillator strength in absorption measurements has rapidly improved in recent years. But, since the measurements were limited only for a few elements and ionization stages [165]. However, large number of precision measurements are required to improve the calculation of oscillator strengths.

In absorption measurements, the spectral line arising from a radiative transition between atomic states k and m can be characterized by its wavelength, intensity and shape. The intensity per atom is determined by the emission transition rate A_{km} or absorption oscillator strength f_{mk}. Precision measurements of oscillator strengths can also provide stringent tests of atomic structure calculations and experimental tests of fundamental theories such as quantum electrodynamic corrections and nonconservation of parity predicted by the unified electro-weak theory.

Consider Egn (3.1.48) with the molar absorption coefficient as a function of wavenumeber $\overline{v}$, a more accurate measure of intensity is the area under the absorption curve, i.e. $\int_{\overline{v_1}}^{\overline{v_2}} \varepsilon(\overline{v}) d\overline{v}$. If the states k and m are separated by an energy difference which is large enough for N_m to be very much less than N_k, then induced emission will be negligible compared to absorption: under these conditions the area under the absorption curve is

related to B_{km} [170, 171] by

$$\int_{\overline{v_1}}^{\overline{v_2}} \varepsilon(\overline{v}) d\overline{v} = \frac{N_a h \overline{v}_{km} B_{km}}{ln(10)} \tag{3.1.53}$$

where $\overline{v}_{km}$ is the average wavenumber of the transition and N_a is Avogadro's constants. Thus, if the absorption is due to a transition between electronic states, a quantity $f_{km} = f$, the oscillator strength of the transition [170, 171, 171], is related to the area under the curve by

$$f = \frac{(4\pi\varepsilon_0)c^2 m_e ln(10)}{\pi e^2 N_a} \int_{\overline{v_1}}^{\overline{v_2}} \varepsilon(\overline{v}) d\overline{v} \tag{3.1.54}$$

where m_e and e are the electron mass and charge respectively.

Einstein Relations

Einstein assumed a nondegenerate two-level system with the total number of atoms $N = N_k + N_m$, with an energy difference $\Delta E = h\nu = E_m - E_k$ in thermal equilibrium with its environment kept at a temperature T. Light interacts with the atoms in the system with through resonant stimulated absorption and emission. The rate of change of population of the upper state, $\frac{dN_m}{dt}$, due to induced absorption is proportional to the population N_k of the lower state and to the radiation density, $\rho(\overline{v})$,[172, 173] as

$$\frac{dN_m}{dt} = B_{km}\rho(\overline{v})N_k \tag{3.1.55}$$

where B_{km} is the Einstein coefficient for induced absorption. Similarly the change of population due to induced emission is

$$\frac{dN_m}{dt} = -B_{mk}\rho(\overline{v})N_m \tag{3.1.56}$$

And, due to spontaneous emission, is

$$\frac{dN_m}{dt} = -N_m A_{mk} \tag{3.1.57}$$

where

$$B_{km} = B_{mk} \tag{3.1.58}$$

The proportionality constants B_{mk} and $A_{mk} = \frac{1}{\tau_{mk}}$ are the **Einstein coefficients** for induced and spontaneous emission, respectively, and τ_{mk} is the natural lifetime from level m to k. These coefficients are commonly used in spectroscopic literatures to characterize light-matter interaction in atoms and molecules.

In the presence of radiation of wavenumber $\overline{v}$ all three processes are going on at once and the overall rate of change of the population of the upper state is

$$\frac{dN_m}{dt} = (N_k - N_m)B_{km}\rho(\overline{v}) - N_m A_{mk} \tag{3.1.59}$$

When the states k and m have their equilibrium Boltzmann populations, $\frac{dN_m}{dt} = 0$, and

$$(N_k - N_m)B_{km}\rho(\overline{v}) - N_m A_{mk} = 0 \tag{3.1.60}$$

N_k and N_m are related from the relation of Eq (3.1.58), and the radiation density of a black body has been shown, by applying Planck's quantum theory to the oscillators emitting the radiation, to be given by

$$\rho(\overline{v}) = 8\pi h\overline{v}^3[exp(hc\overline{v}/k_BT) - 1]^{-1} \tag{3.1.61}$$

From Eqns (3.1.58, 3.1.60 and 3.1.61) [172, 173] it follows that

$$A_{mk} = 8\pi h\overline{v}^3 B_{mk} \tag{3.1.62}$$

This equation illustrates the important point that spontaneous emission increases rapidly relative to induced emission as the wavenumber (or frequency) increases.

The relations among the Einstein coefficients, oscillatory strength, transition dipole moment, and integrated absorption coefficient for a transition between two states k (lower) and m (upper) are the most used terms in spectroscopy[129, 168]. Thus, the Einstein coefficients can be related to the integrated absorption coefficient [170, 171] as

$$A_{mk} = \frac{8\pi cln(10)}{N_a}\overline{v}^2_{max}\int \varepsilon(\overline{v})d\overline{v} \tag{3.1.63}$$

$$A_{mk} = \frac{1}{\tau_{mk}} \tag{3.1.64}$$

$$B_{km} = \frac{c\ \ ln(10)}{hN_a} \int \frac{\varepsilon(\overline{v})}{\overline{v}} d\overline{v} \tag{3.1.65}$$

3.1.4 Dipole Moment Transition

The transition dipole moment (μ_{km}) is a vector that depends on both ground state and excited state and couple the transition to the electric field of light[167, 168]. It describes the strength of the quantum-mechanical interaction of light with the sample at the atomic or molecular level. The quantum mechanical transition depends on the interaction between the electrons and the applied optical radiation field and this oscillating field interacts with the molecular dipole moment of transition states. And, from Einstein's treatment that serve as a bridge between the macroscopic Beer-Lambert relationship and the quantum mechanical microscopic transition moment, we can connect what electrons experience at the molecular scale with what we see at the laboratory scale. Thus, Einstein coefficient for absorption, B_{km}, can be related to the quantum mechanical transition moment as Eq (3.1.44)[129, 167, 168]. And, using Eqns (3.1.44 and 3.1.65) the dipole moment [170, 171] can be calculated from the integrated absorption coefficient as

$$|\overrightarrow{\mu}_{km}|^2 = \frac{(4\pi\varepsilon_0)3hc\ \ ln(10)}{8\pi^3 N_a} \int \frac{\varepsilon(\overline{v})}{\overline{v}} d\overline{v} \tag{3.1.66}$$

3.2 Fluorescence Spectroscopy

Fluorescence spectroscopy deals with the process of excitation and emission in molecular systems. It is a highly sensitive method which can detect few photons accurately, and 100-1000 times more sensitive than other molecular spectroscopic methods such as UV-Vis absorption spectroscopy[174, 175]. It is more commonly and widely used in the investigations of the structure and dynamics of molecules in complex systems [176, 177] such as fluorophores found in biological samples (coenzymes NAD(P)H and FAD, and

vitamins (A, B, D and E)) and so on [178]. This section deals with the mechanisms of fluorescence spectroscopy, the fluorescence quenching process, and the external conditions affecting fluorescence emission.

3.2.1 Mechanism of Fluorescence

The molecular phenomenon of fluorescence was first reported by Herschel in 1845 [179]. Nowadays, the principle and mechanisms of fluorescence is well understood in different disciplines, and can be stated as a process of excitation of a molecule by absorption of a photon and de-excitation of the molecule by emission of another photon with different wavelength [177]. Absorbance only deals with the transition from ground state to excited state and fluorescence involves the relaxation from excited to ground state. In view of this, the mechanism of the excitation and emission of light in fluorescent molecules can be illustrated by the energy level diagram suggested by A. Jabtonski [180] as in Fig (3.1).

The molecules can be excited to different singlet states (S_1, S_2.. etc) depending on the energy of the incident photon hv_k from the ground state S_0, and $hv_k \geq \triangle E_{S_0 \longrightarrow S_1}$ to induce the transition. Where $\triangle E_{S_0 \longrightarrow S_1}$ is the difference in energy of the ground and the first excited state. The other energy ($hv_k - \triangle E_{S_0 \longrightarrow S_1}$) of the excitation photon transfers to vibrational states of S_1 and the fluorophore can be excited by different wavelengths. At each of the electronic energy states, the molecules can exist in a number of vibrational energy levels (V_0, V_1, V_2, etc). When a fluorophore is excited to some higher vibrational excited level, of either S_1 or S_2, most of the molecules rapidly relax to the lowest vibrational level of S_1 due to the process of internal conversion. The fluorophore then releases its energy by emission of a photon (radiative decay or by non-radiative relaxation) in

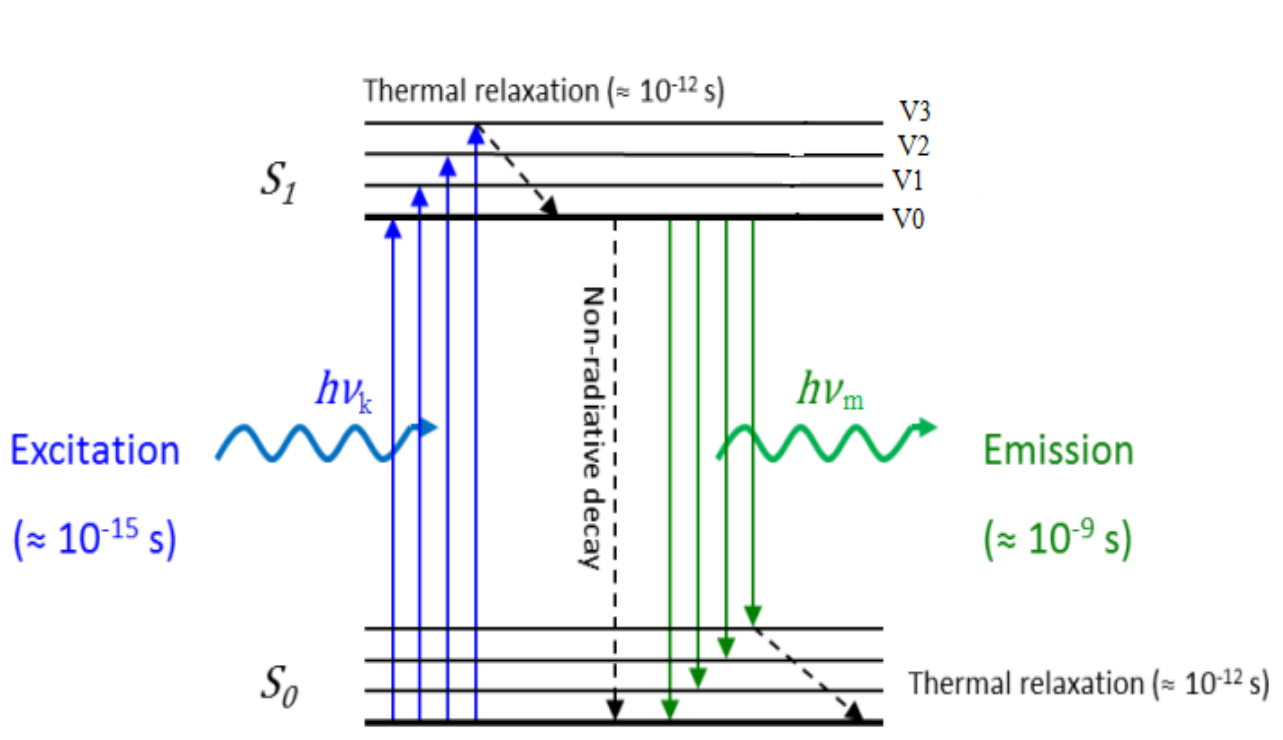

Figure 3.1: Mechanism of fluorescence spectroscopy

which the excitation energy is usually dissipated as heat (vibrations) to the solvent at specific vibrational energy levels. Energy of emitted photon $h\upsilon_m$ is independent of energy of the excitation of photon. A consequence of the thermal relaxation is that the emitted photon has always lower energy than the absorbed photon (i.e. $h\upsilon_m < h\upsilon_k$). Then, the final transition after emission can be any of the vibrational states of S_0 and emission spectrum occurs in a range of wavelength [174, 176, 181, 182]. The emitted light is always red shifted due to energy loss relative to the excitation of light [174, 176].

Emission spectrum measures at a fixed point of excitation wavelength when light is emitted in a range of wavelengths, and the same is true for excitation spectra. Most of the time, emission spectrum has only one maximum peak since it occurs from $S_1 \longrightarrow S_0$ transition, and the shape of excitation and emission spectra is often described as the mirror image rule because vibrational states in S_0 and S_1 are approximately the same repartition.

Emission spectrum from a given molecular compound (fluorophore) measured with different excitation wavelengths is only vary in intensity, but not in shape, since the shape of the emission spectrum is independent of the excitation wavelength[174, 176, 182]. .

Emission efficiency of a fluorescent molecule, also known as quantum yield Q, represents the probability of the fluorophore to lose its excitation by radiative decay. It can be the direct consequence for the existence of competition between radiative and non-radiative decays. And , it can be represented as;

$$Q = \frac{k_r}{k_r + k_{nr}} \tag{3.2.1}$$

Where k_r is the radiative decay rate and k_{nr} is the non-radiative decay rate.

3.2.2 Fluorescence Quenching

Fluorescence quenching refers to a process of decreasing the fluorescence intensity of a given substance due to various processes such as excited state reactions, energy transfer, complex formation, and dynamic (collisional) quenching. Fluorescence quenching has been studied widely in the application of fundamental phenomenon and in biochemical problems due to their favorable properties of quenching process[183, 184].

There are different types of quenching processes such as intrinsic, solvent, static and dynamic (collision) quenching. If a process of quenching is due to environmental perturbations on the competing between spontaneous decay and fluorescence transition at the vibrational levels, they are considered as intrinsic quenching processes because they are principally a function of the electronic structure of the molecule. These intrinsic quenching can be due to intersystem cross process or internal conversion [181].

It is well known fact that the fluorescence quantum efficiency of a molecule is highly dependent on the solvent in which it is dissolved. Solvent quenching occurs through the formation of an intermediate encounter complex [181, 185, 186]. Moreover, both static and dynamic quenching require molecular contact between the fluorophore and quencher.

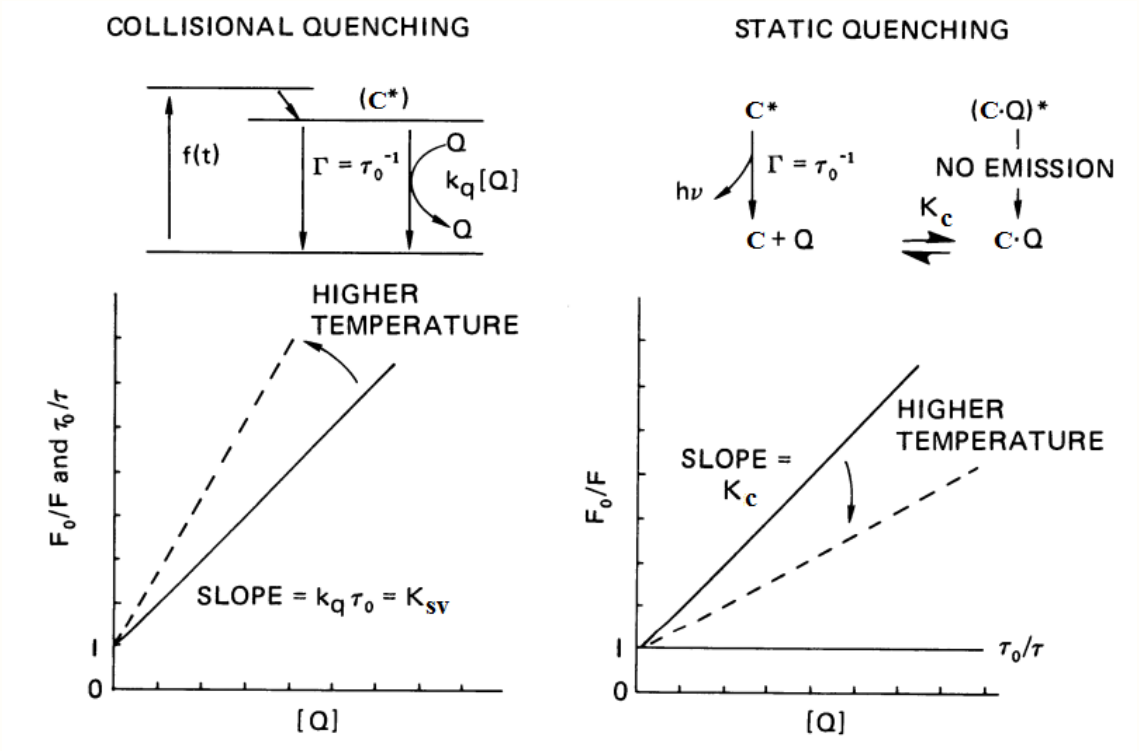

Figure 3.2: Comparison of dynamic and static quenching

Static Quenching

Static quenching occurs due to the formation of a nonfluorescent ground state complex between the fluorophore and quencher that immediately returns to the ground state without emission of a photon after absorption of radiation as shown in Fig (3.2). In this Figure, the slope of the Stern-Volmer equation (the binding constant) is linear and decreases as temperature increase. Besides, the number of the binding sites (τ_0/τ) of static quenching is approaches to unity. Changes in the absorption spectrum upon addition of quencher provides support for the static mechanism.

When molecules are bound independently to a set of equivalent sites on macromolecules, the equilibrium between free and bound molecules is given by [187]:

$$Log\frac{(F_0 - F)}{F} = LogK_C + nLog[CAF] \tag{3.2.2}$$

where K_C is the binding constant, and n is the number of binding sites per molecule.

But, static and dynamic (collision) processes can not be explained fluorescence quenching data obtained from intensity measurements alone. Additional informations such as lifetimes, temperature or viscosity dependence of quenching should be provided in order to distinguish the processes.

Dynamic (Collisional) Quenching

Collisional quenching is a diffusion controlled process which depends on the contact between a potentially fluorescent molecule in an excited state and the quencher as shown in Fig (3.2). In this figure, the slope of the Stern-Volmer equation (the binding constant) is increased as temperature increase. And, it can be described by the Stern-Volmer law [188] that can be derived by considering the fluorescence intensities observed in the absence and presence of quencher. The fluorescence intensity observed for a fluorophore is proportional to its concentration in the excited state (F^*). Under continuous illumination a constant population of excited fluorophores is established and in equilibrium $\frac{dF^*}{dt} = 0$. In the absence and presence of quencher the differential equations describing (F^*) are

$$\frac{dF^*}{dt} = f(t) - \Gamma(F^*)_0 = 0 \tag{3.2.3}$$

$$\frac{dF^*}{dt} = f(t) - [\Gamma + k_q[Q]](F^*) = 0 \tag{3.2.4}$$

where $f(t)$ is the constant excitation function, which can be easily eliminated from these equations. $\Gamma = \tau_0^{-1}$ is the decay rate of the fluorophore in the absence of quencher. Eqns (3.2.3) and (3.2.4) yield [189, 190]:

$$\frac{F_0}{F} = 1 + k_q \tau_0 [Q] = 1 + K_{SV}[Q] \tag{3.2.5}$$

which is the Stern-Volmer equation. Where F_0 is the fluorescence intensity in the absence of the quencher, F is the intensity at quencher concentration $[Q]$, k_q is the bimolecular quenching rate constant, τ_0 is the lifetime of the fluorophore in the absence of quencher, and $K_{SV} = k_q \tau_o$ is the Stern-Volmer quenching constant.

3.2.3 External Conditions Affecting Fluorescence Emission

The fluorescence signal can be affected by different factors of the environment surrounding the fluorophore such as pH, temperature, concentration and polarity. These factors can affect the emission for a given fluorophore in one way or another. The polarity of the solvent is an especially important factor since it causes a shift in the emission. In a highly polar environment, a solvent relaxation will occur that makes the dipole moment between ground and excited state smaller, and thus the energy difference between the two states will be lower [191].

At low concentration, Beer-Lamberts is also valid for fluorescence intensity. Thus, the intensity is dependent on the overall absorbance of the sample and concentration of the fluorophore. But, at high concentrations, the intensity can be affected by concentration quenching or inner filter effect. Some of the excitation or emitted light can be reabsorbed by the sample and the intensity will be quenched (decreased). This quenching effect can be reduced by reducing the absorbance of the sample [174].

3.3 Effects of Solvent Polarity on Absorption and Fluorescence Spectra

3.3.1 Solvent Effect on Absorption Spectra

When absorption spectra are measured in solvents of different polarity, it is found that the positions, intensities, and shapes of the absorption bands are usually modified by these solvents [191–194]. These modification occurs due to the physical intermolecular solute-solvent interaction forces (such as ion-dipole, dipole-dipole, dipole-induced dipole, hydrogen bonding, etc.), and arise from alteration of the chemical nature of the chromophore-containing molecules in the medium (such as proton or electron transfer between solvent and solute, solvent-dependent aggregation, ionization, or isomerization equilibria).

Therefore, solvent effects on absorption spectra can be used to provide information about solute-solvent interactions [192–194]. A qualitative interpretation of solvent shifts is possible by considering (1) the momentary transition dipole moment present during the optical absorption, (2) the difference in permanent dipole moment between the ground and excited state of the solute, (3) the change in ground-state dipole moment of the solute induced by the solvent, and (4) the Franck-Condon principle [195].

3.3.2 Solvent Effects on Fluorescence Spectra

When excited states of a molecule are created in solution, the excited-state molecule interacts to a varying degree with the surrounding solvent molecules, depending on their polarity before returning to the ground state. These interactions found in fluorescent molecules are often reflected in the spectral position and shape of the emission bands

as well as in the lifetimes of the excited-state molecules. The solvent-dependence of the position of emission bands in fluorescence spectra is commonly included in the term solvatochromism [191].

A general explanation of solvent effects on fluorescence spectra is based on the differential solvation of the fluorescent molecules (also called fluorophores) in their ground and excited states, mediated by the various non-specific and specific intermolecular forces acting between the solute and solvent [176, 196]. However, most fluorophores undergo an intramolecular charge transfer upon excitation so that usually $\mu_e > \mu_g$. In such cases, the relaxed excited state S_1 will be energetically stabilized relative to the ground state S_0 and a significant red shift of the fluorescence band will be observed. The stronger the solute/solvent interaction, the lower the energy of the excited state, and the larger the red shift of the emission band and the corresponding Stokes shift.

The fluorescence emission spectra of many fluorophores are sensitive to the polarity of their surrounding environment. If the emission spectrum of a probe is examined in solvents of varying polarity, one finds that the emission spectrum shifts to shorter wavelengths (blue shifts) as the solvent polarity is decreased. Conversely, increasing solvent polarity generally results in shifts of the emission spectrum to longer wavelengths (red shifts).

3.3.3 Stokes' Shifts and Solvent Relaxation

Emission of light from the fluorophors always occurs at a longer wavelength than those of light absorption. This phenomenon of loss of energy between absorption and emission of light is called Stokes shift [197]. This energy loss results from several dynamic processes such as dissipation of vibrational energy, redistribution of electrons in the sur-

rounding solvent molecules induced by the dipole moment of the excited fluorophore, reorientation of the solvent molecules around the excited state dipole, and specific interactions between the fluorophore and the solvent or solutes. Precise interpretation of the solvent sensitivity of fluorophores requires a detailed understanding of the effects of solvents on both the ground and excited state energy levels of fluorophores [191].

The gap between the maximum of the first absorption band and the maximum of the corresponding fluorescence band is called the Stokes shift, and is usually expressed in wavenumbers as $\Delta\overline{v} = \overline{v}_a - \overline{v}_f$. This Stokes' shift provides valuable information on the excited state. When the dipole moment of a fluorescent molecule is larger in the excited state than in the ground state (i.e. $\mu_e > \mu_g$), then the differential solvation of the two states by solvents of varying polarity gives rise to an increase in the Stokes' shift with increasing solvent polarity [176, 198–200].

Solvent effects can be divided in to general and specific effects. General solvent effects result from the refractive index and dielectric constant of the solvent molecules that reflects the freedom of motion of the electrons and the dipole moment of the solvent molecules. And, specific solvent effects are due to specific chemical interactions between the fluorophore and the solvent molecules. Both these effects can result in significant spectral shifts. Moreover, general solvent effects are always present, and specific solvent effects depend on the precise chemical structures of the solvent and the fluorophore.

3.3.4 General Solvent Effects

The physical and chemical interactions between fluorophore and solvent molecules, which are the cause of general solvent effects, can be derived as the Lippert-Mataga equation.

This equation is based on Onsager's reaction-field theory, which assumes that the fluorophore is a point dipole residing in the center of a spherical cavity with radius a in a homogeneous and isotropic dielectric with relative permittivity ε_r. It uses the interaction of the dipole moment of the fluorophore with the solvent and the time scale of the interaction. Consider a point dipole moment in a continuous dielectric medium [191]. The energy of the dipole E_{dipole} in this medium is given by

$$E_{dipole} = -\mu R \tag{3.3.1}$$

where R is the reactive field induced in the dielectric by the dipole and μ is the induced dipole moment. Since the reactive field is parallel and opposite to the direction of the dipole, it is proportional to the magnitude of μ [191] as

$$R = 2\frac{\mu}{a^3}f \tag{3.3.2}$$

where f is the polarizability which results from the mobility of electrons and dipole moments of the solvent molecules, and a is the cavity radius. Reorientation of the electrons in the solvent is essentially instantaneous, and the high frequency polarizability $f(n)$ can be determined from the refractive index n [191] as,

$$f(n) = \frac{n^2 - 1}{2n^2 + 1} \tag{3.3.3}$$

Because of the slower time scale of molecular orientation, the low-frequency polarizability $f(\varepsilon_r)$ can be determined from the dielectric constant of the solvent molecules as

$$f(\varepsilon_r) = \frac{\varepsilon_r - 1}{2\varepsilon_r + 1} \tag{3.3.4}$$

And, orientation polarizability $\triangle f(\varepsilon_r, n)$ is given by

$$\Delta f = \frac{\varepsilon_r - 1}{2\varepsilon_r + 1} - \frac{n^2 - 1}{2n^2 + 1} \tag{3.3.5}$$

If the solvent has no permanent dipole moment, $\varepsilon_r = n^2$ and $\Delta f = O$.

Moreover, the fluorophore- solvent interaction can be determined from the ground and excited state dipole moments, and reactive fields around these dipoles. The fields can be due to electronic factors (R_g^e and R_e^e) and solvent reorientation (R_g^r, and R_e^r), that are given by

$$R_g^e = \frac{2\mu_g}{a^3} f(n), \qquad R_e^e = \frac{2\mu_e}{a^3} f(n) \tag{3.3.6}$$

$$R_g^r = \frac{2\mu_g}{a^3} \Delta f, \qquad R_e^r = \frac{2\mu_e}{a^3} \Delta f \tag{3.3.7}$$

Let the fields be represented as shown in Fig (3.3) on the process of excitation and emission of light. Thus, for absorption of light, the ground energy (E_g) and excited energy (E_e) are given as

$$E_e(abs) = (E_v)_e - \mu_e R_g^r - \mu_e R_e^e \tag{3.3.8}$$

$$E_g(abs) = (E_v)_g - \mu_g R_g^r - \mu_g R_g^e \tag{3.3.9}$$

where E_v is the vapor state energy of the fluorophore unperturbed by the solvent.

Since the electrons of the solvent can follow the rapid change in electron distribution within the fluorophore, energy of absorbed light decreases by the electronic reaction field induced by the excited state dipole (R_e^e). But, the solvent molecules orientation does not change during the absorption of light. Therefore, due to the Franck-Condon principle, the effect of the orientation polarizability is given by $\mu_g R_g^r$ and $\mu_e R_g^r$, contains only the ground state orientational reaction field. Thus, subtracting Eqn (3.3.9) from (3.3.8) yields

$$\Delta E_a = hc\overline{v}_a = hc((\overline{v}_a)_v)_g - (\mu_e - \mu_g)R_g^r - \mu_e R_e^e - \mu_g R_g^e \tag{3.3.10}$$

where $hc((\overline{v}_a)_v)_g = (E_v)_{ge} - (E_v)_g$.

Similarly, the energy of the two electronic levels for emission is given by

$$E_e(em) = (E_v)_e - \mu_e R_e^r - \mu_e R_e^e \tag{3.3.11}$$

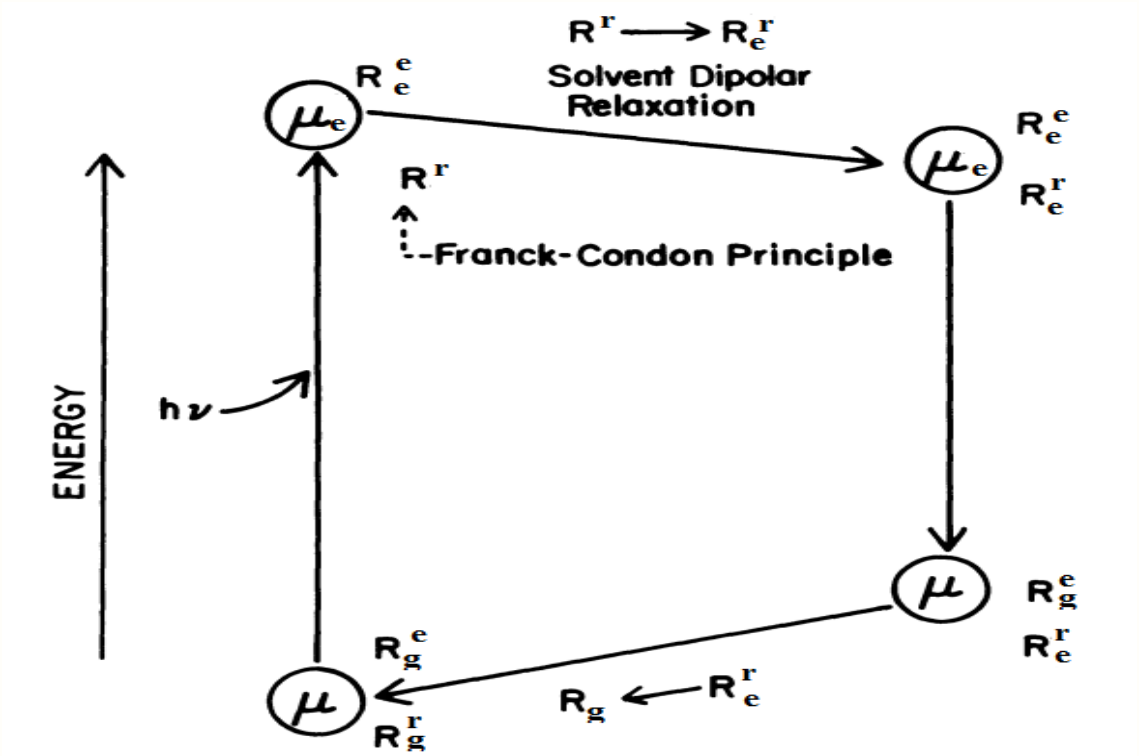

Figure 3.3: Effects of electronic and orientational reaction fields on the energy of a dipole in a dielectric medium

$$E_g(em) = (E_v)_g - \mu_g R_e^r - \mu_g R_g^e \tag{3.3.12}$$

Now, assume that the solvent relaxes quickly as compared to the lifetime of the excited state, and the initial orientation field (R_g^r) changed to R_e^r prior to emission. Thus, using Franck-Condon principle, the electronic field changed during emission with out change in the orientation field, and the frequency of emission is given by

$$hc\overline{v}_f = hc(\overline{v}_e)_v - (\mu_e - \mu_g)R_e^r - \mu_e R_e^e - \mu_g R_g^e \tag{3.3.13}$$

In the absence of environmental effects one may expect $\overline{v}_a = \overline{v}_f$ for atoms in the vapor phase, and $\overline{v}_a - \overline{v}_f$ to be a constant for complex molecules which undergo vibrational relaxation. Hence, subtracting Eqn (3.3.13) from(3.3.10) yields

$$\overline{v}_a - \overline{v}_f = \frac{1}{hc}(\mu_e - \mu_g)(R_g^r - R_e^r) + constant \tag{3.3.14}$$

Substitution from Eqn (3.3.7) yields the Lippert-Mataga equation,

$$\overline{v}_a - \overline{v}_f = \frac{2\Delta f}{hca^3}(\mu_e - \mu_g)^2 \tag{3.3.15}$$

The Lippert-Mataga equation is a completely general expression describing the Stokes shift expected for a given fluorophore in media of varying polarity. But, other alternative expression have been developed for the general solvent effects such as Bilot and Kawski [201, 202], Kawski-Chamma-Viallet [203] and Bakhshiev [204] methods as shown below.

Bilot-Kawski Method

Based on Onsager's reaction field theory which assumes a spherical structure of the molecules with in a cavity radius $'a'$ and employing the simplest quantum mechanical second order perturbation theory of absorption ($\overline{v}_a$) and fluorescence ($\overline{v}_f$) band shifts in various solvents of different relative permittivities (ε_r) and refractive indices (n), the equations for the dipole moments were derived. According to Bilot and Kawski [201, 202], the equations related to the difference and sum of wavenumbers of absorption and fluorescence are expressed as;

$$\tilde{v_a} - \tilde{v_f} = m_1 f(\varepsilon_r, n) + constant \tag{3.3.16}$$

$$\tilde{v_a} + \tilde{v_f} = -m_2 \varphi(\varepsilon_r, n) + constant \tag{3.3.17}$$

where m_1 and m_2 are slopes, and the solvent polarity parameters $f(\varepsilon_r, n)$ and $\varphi(\varepsilon_r, n) = f(\varepsilon_r, n) + 2g(n)$ [154, 205, 206] are expressed as Eqns (3.3.18 and 3.3.20), respectively.

$$f(\varepsilon_r, n) = \frac{2n^2+1}{n^2+2}\left(\frac{\varepsilon_r - 1}{\varepsilon_r + 2} - \frac{n^2-1}{n^2+2}\right) \tag{3.3.18}$$

$$g(n) = \frac{3}{2}\left(\frac{n^4-1}{(n^2+2)^2}\right) \tag{3.3.19}$$

$$\varphi(\varepsilon_r, n) = \frac{2n^2+1}{n^2+2}\left(\frac{\varepsilon_r - 1}{\varepsilon_r + 2} - \frac{n^2-1}{n^2+2}\right) + \frac{3}{2}\left(\frac{n^4-1}{(n^2+2)^2}\right) \tag{3.3.20}$$

The unknown parameters m_1 and m_2 which can be determined from the slope of the straight line of Eqns (3.3.16 and 3.3.17) are given by;

$$m_1 = \frac{2(\mu_e - \mu_g)^2}{hca^3} \tag{3.3.21}$$

and

$$m_2 = \frac{2(\mu_e^2 - \mu_g^2)}{hca^3} \tag{3.3.22}$$

Where h and c are the Planck's constant and the velocity of light in vacuum respectively; $a = (\frac{3M}{4\pi\delta N_a})^{1/3)}$ with the relative molecular mass of the solute molecules (M), the density (δ) and Avogadro's number (N_a).

Assuming the symmetry of the solute molecule remains unchanged upon electronic transition and the dipole moment states are parallel, the values of the ground and excited dipole moments from Eqns (3.3.21) and (3.3.22) can be obtained as [154, 205, 206],

$$\mu_g = \frac{|m_2 - m_1|}{2}(\frac{hca^3}{2m_1})^{\frac{1}{2}} \tag{3.3.23}$$

and

$$\frac{\mu_e}{\mu_g} = \frac{|m_1 - m_2|}{|m_2 - m_1|} \qquad for \qquad m_2 > m_1 \tag{3.3.24}$$

Lippert-Mataga, Kawski-Chamma-Viallet and Bakhshiev Methods

The electric dipole moment of polar solute polarizes the solvent so that the solute itself experiences an electric field, the reaction field, which is proportional to the solute dipole moment in the ground and excited states. Such proportionalities for the difference and sum of absorption and fluorescence maxima maximum wavenumber have been defined by following independent equations [196, 203, 204, 207] used for the estimation of ground and excited state dipole moments:

$$\overline{v}_a - \overline{v}_f = m_3 F_{L-M}(\varepsilon_r, n) + constant \tag{3.3.25}$$

$$\frac{\overline{v}_a + \overline{v}_f}{2} = -m_4 F_{K-C-V}(\varepsilon_r, n) + constant \tag{3.3.26}$$

$$\overline{v}_a - \overline{v}_f = m_5 F_B(\varepsilon_r, n) + constant \tag{3.3.27}$$

The slopes of the linear relationships m_3, m_4 and m_5 corresponding to Eqns (3.3.25-3.3.27) are given by

$$m_3 = \frac{2(\mu_e - \mu_g)^2}{hca^3} \tag{3.3.28}$$

$$m_4 = \frac{2(\mu_e^2 - \mu_g^2)}{hca^3} \tag{3.3.29}$$

and

$$m_5 = \frac{2(\mu_e - \mu_g)^2}{hca^3} \tag{3.3.30}$$

F_{L-M} [196, 207], F_{K-C-V} [203] and F_B [204] are solvent polarity functions corresponding to Lippert-Mataga, Kawski-Chamma-Viallet and Bakhshiev methods and are given as:

$$F_{L-M}(\varepsilon_r, n) = (\frac{\varepsilon_r - 1}{2\varepsilon_r + 1} - \frac{n^2 - 1}{2n^2 + 1}) \tag{3.3.31}$$

$$F_{K-C-V}(\varepsilon_r, n) = \frac{2n^2 + 1}{2(n^2 + 2)}(\frac{\varepsilon_r - 1}{\varepsilon_r + 2} - \frac{n^2 - 1}{n^2 + 2}) + \frac{3(n^4 - 1)}{2(n^2 + 2)^2} \tag{3.3.32}$$

and

$$F_B(\varepsilon_r, n) = \frac{2n^2 + 1}{n^2 + 2}(\frac{\varepsilon_r - 1}{\varepsilon_r + 2} - \frac{n^2 - 1}{n^2 + 2}) \tag{3.3.33}$$

If the fluorophore is now placed in an unknown environment, the polarity of this environment can be estimated from $\Delta\overline{v}$. Alternatively, the sensitivity of the Stokes shift to Δf can be used to estimate the change in dipole moment which occurs upon excitation. Fluorophores which have the largest changes in dipole moment upon excitation should be the most sensitive to solvent polarity.

3.3.5 Specific Solvent Effects

The general effects are determined by the electronic polarizability of the solvent (which is described by the refractive index) and the molecular polarizability (which results from

reorientation of solvent dipoles). In contrast, specific interactions are produced by one or a few neighboring molecules, and are determined by the specific chemical properties of both fluorophores and solvent [208, 209]. Specific effects can be due to hydrogen bonding, acid-base chemistry, or charge transfer interactions, to name a few.

Specific solvent-fluorophore interactions can often be identified by examining emission spectra in a variety of solvents. The presence of specific solvent-fluorophore interactions can also be identified by the dependence of the emission maxima upon solvent composition.

Chapter 4

Materials and Methods

This chapter presents the materials and methods of the thesis. The first section of this chapter presents the various chemicals, samples, and the basic components and working principles of the instruments UV-Vis-NIR spectrophotometry and FluoroMax Fluorophotometry which are used to measure the spectra of the samples. The second section of this chapter describes the methods applied on the investigations of the study. The computational and experimental procedures used to investigate, (i) the self and hetero association of the drug samples with the bioactive compounds of coffee bean, (ii) the optical transition probabilities, (iii) the thermodynamic properties and the interaction mechanisms, (iv) the binding of caffeine with nicotinamide, and (v) the solvent effect on nicotinamide solution and (vi) determination of dipole moment are presented.

4.1 Materials

4.1.1 Chemicals

For standard solution preparation a commercially bought caffeine (Evan, England), nicotinamide, neomycin sulfate, norfloxacin, ciprofloxacin and 5-caffeoylquinic(Aldrich-Sigma, Germany) were used. Moreover, to study the hetero-association, binding mechanism and the thermodynamic properties of nicotinamide and norfloxacin with the bioactive compounds, the solutions of sodium hydroxide dissolved in distilled water were used in order to have constant pH values of the solutions.

Ethanol, Methanol, Butanol, Acetonitrile bought from (Aldrich Sigma, Germany), and doubly distilled water were used as solvents with out further purification. All the solvents were of spectroscopic grade.

4.1.2 Apparatus and Instruments

Some of the basic apparatus and instruments used during the experiment are measuring cylinders, pipettes, and volumetric flasks, magnetic stirrer with hot plate, micro balance and digital balance with accuracy of 0.0001g, beakers and 1cm size of quartz cuvettes. For electronic absorption measurement of standard solutions a double monochromator UV-Vis-NIR spectrometer, Perkin Elmer Lambda 19 (Perkin Elmer, D-7770 Ueberlingen, Germany) in wavelength range of 200-500 nm was used. The instrument operated by a powerful soft ware package termed UVCSS. Similarly, for fluorescence spectra measurement FluoroMax-4 spectrofluorometer (HORIBA, USA) was used. All the instruments provide a wide range of operating mode for the instrument and they also includes comprehensive data handling and file management capabilities. The instruments are a PC-driven spectrometers. The detail working principles of these instruments are presented in the following subsections.

4.1.3 Basic Components and Experimental Set Up of UV-Vis-NIR Spectrophotometer

The basic components of double beam spectrophotometer are light sources (UV, VIS and NIR sources), monochromator (wavelength selector), focusing devices, sample cell compartment, detector and signal processor. The radiation source are deuterium lamp for the ultraviolet region and tungsten-halogen lamp for visible and near infrared region. When

measuring absorbance at the UV spectrum, the other lamp has to be turned off, and vis versa. The monochromator isolates radiant energy of desired wavelength by dispersing the beam in to its components by reflecting grating and placing the light path in a slit that lets pass only a narrow wavelength band. The focusing devices are a combination of lenses, slits, and mirrors inserted in to light path to render the light rays parallel or to isolate narrow portion of the light beam or its spectrum. The detectors are a photo sensetive materials, typically a photomultiplier tube (PMT) for UV and VIS ranges and PbS only for NIR range. When light strikes the PMT, it generates electron which passes through a series of dynode that amplify the signal several times.

Fig (4.1) shows the schematic diagram of UV-Vis-NIR Spectrophotometer. For operation in the near infrared and visible ranges, source mirror 1 reflects the radiation from tungsten-halogen lamp onto mirror 2, at the same time it blocks the radiation from deuterium lamp. Similarly for operation in the ultraviolet range, mirror 1 is raised to permit radiation from deuterium lamp to strike mirror 2. The radiation from the respective source lamp is reflected from mirror 2 via mirror 3 through an optical filter wheel assembly to mirror 4. The filter wheel is driven by a steeping motor to be in synchronization with monochromators. Depending on the wavelength of interest, the appropriate optical filter is located in the beam path to prefilter the radiation before it enters the first monochromator. From mirror 4 the radiation is reflected through the entrance slit of monochromator 1. This radiation is collimated at mirror 5 and reflected to grating table 1. Depending on the current wavelength range, the collimated radiation beam strikes either the UV/VIS grating or the NIR grating. The radiation is dispersed at the grating to produce the spectrum. The rotational position of the grating effectively selects a segment of the spectrum, reflecting this segment to mirror 5 and hence through the exit slit. The exit slit restricts the spectrum segment to a near-monochromatic radiation beam. The

exit slit of monochromator 1 serves as the entrance slit of monochromator 2. The radiation is reflected via mirror 6 to appropriate grating table 2 and hence back via mirror 6 through the exit slit mirror 7. The rational position of grating table 2 is synchronized to that of grating table 1. The radiation emerging from the exit slit exhibits high spectral purity with an extremely low stray radiation content. From mirror 7 the radiation beam is reflected via torroid mirror 8 to the chopper assembly. As the chopper rotates, a mirror segment, a window segment, and dark segment are brought alternatively into radiation beam. When a mirror segment enters the beam, radiation is reflected via mirror 9 to create the sample beam. When a window segment enters the beam the radiation passes through to mirror 10 and is then reflected to form the reference beam. When a dark segment is in the beam path, no radiation reaches the detector, permitting the detector to create the dark signal. The radiation passing alternately through the sample and reference beam is reflected by the optics of the detector assembly onto the appropriate detector.

4.1.4 Basic Components and Experimental Set-up of Spectrofluorometer

Fig (4.2), shows the basic components and experimental ste-up of FluoroMax-4 Spectrofluorometer. The basic components Spectrofluorometer (FluoroMax®-4) are light source (xenon arc-lamp), excitation and emission monocromators, sample compartment, reference (photodiode) and signal (photomultiplier tube) detectors, and instrument controller (computer). The light from continuous light source (xenon arc-lamp) is collected by an elliptical mirror 1, and then focused on the entrance slit of the excitation monochromator. The lamp housing is separated from the excitation monochromator by a quartz window in order to vent heat out of the instrument. The FluoroMax ®-4 contains Czerny-Turner monochromators that is designed using different reflective optics (such as refractive grating) to maintain high resolution over the entire spectral range, and minimize spherical aberrations and re-diffraction. A grating disperses the incident light by means of its verti-

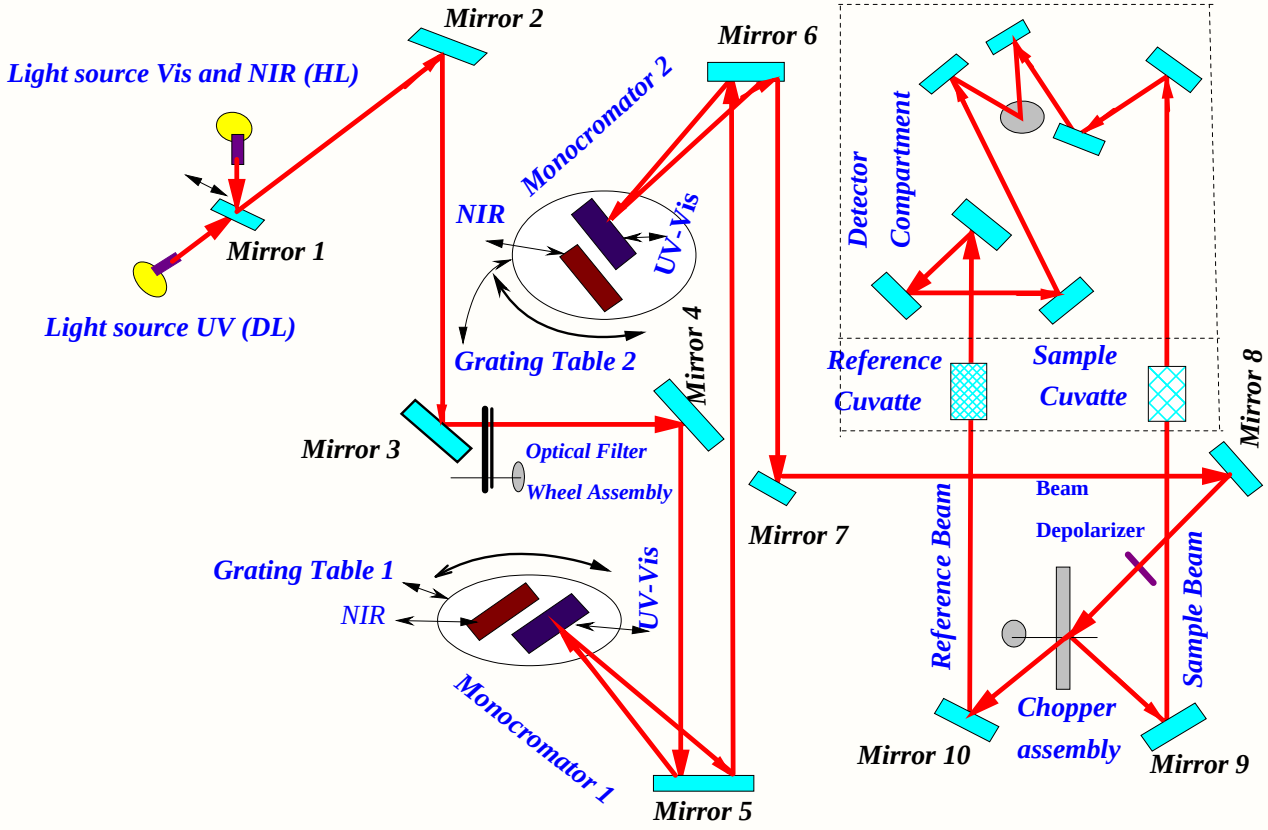

Figure 4.1: The schematic diagram of UV-Vis-NIR spectrophotometer

cal grooves. A spectrum is obtained by rotating the gratings, and recording the intensity values at each wavelength. The wavelengths selected are optimal for excitation in the UV and visible, and for emission in the high-UV to near-IR. Each grating is coated with $MgF2$ for protection against oxidation.

The entrance and exit ports of each monochromator have continuously adjustable slits controlled by FluorEssence^{TM}. The width of the slits on the excitation monochromator determines the bandpass of light incident on the sample. The emission monochromator's slits control the intensity of the fluorescence signal recorded by the signal detector. An excitation shutter, standard on the FluoroMax®-4, is located just after the excitation monochromator's exit slit. The shutter protects samples from photobleaching or photodegradation from prolonged exposure to the light source.

A toroidal mirror focuses the beam from the excitation monochromator on the sample. About 8% of this excitation light is split off, using a beam-splitter, to the reference photodiode. Fluorescence from the sample is then collected and directed to the emission spectrometer. The sample compartment accommodates various optional accessories, as well as fiberoptic bundles to take the excitation beam to a remote sample, and return the emission beam to the emission monochromator.

The signal detector is a photomultiplier tube, which sends the signal to a photoncounting module. The reference detector monitors the xenon lamp, in order to correct for wavelength- and time-dependent output of the lamp. Both the reference and signal detectors have correction-factor files run for them, to correct for wavelength dependencies of each optical component. And, the data's are processed through the host computer with FluorEssence^{TM} software.

4.2 Methods

4.2.1 Self-Association of the Drug Compounds

The self-association of the drugs (NIC, NOMS, NOR and CIP) was studied using UV-Vis spectroscopy at room temperature of 293, 293, 295 and 295K respectively. The experimental method applied to study the self-association of the drugs is based on the change in the shape of the spectrum and shift in maximum absorbance of the species. The analyzed spectra were obtained by subtracting the spectrum of pure solvent from that of the solution containing the compounds. The self-association of NIC, NOMS, NOR and CIP was studied over the concentration range of $(1.0555 - 2.234) \times 10^{-4}M$, $(1.65 - 3.1) \times 10^{-2}M$, $(7.33 - 9.807) \times 10^{-5}M$and $(3.122 - 7.148) \times 10^{-4}M$ respectively. All solutions were made using doubly distilled water. The solutions were stored in the dark to avoid photo

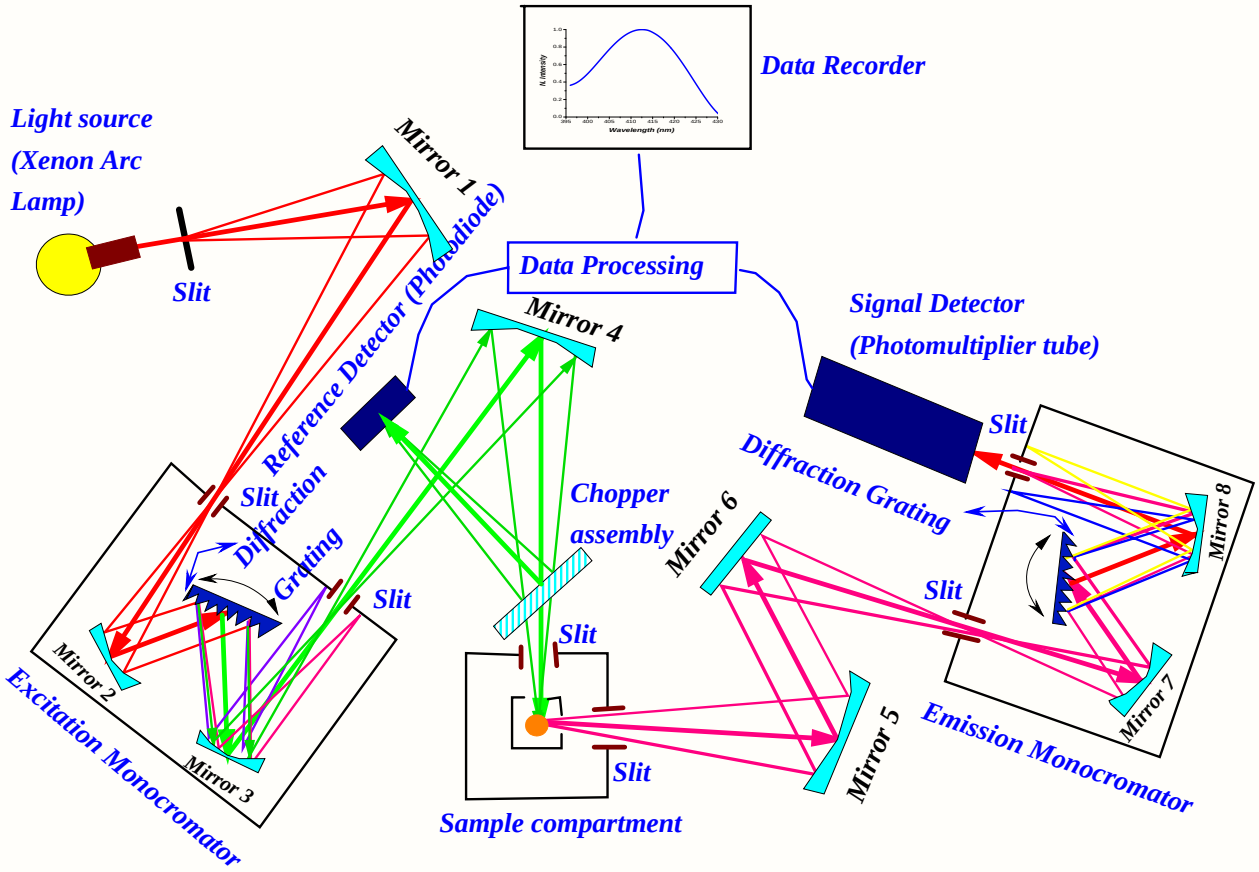

Figure 4.2: The schematic diagram of FluoroMax-4 spectrofluorometer

degradation of the compounds. The absorbance as a function of concentration was measured at absorption maxima 261.6nm, 304.8nm, 272.8nm and 272.8nm for NIC, NOMS, NOR and CIP respectively to obtain the greatest accuracy of detection.

For numerical analysis of the self association, the dimer model Eqn (4.2.1) was used to fit the experimental data. Dimer model equation can be derived by considering a molecular equilibrium in a solutions as in appendix (A.1) [153, 210].

$$\varepsilon = \varepsilon_d + (\varepsilon_d - \varepsilon_m)\frac{1 - \sqrt{8[C_0]K_C + 1}}{4[C_0]K_C} \tag{4.2.1}$$

The non-linear curve fitting based on Levenberg-Marquardt algorithm was used using origin 8 software. The molar extinction coefficients and equilibrium constant were used as searching parameters, in order to achieve minimum discrepancy between the experi-

mental data and theoretical values.

4.2.2 Hetero-Association of Nicotinamide with Chlorogenic Acid and Norfloxacin with Caffeine

The complexes of nicotinamide with chlorogenic acid and norfloxacin with cafffeine was studied using UV-Vis spectroscopy at temperatures of 293 and 295K respectively. The analyzed spectra were obtained by subtracting the spectrum of pure solvent from that of the solution containing the compounds. For the hetero-association of nicotinamide with chlorogenic acid, the constant nicotinamide concentration ($8.49 \times 10^{-5}M$) was titrated with chlorogenic acid solution in a concentration range of $(1.196 - 1.221) \times 10^{-4}M$. And also, for the hetero-association of norfloxacin with caffeine, the constant concentration of norfloxacin ($3.192 \times 10^{-5}M$) was titrated with caffeine solution in a concentration range of $(3.509 - 12.87) \times 10^{-5}M$. All solutions were made using doubly distilled water. The solutions were stored in the dark to avoid photo degradation of the compounds.

The numerical values of the association constant and molar extinction coefficient of the complexes at their maximum wavelength was analysed using the Bensi-Hildebrand approach by a linear curve fitting for the experimental data with that of the experimental values of Eqn (4.2.2). Bensi-Hildebrand equation can be derived by considering a molecular equilibrium in a solutions as in appendix (A.2).

$$\frac{[D_0]}{A} = \frac{1}{\varepsilon} + \frac{1}{\varepsilon K_E}\frac{1}{[C_0]} \tag{4.2.2}$$

The plot of $\frac{[D_0]}{A}$ vs $\frac{1}{[C_0]}$ gives a straight line with y-intercept $\frac{1}{\varepsilon}$ and slope $\frac{1}{\varepsilon K_E}$.

4.2.3 Thermodynamic Properties of the Drugs and their Complexes with Bioactive Compounds of Coffee Beans

In order to characterize the interaction mechanisms of the self and hetero-association of the drugs, the thermodynamic properties were investigated using UV-Vis spectroscopy. Accordingly, the thermodynamic parameters (molar enthalpy change, Gibbs free energy change and entropy change) of the NIC, NOMS, NOR, CIP, NIC-CGA and NOR-CAF were studied in the temperature ranges $(293-299)$, $(295-312)$, $(295-304)$, $(295-304)$, $(293-299)$ and $(295-304)K$, respectively. The thermodynamic parameters at the given temperature have been determined using the model of Vant's Hoff's Eqn (4.2.6) by linear curve fitting for the experimental data with that of the theoretical values. The magnitude of the enthalpy was estimated from the slope of the approximating line according to Vant's Hoff's equation:

$$\frac{dlnK_C}{d(\frac{1}{T})} = -\frac{\Delta H}{R} \tag{4.2.3}$$

where ΔH is the molar enthalpy change, $R = 8.31 J.mol^{-1}.K^{-1}$ is the universal gas constant and T is the temperature in Kelvin. The entropy was derived from Gibb's free energy and enthalpy. The change Gibb's free energy and entropy can be expressed as:

$$\Delta G = -RTln(K_C) \tag{4.2.4}$$

$$\Delta S = -\frac{\Delta G - \Delta H}{T} \tag{4.2.5}$$

Finally, the Vant's Hoff's equation can be written as

$$lnK_C = \frac{\Delta S}{R} - \frac{\Delta H}{R}\frac{1}{T} \tag{4.2.6}$$

Plots of lnK_C versus $\frac{1}{T}$ gives a straight line, whose slope and intercept can be used to determine ΔS and ΔH, and Gibb's free energy can be determined at a specific temperature using Eqn (4.2.5).

4.2.4 Optical Transition Properties of the Drug Compounds

The optical transition probabilities for pure compound of NIC, NOMS, NOR and CIP were studied at the concentration of $(1.0555 - 2.234) \times 10^{-4}M$, $(1.65 - 3.1) \times 10^{-2}M$, $(7.33 - 9.807) \times 10^{-5}M$and $(3.122 - 7.148) \times 10^{-4}M$ respectively. All solutions were made using doubly distilled water. The solutions were stored in the dark to avoid photo degradation of the compounds. These optical transition probabilities were measured by integrating the absorption coefficient and molar decadic absorption coefficients in the wave number regions around their corresponding maximum absorption wavenumber. Usually the UV-Vis spectrometer measures the concentration in terms of absorbance versus wavelength; this was recalculated into absorption coefficient or molar decadic absorption coefficient versus wave number using Origin 8 software. The analyzed spectra were obtained by subtracting the spectrum of pure solvent from that of the solution containing the compounds. Finally, the average of the optical transition probabilities were calculated respectively.

The integrated absorption technique which is more powerful in measuring the intensity of absorption light has been used to calculate the optical transition probabilities (transition dipole moment, oscillator strength, integrated absorption cross-section and Einstein coefficients). The molar decadic absorption coefficient which represents the ability of a molecule to absorb light in a given solvent at a given wavelength was calculated using Beer-Lambert's law of Eqn (3.1.48). And, the integrated absorption coefficient (α_t) which is the sum of absorption coefficient for all frequencies, and the integrated absorption cross-section (σ_t) were calculated using Eqn (3.1.50 and 3.1.52) respectively. Besides, the oscillator strength and the transition dipole moment (μ_{km}) were determined using Eqns (3.1.54 and 3.1.66) respectively. Moreover, the Einstein coefficients (A and B), the

transition time of the compounds were calculated using Eqn (3.1.63, 3.1.65 and 3.1.64) respectively.

4.2.5 Binding of Caffeine with Nicotinamide using Fluorescence Quenching and UV/Vis Spectroscopic Techniques

Stock solutions of NIC $(1.25 \times 10^{-3}M)$ were prepared in sodium phosphate buffer solution for stead-state fluorescence and UV/Vis absorption measurements. The stock solution of CAF $(1.287 \times 10^{-3}M)$ was prepared in doubly distilled water. The fluorescence and UV-Vis spectra measurements were carried out by successive addition of CAF $((2.925 - 9.365) \times 10^{-5}M)$ to a fixed amount of NIC $(2.841 \times 10^{-5}M)$ solution. The spectra of these series of solutions containing different amounts of CAF and definite amounts of NIC were obtained. The excitation wavelengths for NIC $\lambda_{ex} = 250nm$, and their corresponding emission was recorded over a range of $300 - 500nm$. From the fluorescence emission spectral analysis, the quenching rate constant (K_q), Stern-Volmer constant (K_{sv}) were determined using Eqn (3.2.5) at 295 and 303K. Besides, the values of binding constant (K_C) and the number of sites (n) were determined from the slope and intercept of the linear fit of eqn (3.2.2) to the experimental data of the compounds. Moreover, the thermodynamic properties of the interactions were determined at the temperature of 295 and $303K$ using Vant's Hoff's Eqn (4.2.6).

Similarly, the UV-Vis absorption spectra were measured in the range of wavelengths $200 - 500nm$ at a concentration of $((2.01 - 1.897) \times 10^{-5}M)$ to a fixed amount of NIC $(2.275 \times 10^{-5}M)$. This method was used to confirm the binding mechanism obtained from fluorescence analysis of the compounds based on the spectral change.

4.2.6 Effects of Solvent Polarity on Absorption and Fluorescence Spectra and Determination of Dipole Moments of Nicotinamide

The stock solution of nicotinamide were prepared in the solvents water, methanol, ethanol, acetonitrile and butanol at room tempreture 295K. The absorption spectra were recorded in the wavelength regions $200 - 500nm$. The emission spectra were recorded by exciting the sample at the wavelength of $250nm$. The absorption and emission measurements were performed at room temperature keeping the concentration of the molecule very low (<1 a.u), for the fluorescence spectra measurement. The solvent polarity functions were calculated from the dielectric constant and refractive index of the solvents as in table (5.9). The ground and excited dipole moments of NIC were calculated experimentally using the solvent polarity functions and the Stokes' shift of the absorption and emission spectra of NIC in different polar solvents from Bilot and Kawski, Lippert-Mutaga, Kawski-Chamma-Viallet and Bakhshiev methods of eqns (3.3.16, 3.3.17, 3.3.25, 3.3.26 and 3.3.27) respectively.

Ground-and excited-state dipole moments of NIC were also theoretically calculated using the Gaussian 09 program and analysed with the help of Gauss view software [211]. The optimized geometries of ground states were provided using DFT model employing the hybrid Becke3-Lee-Yang-Parr (B3LYP) functional with a $6 - 311 + +G^{**}$ basis set. Vertical energies of the singlet excited state were calculated using time-dependent density functional (TD-DFT) method at the $B3LYP/6 - 311 + +G^{**}$ level. In addition, the parameters that are very important in quantum chemistry called $HOMO - LUMO$ energy gaps of the compound which reflect the chemical activity of the molecules were also determined from the Gaussian 09 software.

Chapter 5

Results and Discussion

In this chapter the results and discussion of the thesis are presented. The first section of this chapter deals with the concentration dependency of the self association of the drug compounds (NIC, NOMS, NOR and CIP) using the known dimer model. In this section, the absorption spectral, dimerization constant, monomer and dimer extinction coefficients of the drugs are determined. The variations of mole fraction of monomer and of dimer with concentration of the drugs are characterized and compared to the results of the self-association in order to indicate the concentration dependency of the dimerization.

The second section deals with the investigation of the hetero-association of nicotinamide and norfloxacin with the biologically active compounds of coffee beans chlorogenic acid and caffeine respectively using the Bensi-Hildebrand approach. In this section, we described the equilibrium constant and the molar extinction coefficient of the interaction of the compounds.

The third section of this chapter deals with the calculations of the thermodynamic parameters (the molar enthalpy change, entropy change and Gibb's free energy change) of NIC, NOMS, NOR, CIP, NIC-CGA, and NOR-CAF interactions using Vant's Hoff's equation. These parameters are used to characterize the force between the molecules and for confirming the binding mode of the compounds.

The fourth section of this chapter contains the calculation of the optical transition probabilities of NIC, NOMS, NOR and CIP. The integrated absorption coefficient, integrated absorption cross-section, oscillator strength, transition dipole moments and the Einstein coefficients are calculated from the absorption spectra that may help in order to characterize the strength of the electron transition, the strength of the quantum mechanical interaction of light with the sample, and interpret the absorption spectra at atomic or molecular level of the samples.

In the fifth section of this chapter we describe (i) the binding interaction of nicotinamide with the biologically active compound of coffee beans using UV-Vis and fluorescence quenching spectroscopy (ii) the investigation of the quenching constant and binding mechanism of the interaction in order to understand the binding reaction mechanism of the compounds.

The last section of this chapter describes the solvent polarity effect on the absorption and fluorescence spectra of nicotinamide. The absorption and emission spectral nature of the compound in the different solvents are characterized. Also, the ground and excited dipole moments of NIC obtained experimentally are compared with theoretically calculated values. These parameters are important to provide information about the change electronic distribution of the ground and excited state molecules.

5.1 Self-Association of the Drug Compounds

Self-association of molecules in a solution is a dimerization of molecules to form and aggregate dimer or higher molecular weight forms [212, 213]. Two monomer molecules

may self-associate to form a dimer. Understanding the factors governing the self-association such as the concentration effect in the solution and the kinetics of the self-association reaction are crucial to the development of a robust manufacturing process and pharmaceutical products [212]. Moreover, the existence of self-association of the compounds may modify the pharmacokinetic properties of the compound. In this study, we investigated the self association of different drug compounds (NIC, NOMS, NOR and CIP).

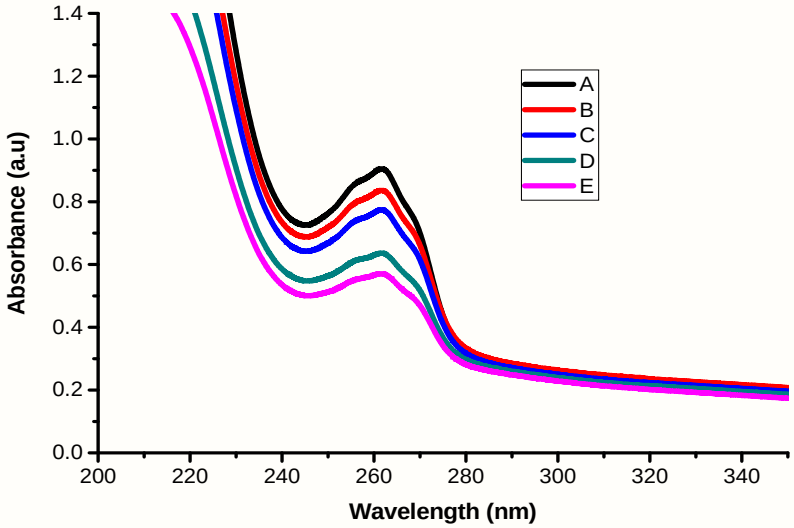

Figure 5.1: Absorbance of nicotinamide with wavelength at various concentration A-E $(2.234, 1.948, 1.656, 1.358, 1.0555) \times 10^{-4} M$

Figs (5.1, 5.2, 5.3 and 5.4) shows the concentration dependence absorption spectra of NIC, NOMS, NOR and CIP measured in doubly distilled water at room temperature with an absorption peak observed at the wavelength 261.6, 304.8, 272.8 and 272.8 nm respectively. The quantitative analysis for self-association of the drug compounds was carried out using the concentration dependent molar extinction coefficient of the molecules at their maximum wavelength. In these figures, the absorbance of all the drug compounds was increased as the concentration increases. It also reflects that the absorption spectra

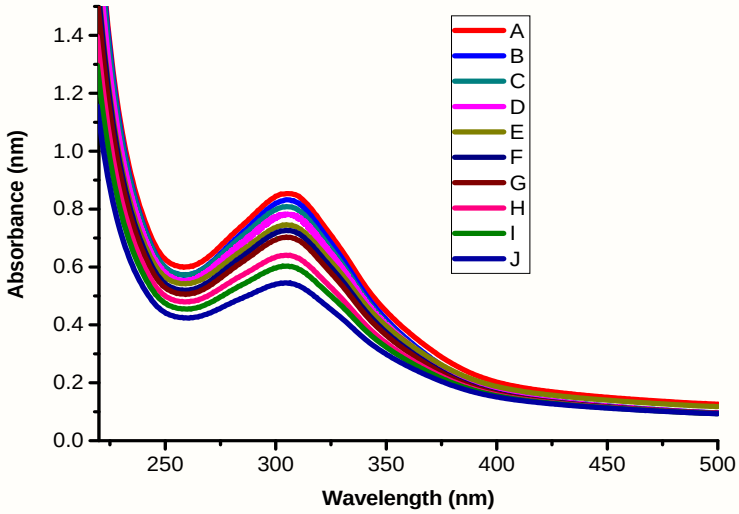

Figure 5.2: Absorbance of neomycin sulfate with wavelength at various concentration J-A $(1.65, 1.95, 2.2, 2.4, 2.56, 2.71, 2.83, 2.93, 3.025, 3.1) \times 10^{-2} M$

of NOMS shows a broad absorption peak as shown in Fig (5.2) and CIP shows a sharp peak as shown in Fig (5.4) as compared to NIC and NOR. From these spectra's we expect that the molecules of CIP are the most sensitive to the UV-Vis light absorption and the molecules of NOMS are less sensitive to absorption as compared to the absorption of the other drugs. Moreover, as we observe in Fig (5.4 and 5.3), the molecules of NOR and CIP have the same structure. Thus, from these compounds we expect that their self-associtition, thermodynamic properties and optical transition probabilities are comparable.

For the numerical analysis of the self-association parameters (the molar monomer extinction coefficients ε_m, molar dimer extinction coefficients ε_d, and equilibrium mole fraction of the molecules K_C), Dimer model Eqn (4.2.1) was fitted to the experimental data as shown in Figs (5.5, 5.6 5.7, and 5.8) respectively for NIC, NOMS, NOR and CIP. And, the obtained values of the dimerization constants, monomer extinction coefficient and dimer

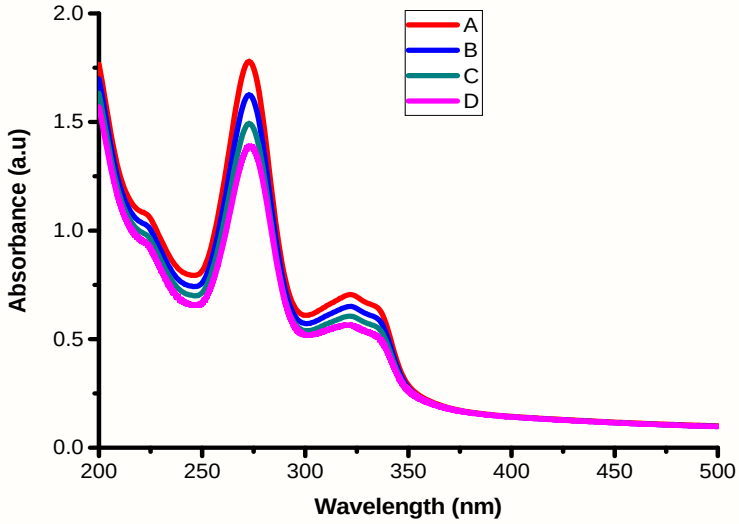

Figure 5.3: UV-Vis absorption spectrum of norfloxacin with wavelength at various concentration D-A $(7.33, 8.171, 8.996, 9.807) \times 10^{-5}M$

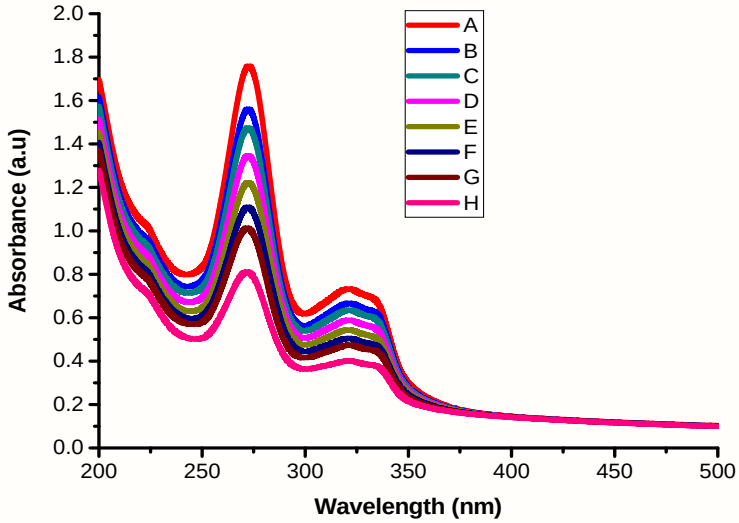

Figure 5.4: UV-Vis absorption spectrum of ciprofloxacin with wavelength at various concentration H-A $(3.122, 3.72, 4.311, 4.894, 5.469, 6.036, 6.596, 7.148) \times 10^{-5}M$

extinction coefficient of the drug compounds are listed in table 5.1 at their peak wavelengths. The deviation of the Beer-Lambert's law at high concentration and dependence on concentration, suggest the existence of self-association process of the drug molecules [153, 214].

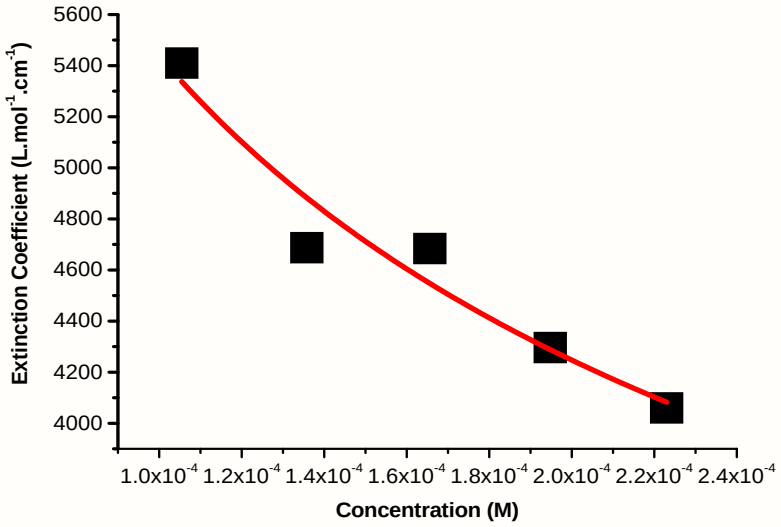

Figure 5.5: Molar extinction coefficient versus concentration of NIC under the peak of 261.6*nm*

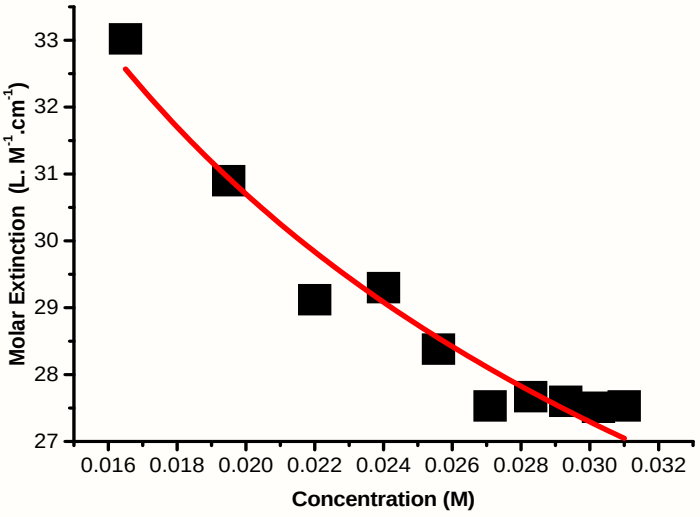

Figure 5.6: Molar extinction coefficient vs concentration of NOMS absorption maxima of 304.8*nm*

As previously reported by Kulkarni [215]using Raman and IR spectral analysis, the molecules of nicotinamide makes a dimerization in the amide-amide homosynthons (head-to-head dimers), and makes a chain on the amide-pyridine group (head-to-tail chains). It is also reported using NMR analysis that the monosubstituted analogue indicated that the

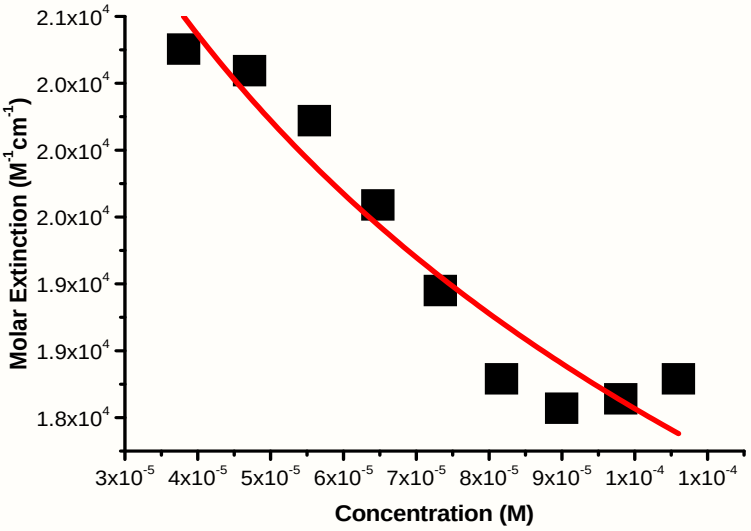

Figure 5.7: Molar extinction coefficient vs concentration of NOR absorption maxima of 272.8nm

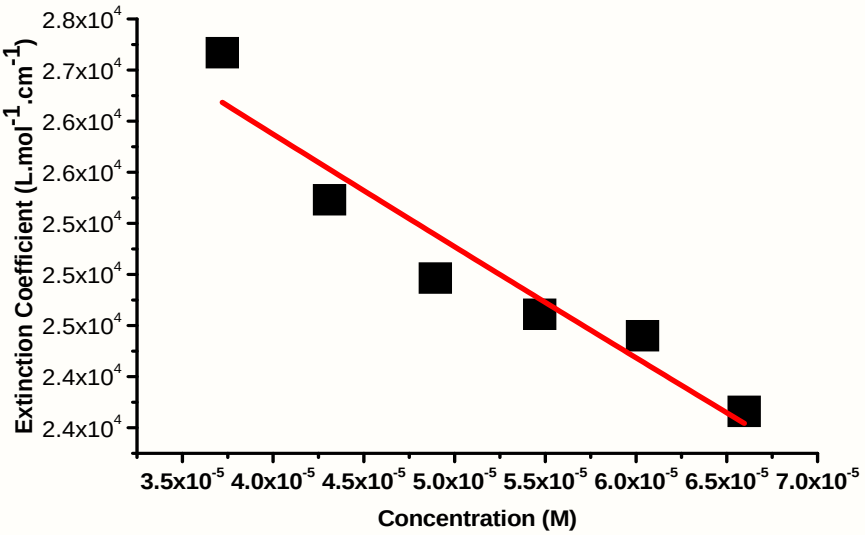

Figure 5.8: Molar extinction coefficient vs concentration of CIP absorption maxima of 272.8nm

self-association of nicotinamide molecules involved the amide group and did not occur through stacking of the pyridine rings[216, 217]. Moreover, our result for the self association constant of nicotinamide of $2.379 \times 10^4 M^{-1}$ is in a good agreement and comparable with the values reported by Peral [218] for self-association constants of $10^3 - 10^7 M^{-1}$ for pyridine derivatives in aqueous solution at $25^0 C$.

On the other hand, the obtained self-association constant (1.06×10^5) value of NOMS in our result is quite reasonable and comparable with the results obtained by Kaplan et al [219] in the dimerization range $(1.2 \times 10^4 - 4.34 \times 10^5)M^{-1}$ for aminoglycoside drug groups. Moreover, it is found Table (5.1) that the magnitude of the self-association constant of NOR and CIP is of the same order of magnitude ($10^2 - 10^3 M^{-1}$) as those found previously by Davis et. al., [220] for molecules with three fused aromatic rings.

Drugs	λ_{max}/nm	$\varepsilon_d/M^{-1}.cm^{-1}$	$\varepsilon_m/M^{-1}.cm^{-1}$	K_C/M^{-1}
NIC	261.6	5.740×10^2	1.389×10^4	2.379×10^4
NOMS	304.8	1.202×10^1	1.239×10^3	1.060×10^5
NOR	272.8	6.770×10^3	2.547×10^4	5.424×10^3
CIP	272.8	8.805×10^3	3.054×10^4	4.377×10^3

Table 5.1: Determined values of the self association parameters of NIC, NOMS, NOR and CIP

Figs (5.9, 5.10, 5.11 and 5.12) shows the mole fraction of monomer and dimer versus concentration of NIC, NOMS, NOR and CIP molecules under the peak of 261.6, 304.8, 272.8 and 272.8nm . The graphs show increase and decrease in the mole fraction of dimer and monomer as the concentrations of the drugs are increased and it indicates the presence of dimerization at low concentration and more favoured at high concentration of the drug compounds. Moreover, NOMS in water have observed less dimer molecules as shown in Fig (5.10) and CIP has highest dimer molecules as shown in Fig (5.12)at low concentration as compared to the other drug compounds. Besides, it has been reported previously that the dimerization of nicotinamide is favourable at high concentrations due to the amide group [217]. Thus, our observations are in conformity with the earlier workers.

From the results of the self association of the drug compounds, we can compare the parameters with their concentration. The concentration of the drugs and their dimerization

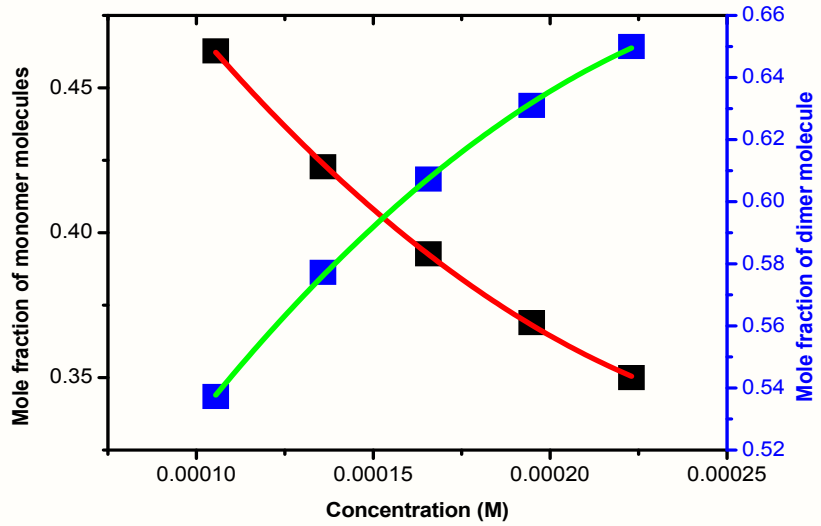

Figure 5.9: The mole fraction of monomer and dimer versus total concentration of NIC under the peak of 261.6*nm*

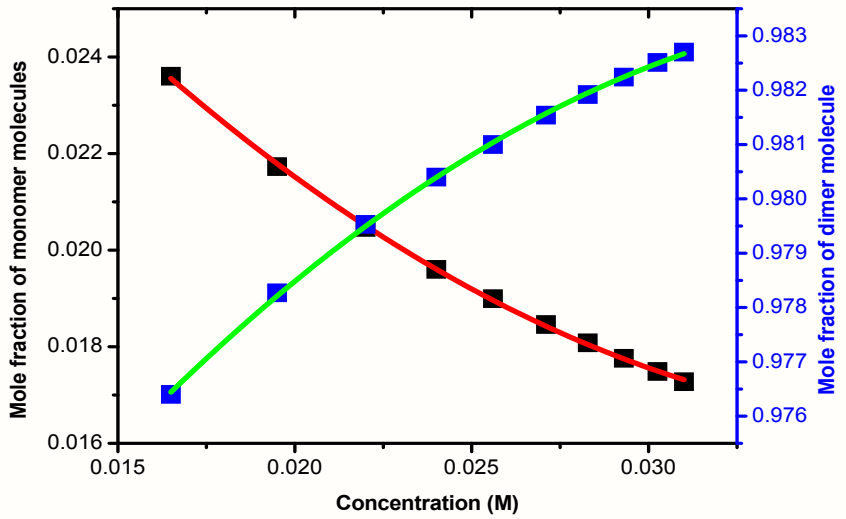

Figure 5.10: The mole fraction of monomer and dimer versus total concentration of neomycin sulfate under the peak of 304.8*nm*

constant can be arranged in descending order as NOMS-NIC-NOR-CIP (i.e NOMS>NIC>NOR>CIP) But, the monomer and dimer extinction coefficient were follow ascending order with their concentration. Thus, we can conclude that CIP molecules are the most sensitive to the UV-Vis light absorption as compared to the absorption of the other drugs.

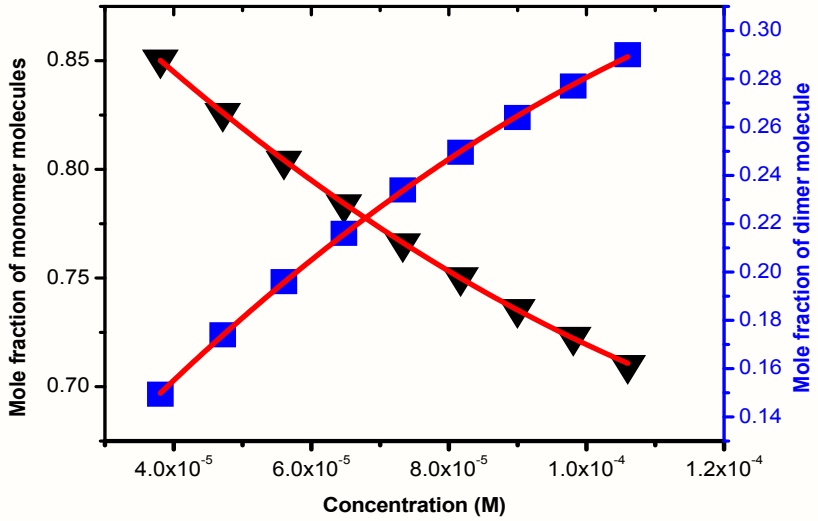

Figure 5.11: The mole fraction of monomer and dimer versus total concentration of NOR under the peak of 272.8nm

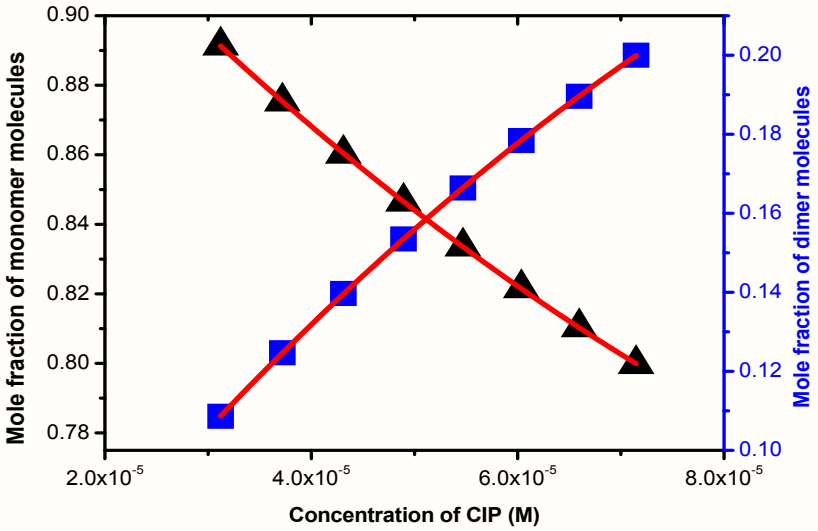

Figure 5.12: The mole fraction of monomer and dimer versus total concentration of CIP under the peak of 272.8nm

5.2 Hetero-Association of Nicotinamide with Chlorogenic Acid and Norfloxacin with Caffeine

The mathematical approach used in physical chemistry for the determination of equilibrium constant called Benesi-Hildebrand approach was used to estimate equilibrium con-

stant for the interaction of nicotinamide with chlorogenic acid and norfloxacin with caffeine [221], under the condition $[C_0] >> [D_0]$. A constant of nicotnamide/norfloxacin solution ($[D_0] = 8.49 \times 10^{-5}M/3.192 \times 10^{-5}M$) with different concentrations range ($[C_0] = (1.24 - 1.196) \times 10^{-4}M/(3.509 - 12.87) \times 10^{-5}M$) of chlorogenic acid/caffeine solutions were used to calculate the equilibrium constant and molar extinction coefficient of the interaction formation. When a chromophoric precursor is converted to product with different spectrums, an isosbestic point is observed in overlaid spectra. In more complex reactions, the wavelength of isosbestic also changes if the molar absorptivity of the precursor changes and the fraction of the precursor converted to multiple product changes[214].

Figs (5.13 and 5.14) shows the effects of CGA/CAF concentration on the UV-Vis absorption spectra of NIC/NOR solutions respectively. The addition of CGA/CAF to NIC/NOR solutions results in important spectral modification and increasing in absorbance (hyperchromic shift) were observed. As shown in Fig (5.13), the absorbance of NIC increases when CGA is added to the NIC solution. Moreover, the existences of isosbestic points were observed at wavelength of about 258 and 265nm of the interaction which indicates the formation of complexes between CGA with NIC [222].

Fig (5.14) shows that the peak absorbance of NOR increases as the concentration of CAF increase. Moreover, the existences of isobestic points at wavelength around 302nm indicate the formation of complexes between NOR and CAF and the presence of one different molecule in the solution[222]. The variation in spectral intensities and presence of isosbestic point is a good indication of the interaction between NOR and CAF, and formation of a NOR-CAF complex in aqueous solution[214]. The interaction of NOR with CAF as reported previously [223] using NMR shows that the aggregation of NOR molecules and association with CAF in solution are driven by the stacking of aromatic chromophores.

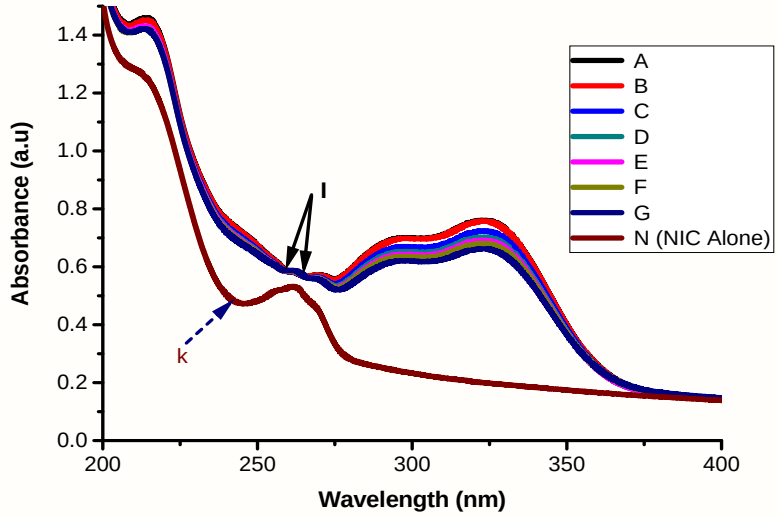

Figure 5.13: UV-Vis absorption spectrum of NIC-CGA at different concentration of chlorogenic acid A-G $((1.24 - 1.196) \times 10^{-4}M)$ and NIC $(8.49 \times 10^{-5}M = constant)$, N is the spectra of NIC alone and I is the isosbetic points

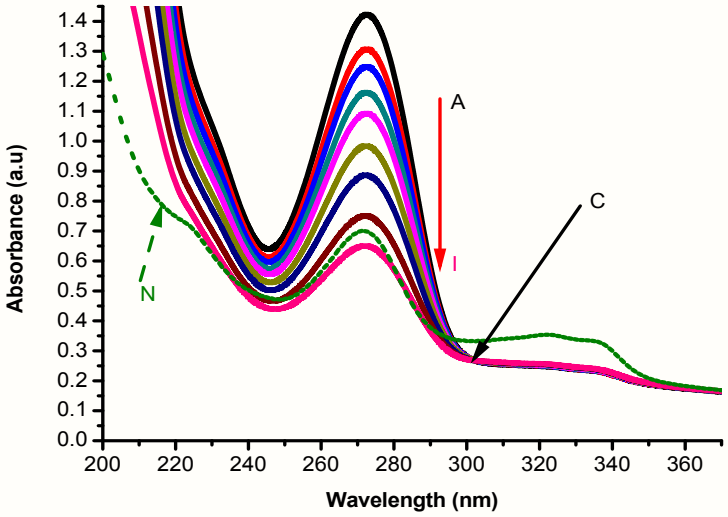

Figure 5.14: UV-Vis absorption spectrum of NOR-CAF at different concentration of CAF A-I $((3.509 - 12.87) \times 10^{-5}M)$ and NOR $(3.192 \times 10^{-5}M = constant)$, N is the spectra of NOR alone and C is the isosbetic point

In order to analyse hetero-association parameters, the Benesi-Hildebrand equation was used [224]. From Eqn (4.2.2), the plot of $\frac{[D_0]}{A}$ vs $\frac{1}{[C_0]}$ gives a straight line with y-intercept $\frac{1}{\varepsilon}$ and slope $\frac{1}{\varepsilon K_E}$ as shown in Fig (5.15) and (5.16). Thus, the equilibrium constant and molar absorption extinction coefficient can be calculated by fitting Eqn (4.2.2) to experimental

data of Fig (5.15) and (5.16). The results are given in table (5.2).

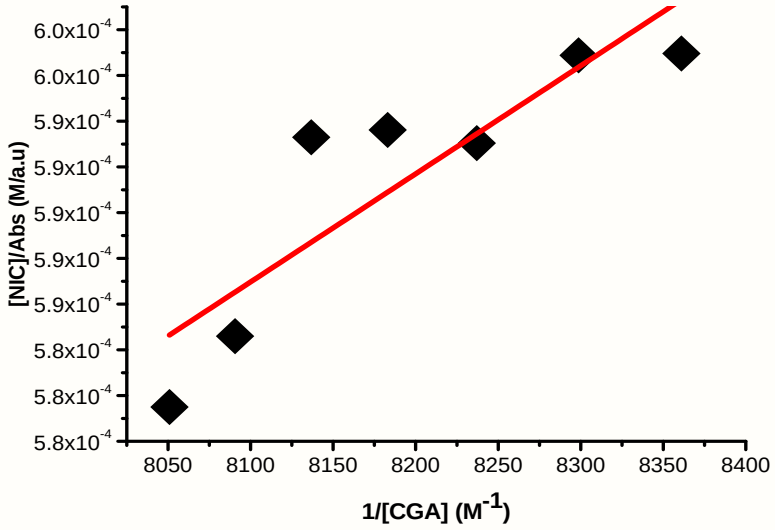

Figure 5.15: Concentration of NIC/Abs versus 1/concentration of CGA at $\lambda_{max}213.6nm$

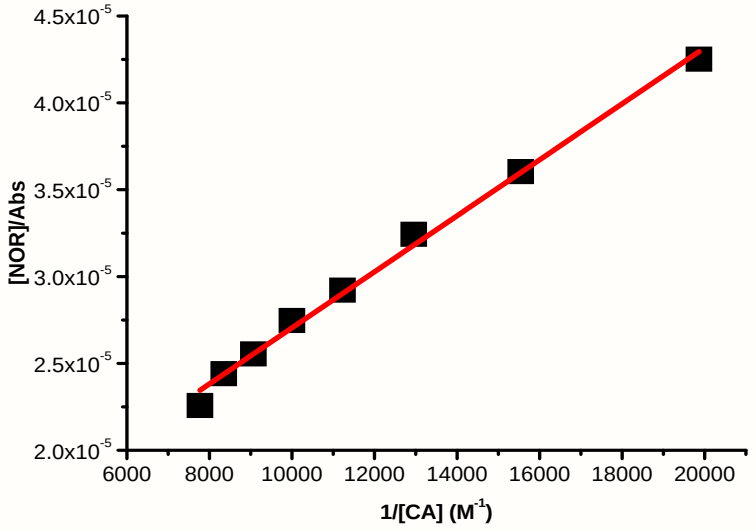

Figure 5.16: Concentration of NOR/Abs versus 1/concentration of CAF at $\lambda_{max}272.8nm$

Compounds	λ_{max}/nm	K_E/M^{-1}	$\varepsilon/M^{-1}.cm^{-1}$
NIC+CGA	213.6	4.3135×10^3	4.903×10^3
NOR+CAF	272.8	6.6700×10^3	9.259×10^4

Table 5.2: Calculated values of the hetero-association parameters of NIC+CGA and NOR+CAF

From the table (5.2), it can be observed that the K_E and ε values for complexes of NOR/CAF greater than corresponding values of NIC/CGA complexes. Thus, this observation shows

that the molecules of NOR/CAF complexes bound together better than the complexes between the molecules of NIC/CGA. On the top of this, the self association constant of NIC and NOR ($2.379 \times 10^4 M^{-1}$ and $1.06 \times 10^5 M^{-1}$) was decreased due to the addition of CGA and CAF respectively. Moreover, the result of the hetero-association constants is comparable with the result reported previously by Davies et. al., [225, 226] for complexation of aromatic drug molecules with short DNA sequences occurs with a binding constant of $10^3 - 10^5 M^{-1}$. Besides, the calculated equilibrium constant for NOR-CAF interaction can also comparable with the result of the binding constants for norfloxacin-DNA complexes system [227]. The results of the hetero association parameters of the compounds may modify the pharmacokinetic properties of the complexes[153, 210, 214].

5.3 Thermodynamic Properties of the Drugs and their Complexes with Bioactive Compounds of Coffee Beans

Performing the experiments at different temperatures and using the estimated associated constants in a Van't Hoff treatment allows the determination of the thermodynamic parameters of the inclusion process, enthalpy change ΔH, entropy change ΔS and Gibb's free energy change ΔG ([228]). The sign and the absolute relative values of these quantities are further used in the discussion of the main forces involved in the inclusion process, i.e. electrostatic, hydrophobic, hydrogen bonds, etc. Heating the aqueous solution of NIC, NOMS, NOR, CIP, NIC-CGA complexes and NOR-CAF shows that the absorption spectra of the molecules are strongly dependent on the temperature in the range of $(293 - 299)K$, $(295 - 312)K$, $(295 - 304)K$, $(295 - 304)K$, $(293 - 299)K$ and $(295 - 304)K$ respectively. The equilibrium constants of the molecules of the compounds at their aforementioned temperatures were calculated at the peak of wavelengths of the

self-association and hetero-association of the drugs. Figs (5.17, 5.18,5.19, 5.20,5.21 and 5.22) shows the graph of lnK_c versus $1/T$ for each drugs.

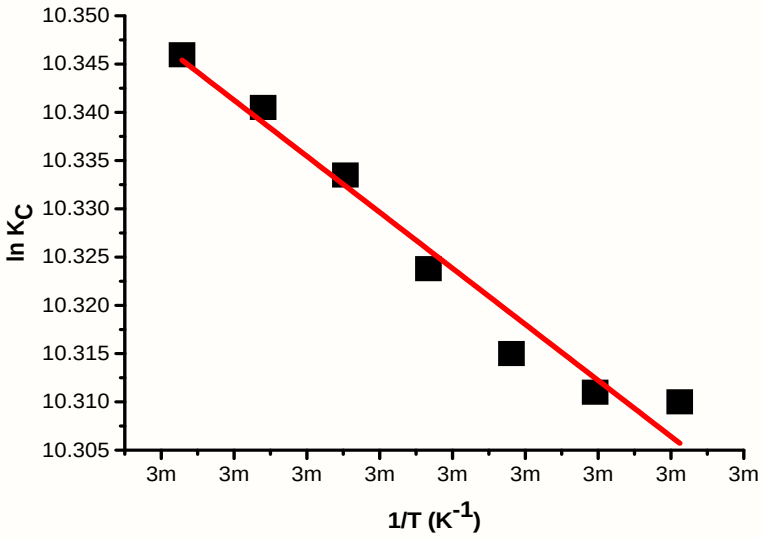

Figure 5.17: $ln(K_C)$ versus $\frac{1}{T}$ of NIC at concentration of $4.5 \times 10^{-4}M$

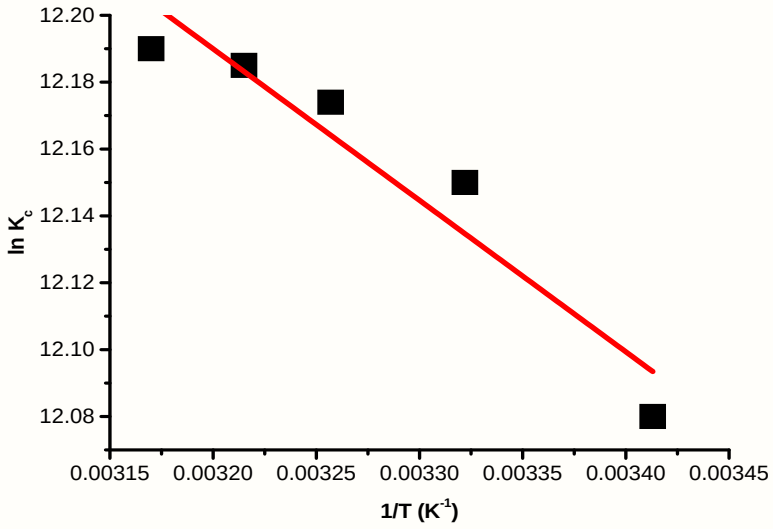

Figure 5.18: $ln(K_C)$ versus $\frac{1}{T}$ of NOMS at concentration of $4.4 \times 10^{-2}M$

The magnitude of the enthalpy was estimated from the slope of the approximating line according to Vant's Hoff's Eqn (4.2.6). Plots of lnK_C versus $\frac{1}{T}$ gives a straight line, whose slope and intercept can be used to determine ΔS and ΔH, and Gibb's free energy can be

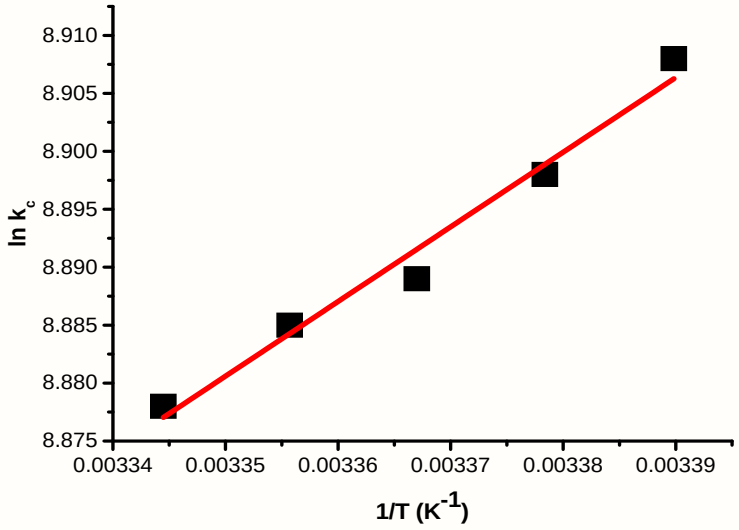

Figure 5.19: $ln(K_C)$ versus $\frac{1}{T}$ of NOR at concentration of $8.312 \times 10^{-5}M$

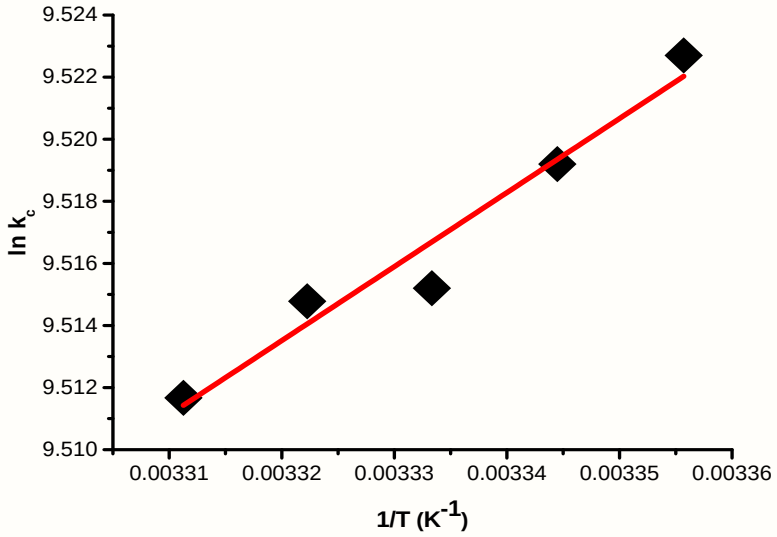

Figure 5.20: $ln(K_C)$ versus $\frac{1}{T}$ of CIP at concentration of $7.148 \times 10^{-5}M$

determined at a specific temperature using Eqn (4.2.5). In order to characterize the force between NIC, NOMS, NOR, CIP, NIC-CGA and NOR-CAF molecules; thermodynamic parameters on the given temperatures were analyzed using Vant's Hoff's equation. The thermodynamic parameters, Gibb's free energy change ΔG, enthalpy change ΔH and entropy change ΔS are important for confirming the binding mode. The calculated values for the Gibb's free energy, enthalpy, and entropy of the molecules for the self and hetero-

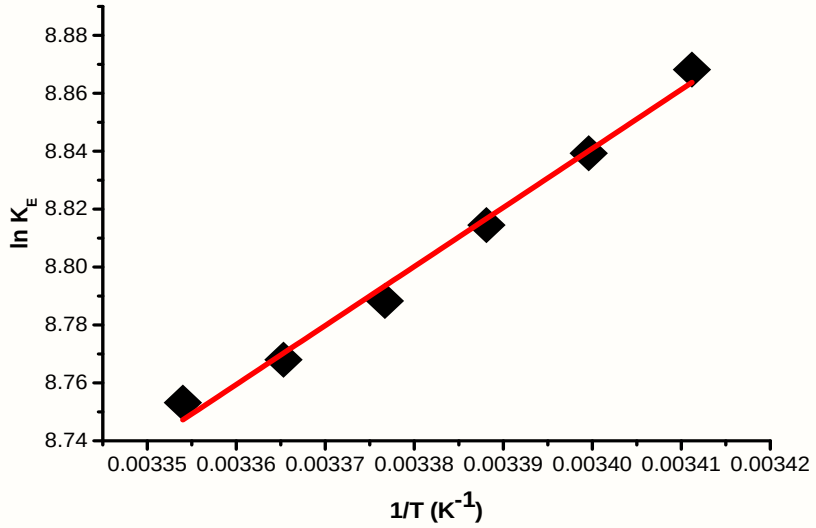

Figure 5.21: $ln(K_C)$ versus $\frac{1}{T}$ of NIC-CGA at concentration of NIC $(4.5 \times 10^{-4}M)$ and CGA $(4.027 \times 10^{-4}M)$

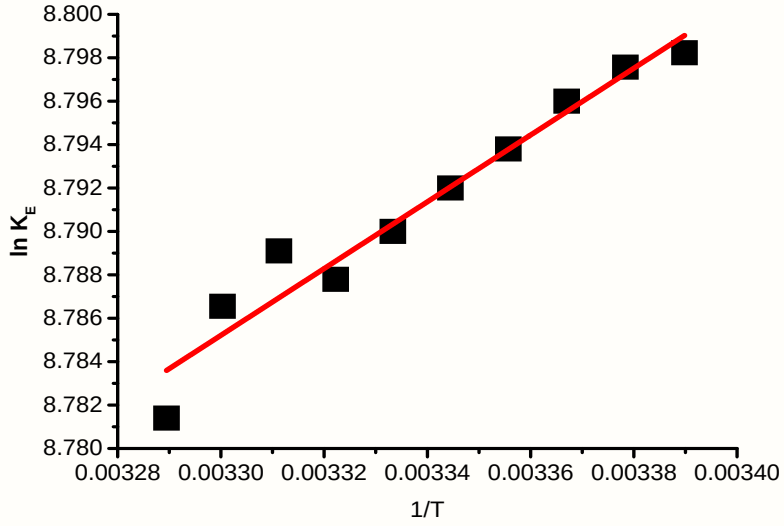

Figure 5.22: $ln(K_C)$ versus $\frac{1}{T}$ of NOR-CAF at concentration of NOR $(3.192 \times 10^{-5}M)$ and CAF $(1.198 \times 10^{-4}M)$

associations are given in Table (5.3). It is shown that NOMS has the highest value of ΔG and ΔS, and NOR has the smallest value of ΔG and ΔS as compared to the other drugs.

As previously reported by zhang et. al., [229], Baosheng Liu et. al., [230] and Wang et. al., [231] if $\Delta H > 0$ and $\Delta S > 0$ hydrophobic interactions are dominant for the in-

Drug	T/K	$\Delta G/kJ.mol^{-1}$	$\Delta H/kJ.mol^{-1}$	$\Delta S/kJ.mol^{-1}K^{-1}$
NIC	$293-299$	$-(25.110 \pm 0.004)$	4.826 ± 0.415	0.102 ± 0.0014
NOMS	$295-312$	$-(31.480 \pm 0.007)$	3.760 ± 0.66	0.113 ± 0.00216
NOR	$295-304$	$-(21.994 \pm 0.92)$	$-(5.350 \pm 0.459)$	0.056 ± 0.0015
CIP	$295-304$	$-(23.725 \pm 4.96)$	$-(1.980 \pm 0.25)$	0.0725 ± 0.001
NIC-CGA	$293-299$	$-(21.590 \pm 1.665)$	$-(16.927 \pm 0.836)$	0.015 ± 0.003
NOR-CAF	$295-304$	$-(19.358 \pm 0.0008)$	$-(1.277 \pm 0.103)$	0.0688 ± 0.0003

Table 5.3: Calculated result of the thermodynamic parameters of NIC, NOMS, NOR, CIP, NIC-CGA and NOR-CAF

teraction process, and if $\Delta H < 0$ and $\Delta S > 0$ electrostatic forces play the major role in the interaction. As a result, from Table (5.3) we observe that hydrophobic interactions are dominant for molecular interaction of NOMS and NIC molecules. Also for the self association of NOR and CIP, and for the complexes NIC-CGA and NOR-CAF molecules, electrostatic forces play the major role in the interaction. Previously, it was reported that the molecular absorption of ciprofloxacin is due the electrostatic effect [232], and the value of $\Delta G = -29.03 kJmol^{-1}$ at 303 K is comparable with our result.

Moreover, Table (5.3) states that both the values of the Gibb's free energy change and enthalpy change are negative for NOR, CIP, NIC-CGA and NOR-CAF, so the absorption process of the compounds indicates the continuous and exothermic reaction respectively [229]. Besides, the values of the enthalpy change for NIC and NOMS is positive, the reaction process of the drug compounds shows that the process is endothermic reaction. The positive value of entropy confirms the increasing randomness of the solution interface during the absorption process of the molecules of the compounds [229, 230]. As previous studies mentioned, if the absolute value of ΔG is in the range of $2.1 - 20.9 KJ/mol$, it is indicative of physical adsorption existing in the adsorption process, while when it is between 80 and $200 KJ/mol$, the adsorption should be associated with chemical adsorption [233, 234]. The values of ΔG at different temperatures in this study were in the range between those of physical adsorption and chemical adsorption. The change in enthalpy

for NOMS is comparable with the change in enthalpy of aminoglycosides drug groups ranging from $-(23-33)kJmol^{-1}$ [235]. Thus, neomycin sulfate be regarded to being aminoglycosides groups.

5.4 Optical Transition Properties of the Drug Compounds

The relations among the Einstein coefficients, oscillatory strength, transition dipole moment, and integrated absorption coefficient for a transition between two states k (lower) and m (upper) are the most used terms in spectroscopy[129, 168]. The optical transition probabilities of NIC, NOMS, NOR and CIP were obtained from the absorption spectra to characterize the strength of the electron transition and to interpret the absorption spectra. The molar decadic absorption coefficient which represents the ability of a molecule to absorb light in a given solvent at a given wavelength was calculated using Beer-Lambert's law[128, 167] and integrated absorption coefficient is the sum of absorption coefficient for all frequencies. Using Eqns (3.1.50,3.1.52,3.1.54 and 3.1.66); the optical transition properties of NIC, NOMS, NOR and CIP respectively were calculated in doubly distilled water at a different concentration. The results are presented in table (5.4). The peak in the visible region of the compounds is due to π to π^* electronic transitions of chromophore groups [236, 237].

Drug	$\alpha_t(10^5 m^{-2})$	$\sigma_t/m.molec^{-1}$	f	$\mu_{km}(Debye)$
NIC	1.700	3.400×10^{-19}	0.070	1.977
NOMS	5.470	4.0975×10^{-6}	0.100	0.263
NOR	6.300	1.220×10^{-17}	0.370	4.646
CIP	3.300	1.060×10^{-17}	0.460	5.156

Table 5.4: Calculated results of the optical transition properties of NIC, NOMS, NOR and CIP

Moreover, the Einstein coefficients were investigated for the drug compounds using equations (3.1.63, 3.1.65 and 3.1.64), results are given in table 5.5.

Tables (5.4 and 5.5) show that the optical transition probabilities and Einstein coeffi-

Drug	$B_{km}/m.kg^{-1}$	A_{mk}/s^{-1}	$\tau_{mk}(s)$
NIC	7.350×10^{19}	6.900×10^{7}	1.450×10^{-8}
NOMS	1.295×10^{18}	7.600×10^{5}	1.300×10^{-6}
NOR	4.070×10^{20}	3.340×10^{8}	2.990×10^{-9}
CIP	5.000×10^{20}	4.100×10^{8}	2.440×10^{-9}

Table 5.5: Results of the Einstein coefficients of NIC, NOMS, NOR and CIP

cients of the drug compounds (NIC, NOMS, NOR and CIP). As the tables revealed the highest values of the optical probabilities (oscillator strength and dipole moment) and Einstein coefficients are obtained on the molecules of ciprofloxacin. This indicates that the molecules of ciprofloxacin have the higher distribution and a strong transition from the ground to the excited level by the incident radiation in water as compared to the other drugs. Besides, the quantum-mechanical interactions of light with the molecules of ciprofloxacin is higher as compared to the other drugs in water solution as expected. On the other side, neomycin sulfate molecules have less ability of absorbing light in the UV-Vis region [171].

The obtained parameters of the optical transition probabilities and Einstein coefficients are important aspects for understanding the nature and strength of the molecular interactions in solution, for characterize the electron transition in different level systems, for interpreting the absorption spectra of the compounds, for direct experimental and theoretical applications in different processes such as emission, absorption and dispersion.

5.5 Binding of Caffeine with Nicotinamide using Fluorescence Quenching and UV/Vis Spectroscopic Techniques

5.5.1 Fluorescence Quenching of Nicotinamide

Fig (5.23) shows the fluorescence spectra of NIC, after the addition of CAF upon excitation at 250 nm and at a temperature of 295 K. The fluorescence intensities of NIC reduced

gradually with increasing CAF concentrations. The quenching mechanisms are usually classified as dynamic and static quenching, which can be distinguished by their different dependence on temperature and viscosity [184, 238]. Since higher temperatures result in large diffusion coefficients for dynamic quenching, the quenching constants are expected to increase with increasing temperature. In contrast, a higher temperature may bring about the decrease in the stability of the complexes, resulting in a lower quenching constant for the static quenching.

The peak of fluorescence spectra of NIC occurs at $424nm$ for both in the absence and presence of CAF. Addition of CAF to NIC produced significant quenching in the fluorescence intensity in a concentration-dependent manner. Furthermore, CAF did not show fluoresce near the emission maximum of NIC that indicated CAF might interact with NIC. The data of Fig (5.23) indicated that CAF quenches the intrinsic fluorescence intensity of the molecules of NIC. The strong quenching effects clearly indicate the existence of binding among the molecules.

In order to interpret the quenching mechanism of the molecules, the fluorescence quenching constant was analyzed according to the Stern-Volmer Eqn (3.2.5). The value of K_{SV} was determined by linear regression of this Stern-Volmer equation and is given in Table (5.6).

Fig (5.24) is the Stern-Volmer plots for the quenching of NIC by CAF at temperatures of 295 and 303 K. The curves showed good linear relationships within the investigated concentrations at the two different temperatures. Linear Stern-Volmer plots indicated to be static quenching rather than dynamic quenching since the plot shows a good linear relationship and decreased as the temperature increase. As reported by Visser [135], the

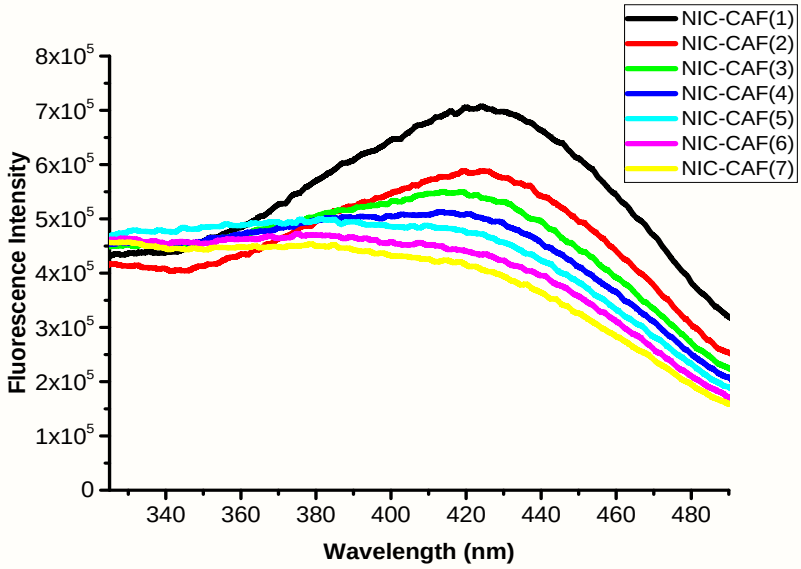

Figure 5.23: Emission spectra of NIC ($\lambda_{ex} = 250nm$) in the presence of caffeine at $295K$. The concentration of caffeine increases from top to bottom $(2.925, 4.058, 5.171, 6.264, 7.338, 8.393, 9.365) \times 10^{-5}M$, and NIC concentration is fixed at $2.841 \times 10^{-5}M$

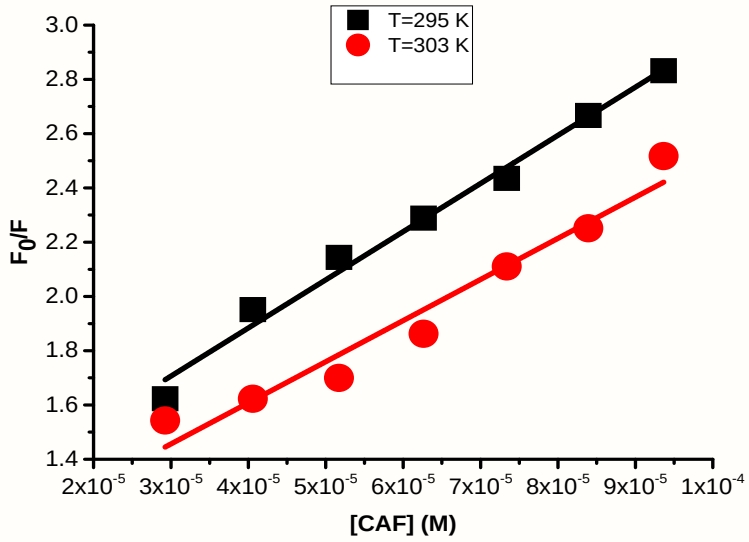

Figure 5.24: Stern-Volmer plots for the quenching of NIC by CAF at 295 and 303 K.

fluorescence lifetime,τ_0, of NIC was taken to be $0.3ns$. From Fig (5.24), the values of K_{SV} was obtained using the the Stern-Volmer equation (3.2.5), and the values of K_{SV}, the quenching rate constant, k_q, determined at the two temperatures are given in Table (5.6). It is clear that the k_q values are of the order $10^{13}L/mol/s$ at both temperatures which

exceed by far the diffusion controlled rate constant $2.0 \times 10^{10} L/mol/s$ in an aqueous solution [239, 240], confirming that the quenching does not involve a dynamic diffusion process, but rather occurs due to the formation of complexes of CAF-NIC.

Temperature (K)	$K_{SV}(1 \times 10^4 L/mol)$	$k_q(1 \times 10^{13} L/mol/s)$	R
295	1.775	5.920	0.980
303	1.515	5.052	0.970

Table 5.6: Stern-Volmer constant, quenching rate constant for the interaction of NIC with CAF at temperature of 295 and 303 K. R is the correlation coefficient.

5.5.2 Binding Constant and Binding Sites

When molecules are bound independently to a set of equivalent sites on macromolecules, the equilibrium between free and bound molecules can be calculated using Eqn (3.2.2). The values of K_C and n were determined from the slope and intercept of the linear fit of this eqn (3.2.2) to the experimental data of Fig (5.25). And, the values of the association constant of CAF with NIC at 295 and 303 K are listed in Table (5.7).

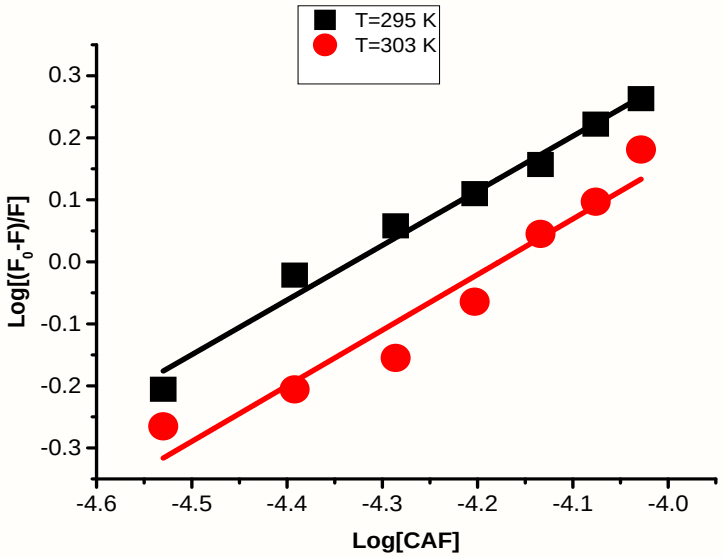

Figure 5.25: Log $\frac{(F_0-F)}{F}$ versus logarithm of concentration of CAF at 295 and 303 K

As it can be seen from the Table (5.7), the value of k_c decreases from $6.5 \times 10^3 L/mol$ to $5.577 \times 10^3 L/mol$ as the temperature increases from 295 to $303K$, which suggested that the binding reaction between the NIC and CAF is exothermic [231].

Temperature (K)	$k_C(1 \times 10^3 L/mol)$	n	R
295	6.500	0.880	0.980
303	5.577	0.897	0.990

Table 5.7: Binding constant (K_C), number of binding sites (n) and correlation coefficient (R) of NIC with CAF at the temperature of 293 and 303 K

Moreover, as previously reported by Chen et al. [241], the binding constant for weak binding affinity of different complexes is less than $1 \times 10^3 M^{-1}$. Thus a moderately strong binding constants were observed between NIC and CAF. The values also decreased with increasing temperature, which indicates the formation of unstable compounds that partly decompose at relatively higher temperatures. The calculated binding site number 'n' that approaches to one, indicates the existence of a single site for the binding of NIC to CAF.

5.5.3 Thermodynamic Parameters and Nature of the Binding Forces

The thermodynamic parameters of binding reaction are the main evidence for confirming the binding mode. The formation of binding between molecules can be described by several biophysical parameters such as the association constant, and other thermodynamic properties. The forces acting between small molecules and macromolecules are mainly hydrogen bonds, electrostatic forces, van der Waal's force and hydrophobic interaction. To obtain further insight into the weak interactions associated with the complexation of NIC with CAF, we endeavored to determine the thermodynamic parameters using Van't Hoff's Eqn (4.2.6). This equation is valid, if the enthalpy change ($\triangle H$) does not vary significantly over the temperature range of the study. And, the free energy change ($\triangle G$) can be calculated at each temperature using eqn (4.2.5).

From the relationship between $ln(K_C)$ and the reciprocal of absolute temperature the values of the thermodynamic parameters were obtained and are listed in Table (5.8).

Accordingly, as previously reported by zhang et. al., [229], Baosheng Liu et. al., [230] and Wang et. al., [231], the negative values of $\triangle H$ and the positive value of $\triangle S$ indicate that electrostatic force played a major role in the reaction between NIC and CAF, whereas the negative sign for $\triangle G$ indicates the spontaneity of the binding for NIC with CAF. Moreover, the negative value of enthalpy indicates that the absorption process of the compounds is exothermic reaction. Besides, the positive value of entropy confirms the increasing randomness of the solution interface of the molecules of the compounds [230, 231]. In addition, the values of ΔH and ΔS for NIC is increased due to the addition of CAF in the solution.

Temperature (K)	$\triangle H(kJ/mol)$	$\triangle S(J/mol/K)$	$\triangle G(kJ/mol)$
295	-14.220	24.764	-21.520
303	-14.220	24.764	-21.720

Table 5.8: Thermodynamic properties determined by fluorescence quenching of CAF with NIC

5.5.4 UV/vis Absorption Spectra

To verify the binding mechanism of CAF-NIC, UV-Vis absorption spectroscopy was investigated. The absorption spectrum can be used to explore the spectral structure changes and to know the complex formation of different compounds [[128, 153, 210]). In dynamic quenching, the spectra of the molecule will not change, however, in static quenching due to the formation of reaction, spectral changes were observed in the compound.

Fig (5.26) shows the absorption spectra of NIC in the presence and absence of CAF. In the absence of CAF, the UV/vis absorption spectra of NIC is characterized by one absorption band with a peak of intensity at $261nm$. With the addition of CAF solution, the interactions between CAF and NIC led to the red shift of the NIC spectra by about $7nm$, with increase in the peak intensity of $268nm$. The curve N was different from the

curves of the complexes of NIC-CAF and isosbestic point occurs at wavelength of around 284nm the complexes. This change of spectral structure is a reasonable result to confirm the binding of CAF with NIC due to ground state complex formation, which is evidence that the static quenching existed in the binding process of the fluorescence quenching.

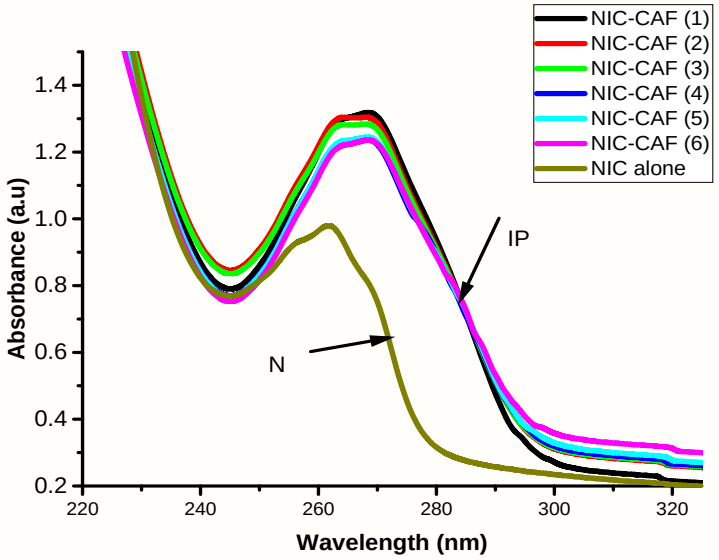

Figure 5.26: UV/Vis absorption spectra of NIC in the presence of caffeine (N) $C(NIC)alone = 2.275 \times 10^{-5}M$; (1-6) C(CAF)= $2.01, 2.189, 1.97, 1.95, 1.92, 1.897 (\times 10^{-5} mol/L)$.

5.6 Effects of Solvent Polarity on the Absorption and Fluorescence Spectra of Nicotinamide: Determination of the Dipole Moments

Determination of the photophysical and photochemistry of different drug compounds is useful for various applications. The values of ground- and excited-state dipole moments of the molecules provide information about the change in electronic distribution of the excited molecule[242, 243]. It elucidates the nature of the excited state of the molecules as it reflects the charge distribution in the molecule[242–244]. In addition, the experimental data on dipole moment are useful in parameterisation in quantum chemical procedures for these states[245]. The excited dipole moments of the fluorescent molecules

have been also used to determine emission energy as a function of the solvent polarity function[242, 243]. As a result, the solvent functions expressed in the in the eqns (3.3.18, 3.3.20, 3.3.31, 3.3.32 and 3.3.33) are calculated and values are given in table (5.9). Accordingly, the ground and excited state dipole moments of NIC can be determined

Solvent	ε^a	n^a	f^b	ϕ^b	F^c_{L-M}	F^d_{K-C-V}	F^e_B
1	80.10	1.3325	0.91375	0.2265	0.32028	0.683392	0.913758
2	33.00	1.3280	0.85573	0.2234	0.30894	0.651335	0.855732
3	24.55	1.3614	0.81293	0.2459	0.28874	0.652459	0.812933
4	17.84	1.3990	0.75370	0.2711	0.26433	0.647996	0.753704
5	37.50	1.3404	0.86408	0.2318	0.30682	0.663891	0.864083

[a] ε =Dielectric constant and n =refractive index.
[b] Bilot-Kawski solvent functions in Eqn (3.3.18) and (3.3.20)
[c] Lippert-Mataga solvent function in Eqn (3.3.31).
[d] Kawski-Chamma-Viallet solvent function in Eqn (3.3.32).
[e] Bakhshiev solvent function in Eqn (3.3.33).
1=Water, 2=Methanol, 3=Ethanol, 4=Butanol 5=Acetonitrile

Table 5.9: Solvent functions used in the Bakhshiev, Kawski-Chamma-Viallet, Lippert-Mataga and Reichardt equations, respectively

based on the solvent polarity functions of Table (5.9) and the Stokes' shift of the absorption and emission spectra of NIC as shown in Table (5.10) in different polar solvents.

5.6.1 Stokes' Shift of NIC

Figs (5.27 and 5.28) show the absorption and fluorescence spectra of NIC obtained in different solvents. The absorption and fluorescence emission spectra of NIC were recorded in solvents of different solvent parameters with the corresponding solvent polarity values as given in table (5.9). The observed absorption and emission spectra of NIC are broad with varying peaks depending on the solvent used.

As compare to the absorption spectra of Fig (5.27), a large spectral shift was observed in the emission spectra of Fig (5.28) as in table (5.10). The less spectral shifts in the absorp-

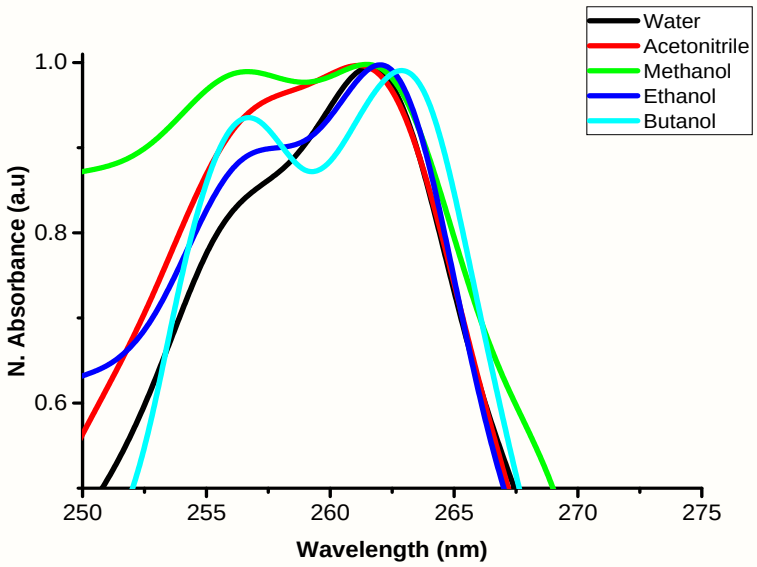

Figure 5.27: Absorbance spectra of NIC in different solvents

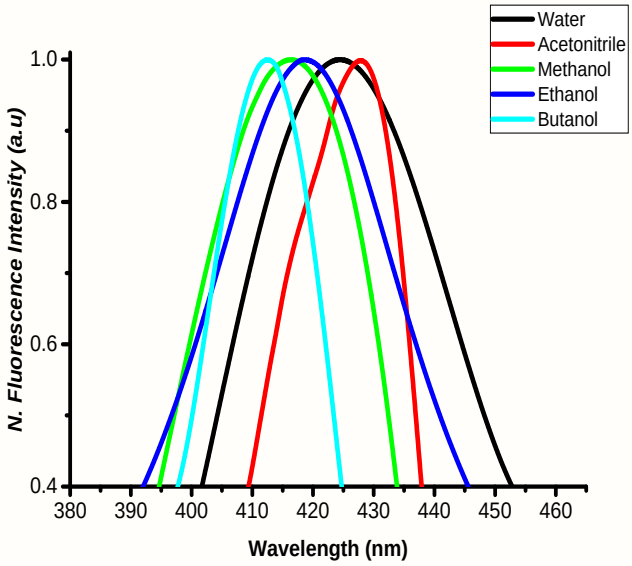

Figure 5.28: Florescence spectra of NIC in different solvents

tion spectra of NIC implies that the ground state energy distribution may not be affected to a greater extent possibly due to the less polar nature of the compound in the ground state rather than in the excited state. The shift in the emission of Fig (5.28) clearly indicates that the dipole moment of the excited state is higher compared to that in the ground state and the relaxed excited state S_1 will be energetically stabilized relative to the ground state S_0 [246].

The absorption and fluorescence emission data of NIC in solution also provided re-

Solvent	$\tilde{v_a}$	$\tilde{v_f}$	$\tilde{v_a} - \tilde{v_f}$	$\tilde{v_a} + \tilde{v_f}$	$(\tilde{v_a} + \tilde{v_f})/2$
1	3822630	2358491	1464139	6181121	3090560
2	3816794	2403846	1412948	6220640	3110320
3	3816794	2392344	1424449	6209138	3104569
4	3802281	2427184	1375097	6229466	3114733
5	3831418	2336449	1494969	6167866	3083933

v_a, absorption maximum in m^{-1}; v_f, fluorescence maximum in m^{-1}
1=Water, 2=Methanol, 3=Ethanol, 4=Butanol, 5=Acetonitrile

Table 5.10: Difference, sum and mean of peak absorption and emission spectra of NIC in different polar solvents

liable information about the solvation effects in the ground and excited states. From table (5.10), we observe that the magnitude of Stokes shift for the compound varies from $13750.97 - 14949.69 cm^{-1}$. The large magnitude of the Stokes shift indicated that the excited state geometry of the compound could be different from that of the ground state and also there will be an increase in dipole moment on excitation. Generally, the pronounced emission band shifts and relatively increase in Stoke's shift values with increase in solvent polarity indicated there is an increase in dipole moment on excitation.

Dipole Moment Calculation

To get a further insight on the solvatochromic behavior of nicotinamide, the spectroscopic properties were correlated with the solvent polarity functions. From the slope of the Bilot-Kawski, Lippert-Mataga, Kawski-Chamma-Viallet and Bakhshiev Eqns (3.3.16, 3.3.17, 3.3.25, 3.3.26 and 3.3.27) respectively, the ground and excited dipole moments were calculated. Figs (5.29 and 5.30) shows the Stokes shift and the sum of the wavenumbers versus solvent polarity function for NIC using the Bilot-Kawski Eqns (3.3.16 and 3.3.17) respectively.

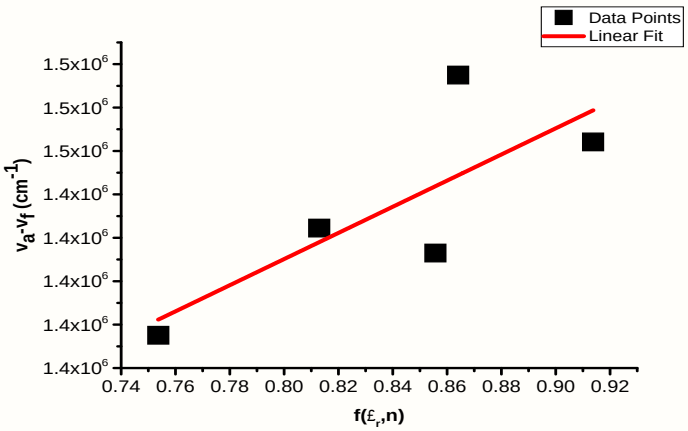

Figure 5.29: Plot of $\overline{v}_a - \overline{v}_f$ versus $f(\varepsilon_r, n)$ of NIC in different polar solvents using Bilot-Kawski equation

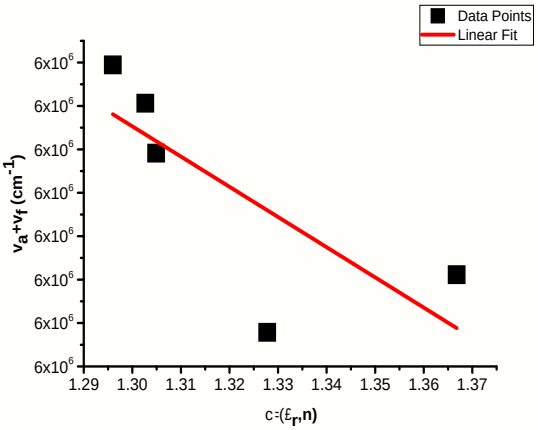

Figure 5.30: Plot of $\overline{v}_a + \overline{v}_f$ versus $\Phi(\varepsilon_r, n)$ of NIC in different polar solvents using Bilot-Kawski equation

Similarly, figs (5.31 and 5.32) are the plots of the Stokes shift and the mean of the wavenumbers versus the solvent polarity function for Lippert-Mataga and Kawski-Chamma-Viallet Eqn (3.3.25 and 3.3.26) respectively.

From the slopes of the graphs of Figs (5.29,5.30,5.31 and 5.32), the ground and excited state dipole moment were calculated and the values are given in Table (5.11).

The calculated values of the ground and excited state dipole moments using eqn (3.3.23 and 3.3.24) are 0.02D and 0.268 D. Thus, the obtained ground and excited state dipole

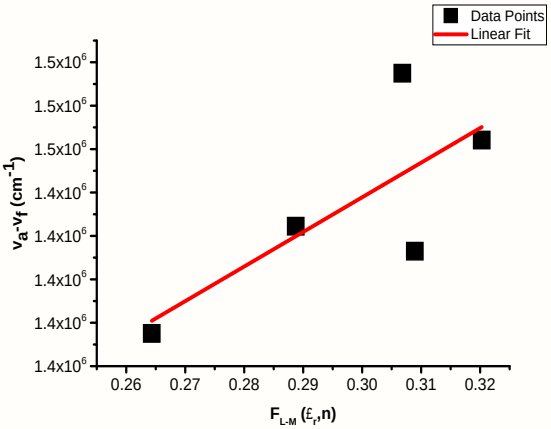

Figure 5.31: Plot of $\overline{v}_a - \overline{v}_f$ versus F_{L-M} of NIC in different polar solvents using Lippert-Mataga equation

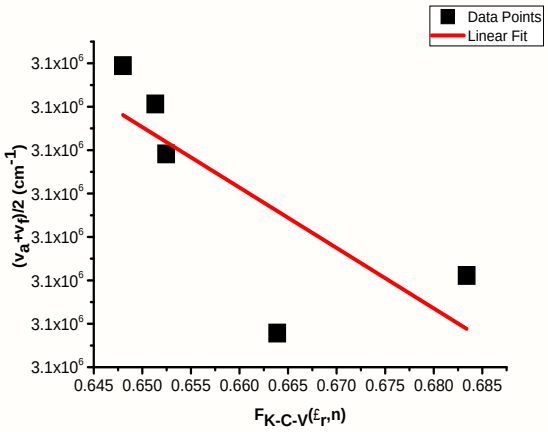

Figure 5.32: Plot of $(\overline{v}_a + \overline{v}_f)/2$ versus F_{K-C-V} of NIC in different polar solvents using Kawski-Chamma-Viallet equation

moments of NIC are quite similar to the results recently obtained and reported by Beat [137], $\mu_g < 0.2$, and μ_e ranges ($0.2 - 0.316D$) from the measurement of individual Stark lobes of the two conformers of nicotinamide (E-nicotinamide and Z-nicotinamide) using microwave spectrum. Also, the above results of the dipole moments are similar to the results as [247], $0.0967D$ on the surface of nicotinamide by the Helmholtz equation on the basis of surface excess values obtained from surface tension measurements, and surface potential changes.

In general, the difference between the excited and ground state dipole moments ($\Delta\mu$)

obtained by experimental and theoretical methods are moderately high, indicating that the excited dipole moment is greater than that in the ground state and also more polar than in the ground state.

From Table (5.11), the change in dipole moment using all the five methods from 0.248 us-

Compound	a^a	μ_g^b	μ_e^c	$\Delta\mu^d$	$\Delta\mu_{L-M}^e$	$(\mu_e^2-\mu_2^2)_{K-C-V}^f$	$\Delta\mu_B^g$	$\Delta\mu^h$
NIC	2.258	0.020	0.268	0.248	0.404	0.076	0.249	0.420

$1D = 3.33564 \times 10^{30} C.m.$
[a] calculated Onsager cavity radius
[b] Ground state dipole moment calculated according to Bilot-Kawski, Eqn (3.3.23)
[c] Excited state dipole moment calculated according to Bilot-Kawski, Eqn (3.3.24).
[d] Calculated according to Bilot-Kawski, Eqn (3.3.24 and 3.3.23).
[e] Calculated according to Lippert-Mataga correlation, Eqn (3.3.28).
[f] Calculated according to Kawski-Chamma-Viallet correlation, Eqn (3.3.29).
[g] Calculated according to Bakhshiev correlation, Eqn (3.3.30).
[h] calculated from Gaussian 9 with $\mu_g = 1.4973$ and $\mu_e = 1.9161D$

Table 5.11: Ground state, excited state dipole moments in Debye (D), and onsager cavity radius $'a'$ (Å), calculated by experimental and theoretical methods of nicotinamide

ing Bilot Kawski method to the values obtained by Gaussian software given by 0.42. As we observe, the change in dipole moment of the theoretical calculations are greater that from the experimental results. This is because, the experimental methods takes solvent and environmental effects in to account. Moreover, from the experimental results, the obtained values from Lippert-Muataga method is higher than from the other used methods. This indicates that Lippert-Muataga method is more sensitive to solvent polarity than the other experimental methods.

5.6.2 Quantum Chemical Calculation

The ground and excited state dipole moments obtained in the gas phase by ab initio calculation, Gaussian 09 program [211] are given in Table 5.11. The theoretical values of μ_g obtained by quantum chemical calculation in the gas phase are 1.4973 D; and by solvatochromic methods: experimental, 0.02 D. The corresponding excited-state dipole moment is also theoretically 1.916 D and experimentally found value is 0.268 D. In the ground state the theoretical values are slightly higher than the experimental results. This

is because, first, the dipole moments that are based on charge densities obtained from eigen functions of the molecular orbital approximations are considerably higher than the actual experimental dipole moments [243]. The other reason is that the experimental methods take solvent and environmental effects into account (solute-solvent interaction), whereas the ab initio calculation gives the values only for a free solid solute molecule.

The other calculated parameters that are very important in quantum chemistry are the $highestoccupiedmolecularorbital - lowestunoccupiedmolecularorbital$(HOMO-LUMO) energy gaps of the compound which reflect the chemical activity of the molecules. Both highest occupied molecular orbital (HOMO) and lowest unoccupied molecular orbital (LUMO) are the main orbitals that take part in chemical stability. A molecule with large HOMO-LUMO gaps is generally stable and unreactive while ones with small gaps are generally reactive. The HOMO-LUMO band gaps for NIC is $5.566eV$. A difference in electronic distribution was also noticed on the HOMO-LUMO molecular orbital plot of NIC and shown in Fig (5.33). Higher electronic distribution was observed on the LUMO orbital level and confirms that the excited states of the molecules have higher dipole moment. The obtained results are also similar with the result reported previously [137, 247].

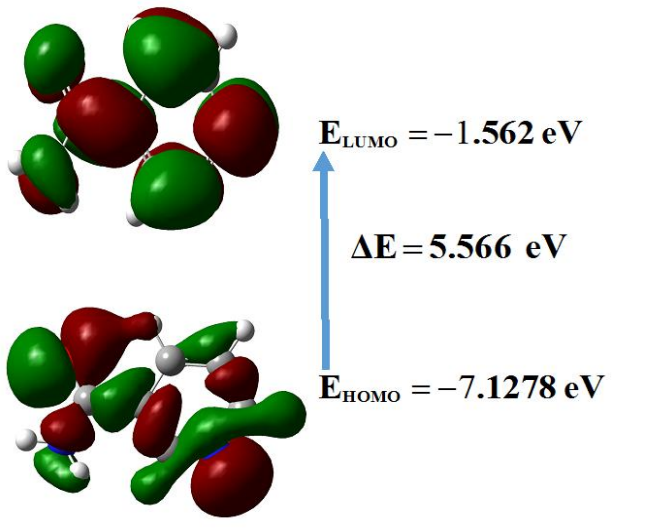

Figure 5.33: Electron distribution of HOMO and LUMO energy levels

Chapter 6

Conclusions and Recommendation for Future Perspective

6.1 Conclusions

This research constitutes the investigation of the optical transition probabilities and interaction of some drugs (NIC, NOMS, NOR and CIP) with biologically active compounds of coffee beans (CGA and CAF) using spectroscopic techniques. The self assciation, heteroassociation, thermodynamic properties, optical transition properties, the binding of caffeine and the effect of solvent polarity of the drugs have been investigated by absorption and fluorescence spectrophotometer. The spectroscopic methods are simple, fast and highly sensitive. Moreover, chemicals and equipments to carry out the analysis are mostly available in moderate equipped laboratories such as ours.

The findings of this research indicates that the molecules of nicotinamide and neomycin sulfate interacts with themselves due to hydrophobic interaction force, and electrostatic forces play the major role on the interaction between the molecules of norfloxacin and ciprofloxacin. It was observed that the molecules of CIP in a water are the most sensitive to the UV-Vis light absorption as compared to the other drugs. Moreover, the molecules of nicotinamide and norfloxacin aggregate with chlorogenic acid and caffeine in the solution respectively due to the electrostatic force between the molecules of the drugs.

Similarly, the binding of CAF with NIC was investigated using fluorescence quenching and UV-vis spectroscopic techniques. From the experimental results, CAF shows a mod-

erately strong binding with NIC, and electrostatic force played a major role in the binding reaction. In addition, the quenching process of the binding between the molecules of CAF and NIC is a static quenching rather than dynamic quenching.

The results of ground and excited state dipole moments of nicotinamide from the solvent polarity effect on absorption and fluorescence showed that the excited state possesses a higher dipole moment than ground state. This indicates that the excited state under investigation of the nicotinamide molecules is more polarized than their ground state and therefore more sensitive to solvent effect.

The calculated parameters for the self-association, hetero-association and thermodynamic properties of the drug compound are used for interpreting the study of binding and kinetic chemical reaction system of the compound in different systems. The thermodynamic parameters which are derived from the temperature dependency of the dimerization constant, have given insight in to the forces that maintain the dimer structures in the solution. The optical transition probabilities and dipole moments are useful for understanding the nature and strength of its molecular interaction in liquid solutions, in order to characterize the electron transition probabilities and interpret the absorption spectra of the compound, for direct experimental application in the emission, absorption and dispersion, and in providing stringent test of atomic and molecular structure calculation in theoretical work.

Knowledge of the mechanism of self-association, hetero-association, thermodynamic properties, solvent effect and optical transition probabilities of the drug compounds are useful in order to design the advanced efficient and controllable carriers of drugs and food components. Therefore, the investigated results will have wider applications in optical char-

acterization, pharmaceutical drug designing and food companies in terms of economic and scientific utility.

6.2 Recommendation for Future Perspective

This study has gone some way towards enhancing our understanding of optical properties of some drugs and their interactions. The research has given rise to the following recommendations in need of further investigation:

1. extend this investigation to other new established drugs and nano-medicinal drugs used in therapy,
2. extend the study of the drugs to real time investigations with biological systems,
3. develop more sophisticated model that estimates the multiple drug regimens and multiple drug interactions, and validating the established predictive model e.t.c.

In addition, the study of drugs on their pharmacokinetics, pharmacodynamics, and drug interactions is critical for the development of safe and effective therapies and for the prevention of drug toxicities and adverse drug reactions. For future pharmaceutical research and development, the use of innovative design in conjunction with advanced technology and/or methodology (spectroscopic techniques of analysis) is encouraged that benefits pharma technology and food industries. The spectroscopic technologies offer attractive options for an opportunity to visualize the effects of various drug incompatibility, and facilitates drug discovery research faster and can open up new applications.

The results of this research will give direction for investigation of some drug properties (optical transition probabilities and interactions), and we are moving toward the right

direction and yet there is still a long way to go until we are able to address all of the scientific issues of drug investigations. This will certainly help to elaborate more effective strategies for the control of the pharmacokinetic and pharmacodynamics activities of the drugs. It will extend the research to other new established drugs and nano-medicinal drugs for effective and efficient drug development. Improvement in investigation of the interaction mechanisms of drug interactions is the most important aspect in the entire drug development process for safe and effective compounds available to combat human diseases.

List of Publications

1. **Ataklti Abraha**, Ashok Gholap, Abebe Belay, "*Determinations of norfloxacin complexes with caffeine, and its optical transition probabilities using UV-Vis spectroscopy*", IJPS, 11(21) (2017) 269-278
2. **Ataklti Abraha**, Ashok Gholap, Abebe Belay, "*Investigation of self-association, optical transition probability and hetero-association with chlorogenic acid of nicotinamide using UV-Vis spectroscopy*", IJPS, 11(21) (2016) 269-278
3. **Ataklti Abraha**, AV Gholap, Abebe Belay, "*Study Self-association, Optical Transition Properties and Thermodynamic Properties of Neomycin Sulfate Using UV-Visible Spectroscopy*", International Journal of Biophysics, 6(2) (2016) 16-20
4. **Ataklti Abraha**, "*Study Self-Association of Norfloxacin and Ciprofloxacin, and their Thermodynamic Properties*", J Pharm Sci Bioscientific Res., 6(3) (2016) 407-413.
5. **Ataklti Abraha**, Ashok Gholap, Abebe Belay, "Binding of caffeine with nicotinamide using fluorescence quenching and UV/Vis spectroscopic techniques ". Progress in Biomaterials, springer (under review)
6. **Ataklti Abraha**, AV Gholap, Abebe Belay, "Effect of solvent polarity on the absorption and fluorescence spectra of nicotinamide: determination of ground and excited state dipole moments". Journal of Theoretical and Applied Physics, springer (under review)

Conference presentation

1. 02/2017 (oral), Investigation of self-, hetero-Association with chlorogenic Acid and optical transition probabilities of nicotinamide using UV-Vis Spectroscopy, Ethiopian Physical Society Annual 11th Conference, Dire Dawa University, 3-4 Feb, 2017.

2. 05/2017 (oral), Investigation of self-, hetero-association with caffeine and optical transition probabilities of norfloxacin using UV-Vis spectroscopy. The role of natural and computational science 1st annual conference, Samara University, 27-28 May, 2017.

References

[1] *Demtroder W. Laser spectroscopy*. Springer, Berline, Germany, 1995. 1, 3.1.2, 3.1.2, 3.1.2, 3.1.2

[2] Benuehll K. Fundamentals of molecular spectroscopy. USSR, 1985. 1

[3] *Rao KN. Molecular spectroscopy: modern research*. Elsevier, New York, 2012.

[4] *Svanberg S. Atomic and molecular spectroscopy: basic aspects and practical applications*. Springer-verlag, Berlin, Germany, 2012. 1

[5] *Platt JR. Ultra-violet and Visible Spectroscopy. Chemical Applications.* J Am Chem Soc, 84(15):3034-3034, 1962. 1

[6] *Bauman RP. Absorption spectroscopy*. John Wiley and Sons, New York, 1962. 1, 3.1.2, 3.1.3

[7] Mccurdy MR, Bakhirkin Y, Wysocki G, Lewicki R, Tittel FK. Recent advances of laser-spectroscopy-based techniques for applications in breath analysis. *J Breath Res.*, 1(1):014001, 2007. 1

[8] *Schmidt F. Laser-based absorption spectrometry: development of NICE-OHMS towards ultra-sensitive trace species detection*. PhD thesis, Fysik, 2007. 1

[9] *Thorne AP. Spectrophysics*. Chapman and Hall Ltd, London, 1988. 1

[10] *Piscitelli SC. Drug interactions in infectious diseases.* Springer, Berlin, Germany., 2011. 1, 2

[11] Winter J. Drug interactions in infectious diseases, Oxford University Press, UK, 2013. 1, 2

[12] Hassan BAR. Vitamins (importance and toxicity). *Pharmaceut Anal Acta*, 3(8):230–240, 2012. 1, 2.1.1, 2.1.1

[13] Waksman SA, Katz E, Lechevalier HA. Antimicrobial properties of neomycin. *J. Lab. Clin. Med.*, 36:93–99, 1950. 2.1.2

[14] Xue L, Xi H, Kumar S, Gray D, Davis E, Hamilton P, Skirba M, Arya DP. Probing the recognition surface of a dna triplex: binding studies with intercalator-neomycin conjugates. *Biochemistry*, 49(26):5540, 2010. 2.1.2, 2.1.2

[15] Sarkozy G. Quinolones: a class of antimicrobial agents. *Vet. Med.- Czech*, 46(9-10): 257–274, 2001. 2.1.3, 2.1.3, 2.1.3

[16] Oliphant CM, Green GM. Quinolones: A comprehensive review. *Am Fam Physician.*, 65(3):455–464, 2002. 1, 2.1.3, 2.1.3

[17] Crowe KM. Designing functional foods with bioactive polyphenols: Highlighting lessons learned from original plant matrices. *J Hum Nutr Food Sci*, 1(3):1018, 2013. 1, 2.2, 2.3

[18] Rowland M, Peck C, Tucker G. Physiologically-based pharmacokinetics in drug development and regulatory science. *Annu Rev Pharmacol Toxicol*, 51:45–73, 2011. 2

[19] *Mathieu MP, Keeney R, Milne CP. New drug development: a regulatory overview*. Parexel International Corp., USA, 2002. 2

[20] Lesko LJ, Salerno RA, Spear BB, Anderson DC, Anderson T, Brazell C, Collins J, Dorner A, Essayan D, Gomez-Mancilla B. Pharmacogenetics and pharmacogenomics in drug development and regulatory decision making: report of the first fda-pwg-phrma-drusafe workshop. *J. Clin. Pharmacol.*, 43(4):342–358, 2003. 2

[21] Lipinski CA, Lombardo F, Dominy BW, Feeney PJ. Experimental and computational approaches to estimate solubility and permeability in drug discovery and development settings. *Adv. Drug Deliv. Rev.*, 23(1-3):3–25, 1997. 2

[22] *Silverman RB, Holladay MW. The organic chemistry of drug design and drug action*. Academic press, USA, 2014. 2

[23] Kraemer K, Semba RD, Eggersdorfer M, Schaumberg DA. Introduction: the diverse and essential biological functions of vitamins. *Ann Nutr Metab*, 61(3):185–191, 2012. 2.1.1

[24] Gonçalves EM, Rego TS, Da Piedade MEM. Thermochemistry of aqueous pyridine-3-carboxylic acid (nicotinic acid). *J. Chem. Thermodyn.*, 43(6):974–979, 2011. 2.1.1

[25] *Yagi T. B vitamins and folate: chemistry, analysis, function and effects*. Number 4. RSC, UK, 2012. 2.1.1, 2.1.1

[26] Dipalma JR, Thayer WS. Use of niacin as a drug. *Annu. Rev. Nutr.*, 11:169–187, 1991. 2.1.1

[27] Park J, Halliday GM, Surjana D, Damian DL. Nicotinamide prevents ultraviolet radiation-induced cellular energy loss. *J. Photochem. Photobiol.*, 86(4):942–948, 2010. 2.1.1

[28] Williams A, Ramsden D. Nicotinamide: a double edged sword. *Parkinsonism Relat Disord*, 11:413–420, 2005. 2.1.1

[29] Rolfe HM. A review of nicotinamide: treatment of skin diseases and potential side effects. *J Cosmet Dermatol*, 13:324–328, 2014. 2.1.1

[30] Shalita AR, Smith JG. Topical nicotinamide compared with clindamycin get in the treatment of inflammatory acne vulgaris. *Int J Dermatol.*, 34(6):434–437, 1995.

[31] Jackson TM, Rawling JM, Roebuck BD, Kirkland JB. Large supplements of nicotinic acid and nicotinamide increase tissue nad+ and poly(adp-ribose) levels but do not affect diethylnitrosamine-induced altered hepatic foci in fischer-344 rats. *J. Nutr.*, 125:1455–1461, 1995. 2.1.1

[32] Surjana D, Halliday GM, Damian DL. Nicotinamide enhances repair of ultraviolet radiation-induced dna damage in human keratinocytes and ex vivo skin. *Carcinogenesis*, 34(5):1144–1149, 2013. 2.1.1

[33] Thompson BC, Surjana D, Halliday GM, Damian DL. Nicotinamide enhances repair of ultraviolet radiation-induced dna damage in primary melanocytes. *Exp Dermatol*, 23(7):509–511, 2014. 2.1.1

[34] Chen AC, Martin AJ, Choy B, Fernández-Peñas P, Dalziell RA, Mckenzie CA, Scolyer RA, Dhillon HM, Vardy JL, Kricker A. A phase 3 randomized trial of nicotinamide for skin-cancer chemoprevention. *NEJM*, 373(17):1618–1626, 2015. 2.1.1

[35] Domínguez GG, Díaz CJ, Chavez BA, Gonzalez FA, Jimenez SJE, Damián MP, Gómez QLE, Dueñas GA. Nicotinamide sensitizes human breast cancer cells to the cytotoxic effects of radiation and cisplatin. *Oncol. Rep.*, 33(2):721–728, 2015. 2.1.1

[36] Maiese K, chong ZZ, Hou J, Shang YC. The vitamin nicotinamide: Translating nutrition into clinical care. *Molecules*, 14:3446–3485, 2009. 2.1.1

[37] Niren NM. Pharmacologic doses of nicotinamide in the treatment of inflammatory skin conditions: a review. *Cutis*, 77(1 Suppl):11–16, 2006. 2.1.1

[38] Omar MA, Nagy DM, Hammad MA, Aly AA. Validated spectrophotometric methods for determination of certain aminoglycosides in pharmaceutical formulations. 2013. 2.1.2

[39] Cai Y, Cai Y, Cheng J, Mou S, Yiqiang L. Comparative study on the analytical performance of three waveforms for the determination of several aminoglycoside antibiotics with high performance liquid chromatography using amperometric detection. *J. Chromatogr. A*, 1085(1):124–130, 2005.

[40] Mcglinchey TA, Rafter PA, Regan F, McMahon GP. A review of analytical methods for the determination of aminoglycoside and macrolide residues in food matrices. *Anal. Chim. Acta*, 624(1):1–15, 2008. 2.1.2

[41] Liu SP, Hu XL, Li NB. Resonance rayleigh scattering method for the determination of aminoglycoside antibiotics with trypan blue. *Anal. Chem.*, 36(13):2805–2821, 2003. 2.1.2

[42] Isoherranen N, Soback S. Chromatographic methods for analysis of aminoglycoside antibiotics. *J. AOAC Int.*, 82:1017–1045, 1999. 2.1.2

[43] Stead DA. Stead DA. Current methodologies for the analysis of aminoglycosides. *J. Chromatogr. B Biomed. Sci. Appl.*, 747(1):69–93, 2000. 2.1.2

[44] Waksman SA. Neomycin: nature, formation, isolation, and practical application. 1953. 2.1.2

[45] Waksman SA. Neomycin its nature and practical application. 1958. 2.1.2

[46] *Zejc A, Gorczyca M. Chemistry of Drugs*. Polish, PZWL, Warszawa, 2002. 2.1.2

[47] Patel AH, Dave RM. Formulation and evaluation of sustained release in situ ophthalmic gel of neomycin sulphate. *Bull. Pharm. Res.*, 5(1):1–5, 2015.

[48] Darwhekar G, Jain DK, Choudhary A. Elastic liposomes for delivery of neomycin sulphate in deep skin infection. *Asian J. Pharm. Sci.*, 7(4):230–240, 2012. 2.1.2

[49] Masur H, Whelton PK, Whelton A. Neomycin toxicity revisited. *Arch Surg*, 111(7): 822–825, 1976. 2.1.2

[50] Cheng G, Hao H, Dai M, Liu Z, Yuan Z. Antibacterial action of quinolones: from target to network. *Eur. J. Med. Chem.*, 66:555–562, 2013. 2.1.3

[51] Zhou XG, Feng JZ, Tong SS. Charge transfer reaction and its application in analytical chemistry, iii study of the determination of norfloxacin. *Fenxi Huaxue*, 21(2): 184–186, 1993. 2.1.3

[52] Amin AS, El-Beshbeshy AM. Utility of certain and-acceptors for the spectrophotometric determination of sildenafil citrate (viagra). *Microchimica Acta*, 1(137):63–69, 2001. 2.1.3

[53] Pharmacopoeia, British. British pharmacopoeia commission secretariat, part of the medicines and healthcare products regulatory agency. 2014. 2014. 2.1.3

[54] Grohe K. Antibiotics-the new generation[including nalidixic acid and fluoroquinolones such as ciprofloxacin]. *Chem Britain*, 28:34–6, 1992. 2.1.3

[55] Zeiler H-J, Grohe K. The in vitro and in vivo activity of ciprofloxacin. In *Ciprofloxacin*, pages 14–18. Springer, Germany, 1986. 2.1.3

[56] Emmerson AM, Jones AM. The quinolones: decades of development and use. *J. Antimicrob. Chemother.*, 51(suppl_1):13–20, 2003. 2.1.3, 2.1.3

[57] Gupta Y, Kapoor S. Fluoroquinolones: a pharmaceutical review. *Int.J. Pharm.Sci. Inv.*, 3(9):66–71, 2014. 2.1.3, 2.1.3

[58] Drlica K, Zhao XK. DNA gyrase, topoisomerase IV, and the 4-quinolones. *Microbiol Mol Biol Rev*, 61(3):377–392, 1997. 2.1.3, 2.1.3

[59] Samanidou VF, Demetriou CE, Papadoyannis IN. Direct determination of four fluoroquinolones, enoxacin, norfloxacin, ofloxacin, and ciprofloxacin, in pharmaceuticals and blood serum by hplc. *Anal. Bioanal. Chem.*, 375(5):623–629, 2003. 2.1.3

[60] Liu RH. Health benefits of fruit and vegetables are from additive and synergistic combinations of phytochemicals. *Am. J. Clin. Nutr.*, 78:517–520, 2003. 2.2

[61] Clifford MN. Chlorogenic acid their complex nature and routine determination in coffee beans. *J. Sci. Food Agr.*, 27:73–84, 1979. 2.2, 2.2.1

[62] Bolton S, Null G. Caffeine, psychological effect, use and abuse. *J. Orthomol.Psychiatry*, 10:202–211, 1981. 2.2, 2.2.2

[63] Buren Jv, Vos Ld, Pilnik W. Measurement of chlorogenic acid and flavonol glycosides in apple juice by a chromatographic-fluorometric method. *J. Food Sci.*, 38(4): 656–658, 1973. 2.2.1

[64] Challis BC, Bartlett CD. Possible cocarcinogenic effects of coffee constituents. *Nature*, 254(5500):532–533, 1975. 2.2.1

[65] Svilaas A, Sakhi AK, Andersen LF, Svilaas T, Strom EC, Jacobs JDR, Ose L, Blomhoff R. Intake of antioxidants in coffee; wine and vegetables are correlated with plasma carotenoids in human. *J. Am. Nutr. Sci.*, 134:562–567, 2004. 2.2.1

[66] Pellegrini N, Serafini M, Colombi B, Del Rio D, Salvatore S, Bianchi M, Brighenti F. Total antioxidant capacity of plant foods, beverages and oils consumed in italy assessed by three different in vitro assays. *J. Nutr.*, 133(9):2812–2819, 2003.

[67] Richelle M, Tavazzi I, Offord E. Comparison of the antioxidants activity of commonly consumed polyphenols beverages (coffee, coca, and tea) prepared per cupping serving. *J. Agri. Food. Chem.*, 49:3438–3442, 2001. 2.2.1

[68] Schwab D. Hepatic uptake of synthetic chlorogenic acid derivatives by the organic anion transport proteins. *J. Pharmacol. Exp. Ther.*, 296:91–98, 2001. 2.2.1

[69] Wang Z, Clifford MN, Sharp P. Analysis of chlorogenic acids in beverages prepared from chinese health foods and investigation, in vitro, of effects on glucose absorption in cultured caco-2 cells. *Food Chem.*, 108:369–373, 2008. 2.2.1

[70] Clifford MN, Wu W, Kirkpatrick J, Jaiswal R, Kuhnert N. Profiling and characterization by liquid chromatography/multi-stage mass spectrometry of the chlorogenic acids in gardeniae fructus. *Rapid Commun. Mass Spectrom*, 24:3109–3120, 2010. 2.2.1

[71] Keles LC, Melo NId, Aguiar GdP, Wakabayashi KAL, Carvalho CEd, Cunha WR Crotti AEM, Lopes JLC, Lopes NP. Lychnophorinae (asteraceae): a survey of its chemical constituents and biological activities. *Quimica Nova*, 33(10):2245–2260, 2010. 2.2.1

[72] Tamura EK, Jimenez RS, Waismam K, Gobbo-Neto L, Lopes NP, Malpezzi-Marinho EAL, Marinho Eduardo AV, Farsky SHP. Inhibitory effects of solidago chilensis meyen hydroalcoholic extract on acute inflammation. *J Ethnopharmacol.*, 122(3): 478–485, 2009. 2.2.1

[73] Pencreac'h G, Lorentz C, Ergan F, Soultani-Vigneron S. Production and properties of chlorogenic acid lipophilic esters. *LT*, 24(5):108–110, 2012. 2.2.1

[74] Villeneuve P. Lipases in lipophilization reactions. *Biotechnology Advances*, 25(6): 515–536, 2007. 2.2.1

[75] Ma BL, Liang SF. Progress report on extraction and separation of chlorogenic acid from eucomia ulmoides [j]. *Shanxi Forest Sci Tech*, 4:023, 2003. 2.2.1

[76] Belay A. Some biochemical compounds in coffee beans and methods developed for their analysis. *IJPS*, 6(28):6373–6378, 2011. 2.2.1

[77] Van Dam RM, Feskens EJM. Coffee consumption and risk of type 2 diabetes mellitus. *The Lancet*, 360(9344):1477–1478, 2002. 2.2.1

[78] Mumin A, Akhter KF, Abedin Z, Hossain Z. Determination and characterization of caffeine in tea, coffee and soft drinks by solid phase extraction and high performance liquid chromatography (spe–hplc). *MJChem*, 8(1):045–051, 2006. 2.2.2

[79] Singh DK, Sahu A. Spectrophotometric determination of caffeine and theophylline in pure alkaloids and its application in pharmaceutical formulations. *Anal. Biochem.*, 349(2):176–180, 2006.

[80] Bolton S, Null G. Caffeine: Psychological effects, use and abuse. 10(3), 202–211. *J. Orthomol. Psychiatry*, 1981. 2.2.2

[81] Davis JM, Zhao Z, Stock HS, Mehl KA, Buggy J, Hand GA. Central nervous system effects of caffeine and adenosine on fatigue. *Am J Physiol Regul Integr Comp Physiol.*, 284(2):R399–R404, 2003. 2.2.2

[82] *Lim J. Attention in the brain under conditions of sub-optimal alertness: Neurobiological effects and individual differences*. PhD thesis, University of Pennsylvania, USA, 2010. 2.2.2

[83] Leonard TK, Watson RR, Mohs ME. The effects of caffeine on various body systems: a review. *J Am Diet Assoc*, 87(8):1048–1053, 1987. 2.2.2

[84] Persad LAB. Energy drinks and the neurophysiological impact of caffeine. *Front Neurosci.*, 5, 2011. 2.2.2

[85] Yukawa GS, Mune M, Otani H, Tone Y, Liang X-M, Iwahashi H, Sakamoto W. Effects of coffee consumption on oxidative susceptibility of low-density lipoproteins and serum lipid levels in humans. *Biochemistry*, 69(1):70–74, 2004. 2.2.2

[86] Nawrot P, Jordan S, Eastwood J, Rotstein J, Hugenholtz A, Feeley M. Effects of caffeine on human health. *Food Addit Contam*, 20(1):1–30, 2003. 2.2.2

[87] De gubareff T, Sleator W. Effects of caffeine on mammalian atrial muscle, and its interaction with adexosine and calcium. *J. Pharmacol. Exp. Ther.*, 148(2):202–214, 1965. 2.2.2

[88] Rizvi SJH, Jaiswal V, Mukerji D, Mathur SN. Antifungal properties of 1, 3, 7-trimethylxanthine, isolated from coffea arabica. *Naturwissenschaften*, 67(9):459–460, 1980. 2.2.2

[89] Ashihara H, Sano H, Crozier A. Caffeine and related purine alkaloids: biosynthesis, catabolism, function and genetic engineering. *Phytochemistry*, 69(4):841–856, 2008. 2.2.2

[90] Butcher RW, Sutherland EW. Adenosine 3′, 5′-phosphate in biological materials. i. purification and properties of cyclic 3′, 5′-nucleotide phosphodiesterase and use of this enzyme to characterize adenosine 3′, 5′-phosphate in human urine. *J. Biol. Chem.*, 237:1244, 1962. 2.2.2

[91] Rizvi SJH, Mukerji D, Mathur SN. Selective phyto-toxicity of 1, 3, 7-trimethylxanthine between phaseolus mungo and some weeds. *Agric Biol Chem.*, 45(5):1255–1256, 1981. 2.2.2

[92] Rizvi SJH, Pandey SK, Mukerji D, Mathur SN. 1, 3, 7-Trimethylxanthine, a new chemosterilant for stored grain pest, callosobruchus chinensis (l.). *J. Appl. Entomol.*, 90(1-5):378–381, 1980. 2.2.2

[93] Greer F, Hudson R, Ross R, Graham T. Caffeine ingestion decreases glucose disposal during a hyperinsulinemic-euglycemic clamp in sedentary humans. *Diabetes*, 50(10):2349–2354, 2001. 2.2.2

[94] Charles BG, Rawal BD. The combined action of methyl xanthines with erythromycin, chloramphenicol and tetracycline on staphylococcus aureus. *Microbios Letters*, 10(39-4):143–148, 1979. 2.2.2

[95] Healy DP, Polk RE, Kanawati L, Rock DT, Mooney ML. Interaction between oral ciprofloxacin and caffeine in normal volunteers. *Antimicrob. Agents Chemother.*, 33 (4):474–478, 1989. 2.2.2, 2.3

[96] Reedijk J. New clues for platinum antitumor chemistry: kinetically controlled metal binding to DNA. *Proc. Natl. Acad. Sci. U.S.A.*, 100(7):3611–3616, 2003. 2.3

[97] *Patrick GL. An introduction to medicinal chemistry*. Oxford university press, Oakland, 2013. 2.3

[98] *Konagaya A. Towards an In Silico Approach to Personalized Pharmacokinetics, Molecular Interactions, Prof. Aurelia Meghea (Ed.), InTech*. InTech, 2012. 2.3

[99] Cechinel FV, Corrêa, Rogério, Vaz Z, Calixto J, Nunes RJ, Pinheiro TR, Andricopulo AD, Yunes RA. Further studies on analgesic activity of cyclic imides. *Il Farmaco*, 53 (1):55–57, 1998. 2.3

[100] Dilip CS, Thangaraj V, Raj AP. Synthesis, spectroscopic characterisation, biological and DNA cleavage properties of complexes of nicotinamide. *ARAB J CHEM*, 9: S731–S742, 2016. 2.3

[101] Smith NA, Zhang P, Salassa L, Habtemariam A, Sadler PJ. Synthesis, characterisa-

tion and dynamic behavior of photoactive bipyridyl ruthenium (II)-nicotinamide complexes. *Inorganica Chim. Acta*, 454:240–246, 2017. 2.3

[102] Hussain MA, Diluccio RC, Maurin MB. Complexation of moricizine with nicotinamide and evaluation of the complexation constants by various methods. *J. Pharm. Sci.*, 82(1):77–79, 1993. 2.3

[103] Bogdanova SV, Sidzhakova D, Karaivanova V, Georgieva Sv. Aspects of the interactions between indomethacin and nicotinamide in solid dispersions. *Int. J. Pharm.*, 163(1):1–10, 1998. 2.3

[104] Evstigneev MP, Evstigneev VP, Santiago AAH, Davies DB. Effect of a mixture of caffeine and nicotinamide on the solubility of vitamin (B 2) in aqueous solution. *Eur. J. Pharm. Sci.*, 28(1):59–66, 2006. 2.3

[105] Abraha A, Gholap A, Belay A. investigation of self-association, optical transition probability and hetero-association with chlorogenic acid of nicotinamide using uv-vis spectroscopy. *IJPS*, 11(21):269–278, 2016. 2.3

[106] Guttman DE, Brooke D. Solution phase interaction of nicotinamide with ascorbic acid. *J. Pharm. Sci.*, 52(10):941–945, 1963. 2.3

[107] Oberoi LM, Alexander KS, Riga AT. Study of interaction between ibuprofen and nicotinamide using differential scanning calorimetry, spectroscopy, and microscopy and formulation of a fast-acting and possibly better ibuprofen suspension for osteoarthritis patients. *J. Pharm. Sci.*, 94(1):93–101, 2005. 2.3, 2.4

[108] Lodhi S, Weiner ND, Schacht J. Interactions of neomycin with monomolecular films of polyphosphoinositides and other lipids. *BBA-Biomembranes*, 557(1):1–8, 1979. 2.3

[109] Dahlberg AE, Horodyski F, Keller P. Interaction of neomycin with ribosomes and ribosomal ribonucleic acid. *Antimicrob. Agents Chemother.*, 13(2):331–339, 1978. 2.3

[110] Reid DG, Gajjar K. A proton and carbon 13 nuclear magnetic resonance study of neomycin b and its interactions with phosphatidylinositol 4, 5-bisphosphate. *J. Biol. Chem.*, 262(17):7967–7972, 1987. 2.3

[111] Larsen RW, Jasuja R, Hetzler RK, Muraoka PT, Andrada VG, Jameson DM. Spectroscopic and molecular modeling studies of caffeine complexes with dna intercalators. *Biophys. J.*, 70(1):443–452, 1996. 2.3

[112] Traganos F, Kaminska-Eddy B, Darzynkiewicz Z. Caffeine reverses the cytotoxic and cell kinetic effects of novantrone (mitoxantrone). *Cell Prolif*, 24(3):305–319, 1991. 2.3

[113] Radandt JM, Marchbanks CR, Dudley MN. Interactions of fluoroquinolones with other drugs: mechanisms, variability, clinical significance, and management. *Clin. Infect. Dis.*, 14(1):272–284, 1992. 2.3

[114] Campbell NR, Kara M, Hasinoff BB, Haddara WM, McKay DW. Norfloxacin interaction with antacids and minerals. *Br. J. Clin. Pharmacol.*, 33(1):115–116, 1992. 2.3

[115] Shikun L, Yanjun W, Qiuyue L, Weidong L, Jiehong D, Yunyun W. Synthesis, crystal structures of novel complexes of rare earth with norfloxacin, interaction with dna and bsa. *J. Rare Earths*, 30(5):460–466, 2012. 2.3

[116] Gao F, Yang P, Xie J, Wang H. Synthesis, characterization and antibacterial activity of novel fe (iii), co (ii), and zn (ii) complexes with norfloxacin. *J Inorg Biochem.*, 60 (1):61–67, 1995. 2.3

[117] Sandström k, wärmländer S, Leijon M, Gräslund A. 1H NMR studies of selective interactions of norfloxacin with double-stranded dna. *Biochem Biophys Res Commun*, 304(1):55–59, 2003. 2.3

[118] Azimi O, Emami Z, Salari H, Chamani J. Probing the interaction of human serum albumin with norfloxacin in the presence of high-frequency electromagnetic fields: Fluorescence spectroscopy and circular dichroism investigations. *Molecules*, 16(12): 9792–9818, 2011. 2.3

[119] Lu Y, Wang G, Lu X, Lv J, Xu M, Zhang W. Molecular mechanism of interaction between norfloxacin and trypsin studied by molecular spectroscopy and modeling. *Spectrochim. Acta A*, 75(1):261–266, 2010. 2.3

[120] Hojgaard A, Szerlong H, Tabor C, Kuempel P. Norfloxacin-induced dna cleavage occurs at the dif resolvase locus in escherichia coli and is the result of interaction with topoisomerase iv. *Mol. Microbiol.*, 33(5):1027–1036, 1999. 2.3

[121] Thomson DJ, Menkis AH, McKenzie FN. Norfloxacin-cyclosporine interaction. *Transplantation*, 46(2):312, 1988. 2.3

[122] More VR, Mote US, Patil SR, Kolekar GB. Fluorescence quenching studies of the interaction between riboflavin and norfloxacin and analytical application in the determination of vitamin b2. *J. Solution Chem.*, 39(1):97–106, 2010. 2.3

[123] Dalle JH, Auvrignon A, Vassal G, Leverger G. Interaction between methotrexate and ciprofloxacin. *J Pediatr Hematol*, 24(4):321–322, 2002. 2.3

[124] Thomson AH, Thomson GD, Hepburn M, Whiting B. A clinically significant interaction between ciprofloxacin and theophylline. *Eur J Clin Pharmacol*, 33(4):435–436, 1987. 2.3

[125] Elston RA, Taylor J. Possible interaction of ciprofloxacin with cyclosporin a. *J. Antimicrob. Chemother.*, 21(5):679–680, 1988. 2.3

[126] Nawaz H, Rauf S, Akhtar K, Khalid AM. Electrochemical DNA biosensor for the study of ciprofloxacin–DNA interaction. *Anal. Biochem.*, 354(1):28–34, 2006. 2.3

[127] Kamada AK. Possible interaction between ciprofloxacin and warfarin. *DICP*, 24(1): 27–28, 1990. 2.3

[128] Belay A. The hetero-association of caffeine with 5-caffeoylquinic acid and ethidium bromide. *J. Bio. Phys. Chem.*, 13:30–35, 2013. 2.3, 2.4, 3.1.3, 5.4, 5.5.4

[129] *Milonni PW, Eberly JH. Lasers*. Wiely, New York, 1988. 3.1.3, 3.1.3, 3.1.3, 3.1.3, 3.1.4, 5.4

[130] Abraha A, Gholap AV, Belay A. Study self-association, optical transition properties and thermodynamic properties of neomycin sulfate using uv-visible spectroscopy. *Int. J. Biophys*, 6(2):16–20, 2016.

[131] Bayliss NS. The effect of the electrostatic polarization of the solvent on electronic absorption spectra in solution. *J. Chem. Phys.*, 18(3):292–296, 1950.

[132] Mac RGE. Theory of solvent effects on molecular electronic spectra. *J. Phy. Chem*, 61:562, 1957. 2.3

[133] Shayanfar A, Velaga S, Jouyban A. Solubility of carbamazepine, nicotinamide and carbamazepine–nicotinamide cocrystal in ethanol–water mixtures. *Fluid Ph. Equilibria*, 363:97–105, 2014. 2.4

[134] Atac A, Karabacak M, Kose E, Karaca C. Spectroscopic (NMR, UV, FT-IR and FT-Raman) analysis and theoretical investigation of nicotinamide N-oxide with density functional theory. *Spectrochim. Acta A*, 83(1):250–258, 2011. 2.4

[135] Visser A, Hoek Av. The fluorescence decay of reduced nicotinamides in aqueous solution after excitation with a uv-mode locked ar ion laser. *J. Photochem. Photobiol.*, 33(1):35–40, 1981. 2.4, 5.5.1

[136] Xu H, Liu Q, Wen Y. Spectroscopic studies on the interaction between nicotinamide and bovine serum albumin. *Spectrochim. Acta A*, 71(3):984–988, 2008. 2.4

[137] Beat V, Ronaldd B, Peter DG, Anthonyp P. The microwave spectrum of a vitamin: Nicotinamide. *J. Mol. Spectrosc.*, 145:1–11, 1991. 2.4, 5.6.1, 5.6.2

[138] Lang R, Yagar EF, Eggers R, Hofmann T. Quantitative investigation of trigonelline, nicotinic acid, and nicotinamide in foods, urine, and plasma by means of lc-ms/ms and stable isotope dilution analysis. *J. Agric. Food Chem.*, 56(23):11114–11121, 2008. 2.4

[139] Hees PS, Sotak CH. Assessment of changes in murine tumor oxygenation in response to nicotinamide using 19F NMR relaxometry of a perfluorocarbon emulsion. *Magn. Reson. Med.*, 29(3):303–310, 1993. 2.4

[140] Baranowska I, Kadziolka A. RPTLC and derivative spectrophotometry for the analysis of selected vitamins. *ACTA CHROMATOGR.*, pages 61–71, 1997. 2.4

[141] Takeshima T, Takeuchi H, Egawa T, Konaka S. Gas-phase molecular structure of nicotinamide studied by electron diffraction combined with mp2 calculations. *J. Mol. Struct*, 644(1):197–205, 2003. 2.4

[142] Clarot I, Regazzeti A, Auzeil N, Laadani F, Citton M, Netter P, Nicolas A. Analysis of neomycin sulfate and framycetin sulfate by high-performance liquid chromatography using evaporative light scattering detection. *J. Chromatogr. A*, 1087(1): 236–244, 2005. 2.4

[143] Adams E, Schepers R, Roets E, Hoogmartens J. Determination of neomycin sulfate by liquid chromatography with pulsed electrochemical detection. *J. Chromatogr. A*, 741(2):233–240, 1996. 2.4

[144] Botto RE, Coxon B. Nitrogen-15 nuclear magnetic resonance spectroscopy of neomycin b and related aminoglycosides. *J. Am. Chem. Soc*, 105(4):1021–1028, 1983. 2.4

[145] Lacourciere KA, Stivers JT, Marino JP. Mechanism of neomycin and rev peptide binding to the rev responsive element of hiv-1 as determined by fluorescence and nmr spectroscopy. *Biochemistry*, 39(19):5630–5641, 2000. 2.4

[146] Pal MK, Ghosh JK. Spectroscopic probe of the competitive binding of ethidium bromide and neomycin to DNA. *Spectrochim. Acta A*, 51(3):489–498, 1995. 2.4

[147] Tsuji K, Goetz JF, Van Meter W, Gusciora KA. Normal-phase high-performance liquid chromatographic determination of neomycin sulfate derivatized with 1-fluoro-2, 4-dinitrobenzene. *J. Chromatogr. A*, 175(1):141–152, 1979. 2.4

[148] Liu C, Nanaboina V, Korshin GV, Jiang W. Spectroscopic study of degradation products of ciprofloxacin, norfloxacin and lomefloxacin formed in ozonated wastewater. *Water Res*, 46(16):5235–5246, 2012. 2.4

[149] Belal F, Al-Majed AA, Al-Obaid AM. Methods of analysis of 4-quinolone antibacterials. *Talanta*, 50(4):765–786, 1999. 2.4

[150] Kamat BP. Study of the interaction between fluoroquinolones and bovine serum albumin. *J Pharm Biomed Anal*, 39(5):1046–1050, 2005. 2.4

[151] Refat MS, Elfalaky A, Elesh E. Spectroscopic and physical measurements on charge-transfer complexes: Interactions between norfloxacin and ciprofloxacin drugs with

picric acid and 3, 5-dinitrobenzoic acid acceptors. *âĂŐJ. Mol. Struct*, 990(1):217–226, 2011. 2.4

[152] Niazi A, Yazdanipour A, Ghasemi J, Kubista M. Spectrophotometric and thermodynamic study on the dimerization equilibrium of ionic dyes in water by chemmetrics method. *Spectrochim. Acta A*, 65:73–78, 2006. 2.4

[153] Belay A. Spectrophotometric method for the determination of caffeic acid complexation and thermodynamic properties. *Int. J. Biophys*, 2:12–17, 2012. 4.2.1, 5.1, 5.2, 5.5.4, A.1

[154] Belay A, Libnedengel E, Kim HK, Hwang YH. Effects of solvent polarity on the absorption and fluorescence spectra of chlorogenic acid and caffeic acid compounds: determination of the dipole moments. *Luminescence*, 31(1):118–126, 2016. 3.3.4, 3.3.4

[155] Belay A, Kim HK, Hwang YH. Binding of caffeine with caffeic acid and chlorogenic acid using fluorescence quenching, uv/vis and ftir spectroscopic techniques. *Luminescence*, 31(2):565–572, 2016. 2.4

[156] *Condon EU, Shortley GH. The theory of atomic spectra*. Cambridge University Press, UK, 1951. 3

[157] *Cowan RD. The theory of atomic structure and spectra*. Number 3. Univ. California Press, Oakland, 1981. 3

[158] *Lindon JC, Tranter GE, Koppenaal D. Encyclopedia of spectroscopy and spectrometry*. Academic Press, USA, 2016. 3.1.1

[159] *Atkins PW, Friedman RS. Molecular quantum mechanics*. Oxford university press, UK, 2011. 3.1.1

[160] *Thyagarajan K, Ghatak A. Lasers: fundamentals and applications*. Springer Science & Business Media, Germany, 2010. 3.1.1

[161] *Piepho SB, Schatz PN. Group theory in spectroscopy: with applications to magnetic circular dichroism*, volume 1. Wiley-Interscience, New York, 1983. 3.1.2, 3.1.3

[162] *Levine IN. Molecular spectroscopy*. Wiley, New York, 1975. 3.1.2

[163] *Barrow GW. Introduction to molecular spectroscopy*. Mc Graw-Hill, New York, 1962. 3.1.2, 3.1.2, 3.1.3

[164] John Weiner and P-T Ho. *Weiner J, Ho PT. Light-Matter Interaction, Volume 1: Fundamentals and Applications*, volume 1. John Wiley & Sons, 2008. 3.1.2, 3.1.2, 3.1.2

[165] Huber MCE, Sandeman RJ. The measurement of oscillator strengths. *Rep. Prog. Phys.*, 49(4):397, 1986. 3.1.3, 3.1.3

[166] *Bohren CF, Huffman DR. Absorption and scattering of light by small particles*. John Wiley & Sons, New York, 2008. 3.1.3

[167] Liptay W. Electrochromism and solvatochromism. *Angew. Chem. Int. Ed. Engl.*, 8: 177–187, 1969. 3.1.3, 3.1.4, 5.4

[168] *Michale JL. Molecular spectroscopy*. Prentice-Hall, Inc., USA, 1999. 3.1.3, 3.1.3, 3.1.4, 5.4

[169] Georgakopoulou S, Van Grondelle R, Van Der Zwan G. Circular dichroism of carotenoids in bacterial lightharvesting complexes: Experimental modeling. *Biophys. J.*, 87:3010–3022, 2004. 3.1.3

[170] Orti E, Planelles J. A revision of the paper grid of expressions related to the einstein coefficients. *Journal of chemical education*, 69(8):685, 1992. 3.1.3, 3.1.3, 3.1.3, 3.1.4

[171] *Hollas JM. High resolution spectroscopy*. Butterworth-Heinemann, UK, 2013. 3.1.3, 3.1.3, 3.1.3, 3.1.4, 5.4

[172] *Kneubühl FK, Sigrist MW. Laser*. Springer-Verlag, Germany, 2008. 3.1.3, 3.1.3

[173] Eichhorn M. Quantum-mechanical fundamentals of lasers. In *Laser Physics*, pages 1–21. Springer, Germany, 2014. 3.1.3, 3.1.3

[174] *Lakowicz JR. Principles of Fluorescence Spectroscopy*. Springer, Germany, 2006. 3.2, 3.2.1, 3.2.3

[175] Strasburg GM, Ludescher RD. Theory and applications of fluorescence spectroscopy in food research. *Trends Food Sci Technol*, 6:69–75, 1995. 3.2

[176] *Valeur B, Berberan-Santos M. Molecular fluorescence: principles and applications*. John Wiley & Sons, New York, 2012. 3.2, 3.2.1, 3.3.2, 3.3.3

[177] *Lakowicz JR. Topics in fluorescence spectroscopy: principles*, volume 2. Springer Science & Business Media, Germany, 1992. 3.2, 3.2.1

[178] Christensen J, Norgaard L, Bro R, Engelsen SB. Multivariate autofluorescence of intact food systems. *Chem. Rev.*, 106:1979–94, 2006. 3.2

[179] Herschel JFW. A$\mu o \rho \Phi \omega \tau \alpha$ No. I. On a case of superficial colour presented by a homogeneous liquid internally colourless. *Philos Trans R Soc Lond B Biol Sci.*, pages 143–145, 1845. 3.2.1

[180] Jabłoński A. Über den mechanismus der photolumineszenz von farbstoffphosphoren. *Z PHYS A-HADRON NUCL*, 94(1):38–46, 1935. 3.2.1

[181] *Hercules DM (Ed.). Fluorescence and Phosphorescence Analysis*. Interscience Publishers, New York, 1966. 3.2.1, 3.2.2

[182] Kasha M. Characterization of electronic transitions in complex molecules. *Disc. Faraday Soc.*, 14(9), 1950. 3.2.1

[183] Albrecht C, Lakowicz JR. Principles of fluorescence spectroscopy. *Anal. Bioanal. Chem.*, 390(5):1223–1224, 2008. 3.2.2

[184] Lakowicz JR. Quenching of fluorescence. In *Principles of fluorescence spectroscopy*, pages 237–265. Springer, Germany, 1999. 3.2.2, 5.5.1

[185] Bowen EJ, West K. Solvent quenching of the fluorescence of anthracene. *J. Chem. Soc.*, page 4394, 1955. 3.2.2

[186] Van Duuren BL. Effects of the environment on the fluorescence of aromatic compounds in solution. *Chem. Rev.*, 63(4):325–354, 1963. 3.2.2

[187] Kang J, Liu Y, Xie MX, Li S, Jiang M, Wang YD. Interactions of human serum albumin with chlorogenic acid and ferulic acid. *Biochim. Biophys. Acta*, 1674(2):205–214, 2004. 3.2.2

[188] Schilt AA, Smith GF. Acid dissociation constants of substituted 1, 10-phenanthrolines. *J. Phys. Chem.*, 60:1546, 1956. 3.2.2

[189] Bowen EJ, Wokes F. Fluorescence of solutions longmans and green, London, 1953. 3.2.2

[190] *Parker CA. Photoluminescence of Solutions: with applications to photochemistry and analytical chemistry*. Elsevier Publishing Company, New York, 1968. 3.2.2

[191] *Reichardt C, Welton T. Solvents and solvent effects in organic chemistry*. John Wiley & Sons, New York, 2011. 3.2.3, 3.3.1, 3.3.2, 3.3.3, 3.3.4, 3.3.4, 3.3.4

[192] Lutskii AE, Prezhdo VV, Degtereva L, Gordienko VG. Spectroscopy of intermolecular field interactions in solutions. *Russ. Chem. Rev.*, 51(8):802–817, 1982. 3.3.1

[193] Gough TE, Irish DE, Lantzke IR. Spectroscopic Measurements (electron absorption, infrared and Raman, ESR and NMR spectroscopy), Phys Chem Organic Solv System, Page 405, 1973.

[194] Rao CNR, Singh S, Senthilnathan VP. Spectroscopic studies of solute–solvent interactions. *Chem. Soc. Rev.*, 5:297–316, 1976. 3.3.1

[195] Bayliss NS, McRae EG. Solvent effects in organic spectra: dipole forces and the franck–condon principle. *J. Phys. Chem. A*, 58(11):1002–1006, 1954. 3.3.1

[196] Lippert E. Spektroskopische bestimmung des dipolmomentes aromatischer verbindungen im ersten angeregten singulettzustand. *Ber. Bunsenges. Phys. Chem.*, 61(8):962–975, 1957. 3.3.2, 3.3.4, 3.3.4

[197] Stokes GG. On the change of refrangibility of light. *Philos Trans R Soc Lond B Biol Sci.*, 142:463–562, 1852. 3.3.3

[198] Van der ZG, Hynes JT. Time-dependent fluorescence solvent shifts, dielectric friction, and nonequilibrium solvation in polar solvents. *J. Phys. Chem. A*, 89(20):4181–4188, 1985. 3.3.3

[199] Kosower EM. Mechanism of fast intramolecular electron-transfer reactions. *J. Am. Chem. Soc*, 107(5):1114–1118, 1985.

[200] *Wolfbeis OS. Fluorescence spectroscopy: new methods and applications*. Springer Science & Business Media, Germany, 2012. 3.3.3

[201] Kawaski A, Rabek JF. Progress in photochemistry and photophysics. vol. 5, crc press, boca raton, fl, 1992. 3.3.4

[202] Bilot VL, Kawski A. Zur theorie des einflusses von lösungsmitteln auf die elektronenspektren der moleküle. *Z Naturforsch A*, 17(7):621–627, 1962. 3.3.4

[203] Chamma A, Viallet PCR. Determination du moment dipolaire dâĂŹune molecule dans un etat excite singulet. *CR Acad Sci Paris Ser C*, 270:1901–1904, 1970. 3.3.4, 3.3.4, 3.3.4

[204] Bakhshiev NG. Universal molecular interactions and their effect on the position of the electronic spectra of molecules in two-component solutions. i. theory (liquid solutions). *Opt. Spec.*, 10:379, 1961. 3.3.4, 3.3.4, 3.3.4

[205] Kawski A. Untersuchungen zum zwischenmolekularen energieübergang in fluoreszierenden lösungen. *Z. Naturforsch. A*, 18(8-9):961–966, 1963. 3.3.4, 3.3.4

[206] Kawski A. On the estimation of excited-state dipole moments from solvatochromic shifts of absorption and fluorescence spectra. *Z. Naturforsch. A*, 57(5):255–262, 2002. 3.3.4, 3.3.4

[207] Mataga N, Kaifu Y, Koizumi M. Solvent effects upon fluorescence spectra and the dipolemoments of excited molecules. *Bull Chem Soc Jpn.*, 29(4):465–470, 1956. 3.3.4, 3.3.4

[208] Perov AN. Energy of intermolecular pair interactions as a characteristic of their nature. theory of the solvato (fluoro) chromism of three-component solutions. *Opt Spec*, 49:371–374, 1980. 3.3.5

[209] Neporent BS, Bakhshiev NG. On the role of universal and specific intermolecular interactions in the influence of the solvent on the electronic spectra of molecules. *Opt Spec*, 8:408, 1960. 3.3.5

[210] Belay A. Determination of self - associated 5-caffeoylquinic acid and its complexation with sodium hydroxide using uv-vis spectroscopy. *Int. J. Phys. Sci.*, 5(5):459–464, 2012. 4.2.1, 5.2, 5.5.4, A.1

[211] Frisch MJ. Guassian 09, gaussian, wallingford, ct. 2009. 4.2.6, 5.6.2

[212] *Murphy R, Tsai A. Misbehaving proteins: Protein (mis) folding, aggregation, and stability*. Springer Science & Business Media, Germany, 2007. 5.1

[213] Davey RJ, Schroeder SLM, ter Horst JH. Nucleation of organic crystalsâĂŤa molecular perspective. *Angewandte Chemie International Edition*, 52(8):2166–2179, 2013. 5.1

[214] Antonov L, Gergov G, Petrov V, Kubista M, Nygren J. UV-vis spectroscopic and chemo metric study on aggregation of ionic dyes in water. *Talanta*, 49:99–106, 1999. 5.1, 5.2, 5.2

[215] Kulkarni SA, Weber CC, Myerson AS, Ter Horst JH. Self-association during heterogeneous nucleation onto well-defined templates. *Langmuir*, 30(41):12368–12375, 2014. 5.1

[216] Charman WN, Lai CSC, Craik DJ, Finnin BC, Reed BL. Self-association of nicotinamide in aqueous-solution: Nmr studies of nicotinamide and the mono-and dimethyl-substituted amide analogs. *Australian Journal of Chemistry*, 46(3):377–385, 1993. 5.1

[217] Gallego E, Peral F. Self-association of nicotinamideâĂŤadenine dinucleotides in aqueous solution. *Journal of molecular structure*, 298:87–94, 1993. 5.1, 5.1

[218] Peral F. Substituent and ph effects on self-association of pyridine derivatives in aqueous solution. an ultraviolet study. *Journal of molecular structure*, 266:373–378, 1992. 5.1

[219] Kaplan E, Guichou JF, Chaloin L, Kunzelmann S, Leban N, Serpersu EH, Lionne C. Aminoglycoside binding and catalysis specificity of aminoglycoside 2"-

phosphotransferase iva: A thermodynamic, structural and kinetic study. *Biochimica et Biophysica Acta*, 1860:802–âĂŞ813, 2016. 5.1

[220] Davies DB, Djimant LN, Veselkov AN. 1 H NMR investigation of self-association of aromatic drug molecules in aqueous solution. structural and thermodynamical analysis. *Journal of the Chemical Society, Faraday Transactions*, 92(3):383–390, 1996. 5.1

[221] Benesi HA. Spectrophotometric investigation of iodine with aromatic hydrocarbons. *J. Am. Chem. Soc*, 71:2703–2707, 1949. 5.2

[222] *Khopkar SM. Basic concepts of analytical chemistry, 2nd ed.* New Delhi, 1998. 5.2

[223] Evstigneev MP, Rybakova KA, Davies DB. Complexation of norfloxacin with dna in the presence of caffeine. *Biophys. Chem.*, 121(2):84–95, 2006. 5.2

[224] Benesi HoA, Hildebrand JHJ. A spectrophotometric investigation of the interaction of iodine with aromatic hydrocarbons. *Journal of the American Chemical Society*, 71 (8):2703–2707, 1949. 5.2

[225] Davies DB, Veselkov DA, Djimant LN, Veselkov AN. Hetero-association of caffeine and aromatic drugs and their competitive binding with a dna oligomer. *European Biophysics Journal*, 30(5):354–366, 2001. 5.2

[226] Davies DB, Eaton RJ, Baranovsky SF, Veselkov AN. NMR investigation of the complexation of daunomycin with deoxytetranucleotides of different base sequence in aqueous solution. *Journal of Biomolecular Structure and Dynamics*, 17(5):887–901, 2000. 5.2

[227] Vijan LE, Conci M. Absorption study of norfloxacin–dna interaction. In *Macromolecular symposia*, volume 265, pages 260–267. Wiley Online Library, 2008. 5.2

[228] Tablet C, Hillebrand M. Theoretical and experimental study of the inclusion complexes of the 3-carboxy-5, 6-benzocoumarinic acid with cyclodextrins. *Spectrochimica Acta Part A: Molecular and Biomolecular Spectroscopy*, 70(4):740–748, 2008. 5.3

[229] Zhang YZ, Dai J, Zhang XP, Yang X, Liu Y. Studies of the interaction between sudan i and bovine serum albumin by spectroscopic methods. *Journal of Molecular Structure*, 888(1-3):152–159, 2008. 5.3, 5.5.3

[230] Guo Y, Liu B, Li Z, Zhang L, Lv Y. Study of the combination reaction between drugs and bovine serum albumin with methyl green as a fluorescence probe. *J. Chem. Pharm. Res.*, 6(5):968–974, 2014. 5.3, 5.5.3

[231] Wang Z, Wang N, Han X, Wang R, Chang J. Fluorescence quenching and molecular docking study on the binding of four hydroxyanthraquinones to fto. *Physics and Chemistry of Liquids*, pages 1–14, 2017. 5.3, 5.5.2, 5.5.3

[232] Danyang Y, Zhengwen X, Jing S, Lili S, Zexiang H. Adsorption characteristics of ciprofloxacin on the schorl: kinetics, thermodynamics, effect of metal ion and mechanisms. *Journal of Water Reuse and Desalination*, 2017. 5.3

[233] Liu Y, Liu YJ. Biosorption isotherms, kinetics and thermodynamics. *Separation and Purification Technology*, 61(3):229–242, 2008. 5.3

[234] Yuanfeng W, Lei Z, Jianwei M, Shiwang L, Jun H, Yuru Y, Lehe M. Kinetic and thermodynamic studies of sulforaphane adsorption on macroporous resin. *Journal of Chromatography B*, 1028:231–236, 2016. 5.3

[235] Serpersu EH, Lionne C. Aminoglycoside binding and catalysis specificity of aminoglycoside 2 âĂş-phosphotransferase iva: A thermodynamic, structural and kinetic study. *Biochimica et Biophysica Acta*, 2016:802–813, 1860. 5.3

[236] Bakhkshiev NG. Universal intermolecular interactions and their effects on the position and electronic spectra of molecules in two components solutions. *Optic. Spectrosc.*, 10:379–384, 1961. 5.4

[237] Firth WJ, Watkins CL, Graves DE, Yielding LW. Synthesis and characterization of ethidium analogs, emphasis on amino and azido substituent. *J. Heterocycl. Chem.*, 20:759–765, 1983. 5.4

[238] Paramaguru G, Kathiravan A, Selvaraj S, Venuvanalingam P, Renganathan R. Interaction of anthraquinone dyes with lysozyme: evidences from spectroscopic and docking studies. *J Hazard Mater*, 175(1):985–991, 2010. 5.5.1

[239] *Atkins P, De Paula J, Keeler J. Atkins' physical chemistry*. Oxford university press, UK, 2018. 5.5.1

[240] Chou KC, Jiang SP. Studies on the rate of diffusion-controlled reactions of enzymes. *Scientia Sinica*, 17:664–680, 1974. 5.5.1

[241] Chen J, Sawyer N, Regan L. Protein–protein interactions: General trends in the relationship between binding affinity and interfacial buried surface area. *Protein Science*, 22(4):510–515, 2013. 5.5.2

[242] Inamdar SR, Nadaf YF, Mulimani BG. Ground and excited-state dipole moments of exalite 404 and exalite 417 uv laser dyes determined from solvatochromic shifts of absorption and fluorescence spectra. *J Mol Struct (Theochem)*, 624:47âĂŞ51, 2003. 5.6

[243] Manohara SR, Kumar VU, Shivakumaraiah GL. Estimation of ground state dipole moments of 1,2-diazines by solvatochromic method and quantum-chemical calculation. *J Mol Liq*, 181:97âĂŞ104, 2013. 5.6, 5.6.2

[244] Sidir I, Sidir YG. Ground state and excited state dipole moment of 6, 8-diphenylimidazo[1,2-alph]pyrazine, determined from solvatochromic shift of absorption and fluorescence spectra. *Spectrochim Acta A*, 79:1220–1225, 2011. 5.6

[245] Raikar US, Renuka CG, Nadaf YF, Mulimani BG, Karguppikav AM, Soudagar MK. Solvent effects on the absorption and fluorescence spectra of coumarines 6 and 7 molecules: determination of ground and excited state dipole moment. *Spectrochimica Acta A*, 65:673–677, 2006. 5.6

[246] Patil NR, Melavanki RM, Kapatkar SB, Ayachit NH, Saravanan J. Solvent effect on absorption and fluorescence spectra of three biologically active carboxamides (c1, c2 and c3). estimation of ground and excited state dipole moment from solvatochromic method using solvent polarity parameters. *Journal of fluorescence*, 21(3): 1213–1222, 2011. 5.6.1

[247] Paluch M, Dynarowicz P. The influence of nicotinamide on the adsorption equilibrium of aspirin at the aqueous solution-air interface. *Colloid Polym. Sci*, 266:180–183, 1988. 5.6.1, 5.6.2

Appendix A

Dimer and Benesi-Hildebrand Model

A.1 Dimer Model

For the case of numerical analysis dimer model was derived by considering the following molecular equilibrium in solutions[153, 210].

$$C_1 + C_1 \quad \xleftrightarrow{K_C} \quad C_2 \tag{A.1.1}$$

where C_1 and C_2 are monomers and dimers of the compounds, respectively and K_C is the equilibrium dimerization constant. The overall concentration of the dissolved molecules in the solution, using the mass conservation law can be written as:

$$[C_0] = [C_1] + 2[C_2] \tag{A.1.2}$$

where $[C_0]$, $[C_1]$ and $[C_2]$ are the total concentration, the concentration of the monomers and concentrations of the dimer molecules respectively. where,

$$[C_2] = K_C[C_1]^2 \tag{A.1.3}$$

The contribution of the monomer and dimer to the molar extinction coefficient of the solution is commonly considered to be additive and

$$\varepsilon = \varepsilon_m f_m + \varepsilon_d f_d \tag{A.1.4}$$

$$f_m = \frac{C_1}{C_0}$$

$$f_d = 2K_C \frac{C_1^2}{C_0}$$

where $\varepsilon_m, \varepsilon_d, f_m$ and f_d are molar monomer extinction coefficients, molar dimer extinction coefficients, equilibrium mole fraction of the molecules in the monomer concentration and equilibrium mole fraction of the molecules in the dimer concentration, respectively.

The concentration can be derived from the mass conservation law given in Eqn (A.1.2) by substituting on the account of Eqn (A.1.4). Thus, we obtain,

$$\varepsilon = \varepsilon_d + (\varepsilon_d - \varepsilon_m)\frac{1 - \sqrt{8[C_0]K_C + 1}}{4[C_0]K_C} \tag{A.1.5}$$

In Eqn (A.1.5), there are three unknown parameters $\varepsilon_d, \varepsilon_m$ and K_C which can be obtained from fitting dimer model equation to the experimental data of the compounds.

A.2 Benesi-Hildebrand Model

In order to analyse hetero-association parameters, the Benesi-Hildebrand equation was used. The equilibrium constant for the complex formation K_E, is given by:

$$C + D \quad \xleftrightarrow{K_E} \quad CD \tag{A.2.1}$$

From Eqn (A.2.1), the equilibrium constant for the complex formation K_E can be defined as:

$$K_E = \frac{[CD]}{[C].[D]} \tag{A.2.2}$$

where $[C]$, $[D]$, and $[CD]$ are the equilibrium concentrations of CGA/CAF, NIC/NOR, and association of NIC-CGA/NOR-CAF, respectively. The initial concentration of NIC/NOR and CGA/CAF is designated as:

$$[D_0] = [D] + [CD] \tag{A.2.3}$$

$$[C_0] = [C] + [CD] \tag{A.2.4}$$

Substituting Eqns (A.2.3 and A.2.4) into Eqn (A.2.2) gives,

$$K_E = \frac{[CD]}{([C_0] - [CD]).([D_0] - [CD])} \tag{A.2.5}$$

where $[C_0]$ and $[D_0]$ are the initial concentrations of CGA/CAF and NIC/NOR respectively.If $[C] >> [D]$, then $[C_0] - [CD] \approx [C_0]$. So, Eqn (A.2.5) can be written as,

$$K_E = \frac{[CD]}{[C_0]([D_0] - [CD])} \tag{A.2.6}$$

After re-arranging Eqn (A.2.6), we have

$$[CD] = \frac{K_E[C_0].[D_0]}{1 + K_E[C_0]} \tag{A.2.7}$$

The absorbance (A) for concentration $[CD]$ according to Beers law is

$$A = \varepsilon l[CD] = \varepsilon l \frac{K_E[C_0].[D_0]}{1 + K_E[C_0]} \tag{A.2.8}$$

By re-arranging Eqn (A.2.8), and when the path length l of the cuvette is $1cm$, Eqn (A.2.8) can be written in the form of Benesi-Hildebrand equation as:

$$\frac{[D_0]}{A} = \frac{1}{\varepsilon} + \frac{1}{\varepsilon K_E}\frac{1}{[C_0]} \tag{A.2.9}$$

The plot of $\frac{[D_0]}{A}$ vs $\frac{1}{[C_0]}$ gives a straight line with y-intercept $\frac{1}{\varepsilon}$ and slope $\frac{1}{\varepsilon K_E}$. Thus, the equilibrium constant and molar absorption extinction coefficient can be calculated by fitting Eqn (A.2.9) to experimental data of the compounds.